Expanding the Horizon of Proteolysis Targeting Chimeras (PROTACs) in RAPID Platforms, CLIPTAC, and the Exploration of E3 Ligase Substrate Receptors

By

Zhongrui Zhang

A dissertation submitted in partial fulfillment of the requirements for the degree of

Doctor of Philosophy

(Chemistry)

at the

UNIVERSITY OF WISCONSIN-MADISON

2023

Date of final oral examination: 08/28/2023

The dissertation is approved by the following members of the Final Oral Committee:

Weiping Tang, Professor, Organic Chemistry and Chemical Biology

Andrew R. Buller, Assistant Professor, Chemical Biology

Samuel H. Gellman, Professor, Organic Chemistry and Chemical Biology

Ying Ge, Professor, Cell and Regenerative Biology

© Copyright by Zhongrui Zhang 2023

All Rights Reserved

Abstract

This dissertation will focus on my efforts for the development of innovative strategies to advance Proteolysis Targeting Chimeras (PROTACs) for therapeutic applications. Chapter 1 presents my efforts in the development of RAPID-TAC and RAPID-GLUE, two novel platforms that expedite the discovery and optimization of PROTACs. Included in this chapter is the successful application of the first generation of RAPID-TAC platform towards the development of degraders for Receptor Interacting Protein Kinase 1 (RIPK1), which shows promise in advancing cancer immunotherapy. Further, this chapter unveils the second generation of the RAPID-TAC platform, revealing its efficiency in producing a wider array of BRD4 degraders. Finally, a new platform, RAPID-GLUE, is introduced for the swift synthesis of molecular glues for direct biological screening. In Chapter 2, a new class of in-cell self-assembled PROTACs is developed by employing covalent E3 ligase ligands. This chapter brings to the fore an innovative tactic that bypasses the need for individual PROTAC synthesis, thus expediting the development of degraders for target proteins. Chapter 3 probes the potential of DDB1 and CUL4associated factors 1 (DCAF1) and 15 (DCAF15) as new E3 ligase substrate receptors for PROTACs. Through rigorous experimentation, it is demonstrated that DCAF1 and DCAF15 are effective in mediating the degradation of BRD4 and Androgen Receptor

(AR), respectively. This research opens new horizons in PROTAC technology and lays a solid foundation for the next wave of therapeutic applications.

Acknowledgements

I would like to express my deepest appreciation to all those who provided me the possibility to complete this thesis. I want to express my special gratitude to my thesis advisor, Dr. Weiping Tang, who has continually and convincingly conveyed a spirit of adventure regarding research, and excitement regarding teaching. Without his guidance and persistent help, this thesis would not have been possible.

I also want to extend my thanks to Dr. Sam Gellman, Dr. Andrew Buller and Dr. Ying Ge for their insightful comments and encouragement, but also for the hard questions which incited me to widen my research from various perspectives.

Special Thanks to my fellow researchers and lab mates. Yin Dan, Le Guo, Yunxiang Wu, Jingyao Li, Hua Tang and Zhen Zhang for their hard work of synthesizing degraders. I am grateful to Dr Chunrong Li for helping me a lot in biological assays in testing RAPID-GLUE and building plasmids for nanoBRET assays. I would also like to thank small molecule screening facility in WIMR and Junming Peng's lab in St. Jude Children's Research Hospital.

Lastly, but by no means least, I wish to acknowledge the love, support, and encouragement of my family. They have been a constant source of strength throughout

my academic journey. This accomplishment would not have been possible without them. Thank you.

This journey would not have been possible if not for them, and I dedicate this milestone to them.

Contents

1. Chapter 1 Expediting Drug Discovery through RAPID-TAC and RAPID-GLUI	Е
Platforms	1
1.1 Introduction	1
1.2 Two-stage strategy for RIP kinase degraders development	6
1.2.1 Introduction	6
1.2.2 Result and discussion	10
1.3 Second generation of Rapid-TAC platform for BRD4 degrader development	nt 20
1.3.1 Introduction	20
1.3.2 Results and discussions	23
1.4. A Platform for the Rapid Synthesis of Molecular Glues (Rapid-Glue) under	
Miniaturized Conditions for Direct Biological Screening.	29
1.4.1 Introduction	29
1.4.2 Results and discussions	32
1.5 Conclusions and future perspectives.	42

	1.6 Experimental Procedures.	44
	1.6.1 Procedures for RIPK1 degrader development	44
	1.6.2 Procedures for BRD4 degraders development	46
	1.6.3 Procedures for GSPT1 degraders development	46
2.	Chapter. 2. In-cell self-assembly of Proteolysis Targeting Chimeras (PROTAC) w	ith
co	valent E3 ligase ligand	50
	2.1 Introduction	50
	2.2 Results and Discussions	54
	2.3 Conclusions and Future perspectives.	65
	2.4 Experimental Procedures.	67
3.	Chapter. 3. Exploring the Utility of Novel E3 Ligase Substrate Receptors DCAF1	l
an	d DCAF15 in PROTACs for Targeted Protein Degradation	68
	3.1 Introduction	68
	3.2 BRD4 degraders recruiting DCAF1	71
	3.3 AR degraders recruiting DCAF15.	78
	3.4 Discussion and Future perspectives	91
	3.5 Experimental Procedures	93
	Abbreviations	96
	References	99

Table of Figures

Figure 1.1.1 Scheme of PROTAC and molecular glue strategy.	2
Figure 1.1.2. Platforms for the rapid synthesis of PROTACs (Rapid-TAC) under	
miniaturized conditions for direct screening without further manipulations	5
Figure 1.1.3. Co-crystallization structure of binding between RIPK1 kinase domain	
and GSK2982772 (PDB 5TX5)	7
Figure 1.2.3 Structures of RIPK1 degraders recruiting VHL1	0
Figure. 1.2.4 Screening of degraders in NOMO-1 cells. 11	
Figure 1.2.5 Structure of AM-DY-2	2
Figure 1.2.6 Western blot analysis of AM-DY2 degrading RIP114	4
Figure 1.2.7 Time-course study of AM-DY2 in NOMO1 cells	5
Figure 1.2.8. Wash-off study of AM-DY21	7
Figure 1.2.9. Mechanistic study of AM-DY2. 18	
Figure 1.3.1 Synthesis of 21 BRD4 PROTACs using the Rapid-TAC platform 22	2
Figure 1.3.2 . A library of 21 members of BRD4 PROTACs was tested by Western	
blot in MV-4-11 cell line for 24 h at 1 μM and 10 μM concentrations24	4
Figure 1.3.3 Dose response test for LG-BRD-122	5

Figure 1.3.4 The western blot analysis of LG-BRD-12 enantiomers
Figure 1.4.1 The strategy for Rapid-Glue platform
Figure 1.4.2 Design of Rapid-Glue libraries. Designed by Jingyao Li
Figure 1.4.3 Potent GSPT1 degraders and their corresponding negative-control were
tested by Western blot in RS4;11 cells
Figure 1.4.4 Proteomics analysis of 15O and 18J
Figure 1.4.5 GSPT1 degraders with stable amide linkers were tested in RS4;11 cells.
41
Figure 2.1.1 The scheme of cCLIPTAC.
Figure 2.1.2 Structure of JP2 and PL
Figure 2.2.1 Structures of cCLIPTAC components
Figure 2.2.2 cCLIPTACs were tested by western blot in SU-DHL-4 cells 57
Figure 2.2.3 cCLIPTACs were tested by western blot in Hela and MCF-7 cells 59
Figure 2.2.3 cCLIPTACs were tested by western blot in MCF-7 cells
Figure 2.2.5 Comparative Analysis of Sequential cCLIPTAC and Pre-Assembled
PROTAC (PRE-MIX) Treatments
Figure 2.2.6 Validation of the Ubiquitin-Proteasome Pathway Mechanism in
cCLIPTAC
Figure 3.1.1 Scheme of PROTAC pathway recruiting DCAF1
Figure 3.1.2 Domain map of DCAF1
Figure 3.2.1 The binding between DCAF1 and CYCA-117-70 (PDB 7SSE)71
Figure 3.2.2 Structures of BRD4 degrader library recruiting DCAF172
Figure 3.2.3 Screening of BRD4 degraders recruiting DCAF1

Figure 3.2.4 Structure of degraders with CYCA-117-70 as DCAF1 ligand75
Figure 3.2.5 Western blot results of degraders tested in SU-DHL-4 cells70
Figure 3.2.6 Mechanistic study of 2036. DCAF1 ligand was pre-treated for 1 hour. 7'
Figure 3.3.1 Binding between E7820 and DCAF15
Figure 3.3.2 Structure of the AR degraders recruiting DCAF15
Figure 3.3.4 Western blot results for AR degraders
Figure 3.3.5 Structure of second AR degraders library
Figure 3.3.7 Western blot results for second AR degraders library
Figure 3.3.8 Structure of the third AR degraders library
Figure 3.3.9 Western blot results for third AR degraders library8
Figure 3.3.10 Antiproliferation effect for 72-hour treatment in LN-CAP cells 89
Figure 3.3.11 nanoBRET assay for confirming ternary complex formation 90

1. Chapter 1 Expediting Drug Discovery through RAPID-TAC and RAPID-GLUE Platforms

1.1 Introduction

Protein homeostasis, a fundamental principle of cell biology, requires a delicate balance between protein synthesis and degradation¹. Disruptions to this balance can lead to disease states, underscoring the importance of understanding and potentially harnessing protein degradation pathways for therapeutic purposes². In recent years, targeted protein degradation (TPD) has emerged as a promising approach for drug discovery, aiming to selectively degrade disease-causing proteins³. This research leverages the ubiquitinproteasome system, the cell's principal machinery for controlled protein degradation. Two novel technologies are at the forefront of this field: Proteolysis-targeting chimeras (PROTACs) and molecular glues⁴. These molecules function by recruiting an E3 ubiquitin ligase to a specific target protein, marking it for degradation by the proteasome. PROTACs and molecular glues provide a unique avenue to 'drug the undruggable',⁵ thereby opening up new opportunities for treating diseases, including cancer, neurodegenerative disorders, and more⁶. This thesis chapter will delve into the current understanding and future potential of PROTACs and molecular glues, discussing their mechanisms, advances in their design, and their therapeutic applications.

Proteolysis-targeting chimeras (PROTACs) and molecular glues are two leading strategies in the TPD field⁷. PROTACs work by hijacking a target protein to an E3 ligase, thereby marking the target protein for ubiquitination and degradation⁸. Molecular glues function similarly but typically induce conformational changes that enhance the

interaction between the target protein and the E3 ligase, leading to proteasomal degradation⁹. These innovative approaches have the potential to revolutionize the therapeutic landscape, particularly for diseases with few existing treatment options or those that have developed resistance to conventional therapies¹⁰ (**Figure 1.1**).

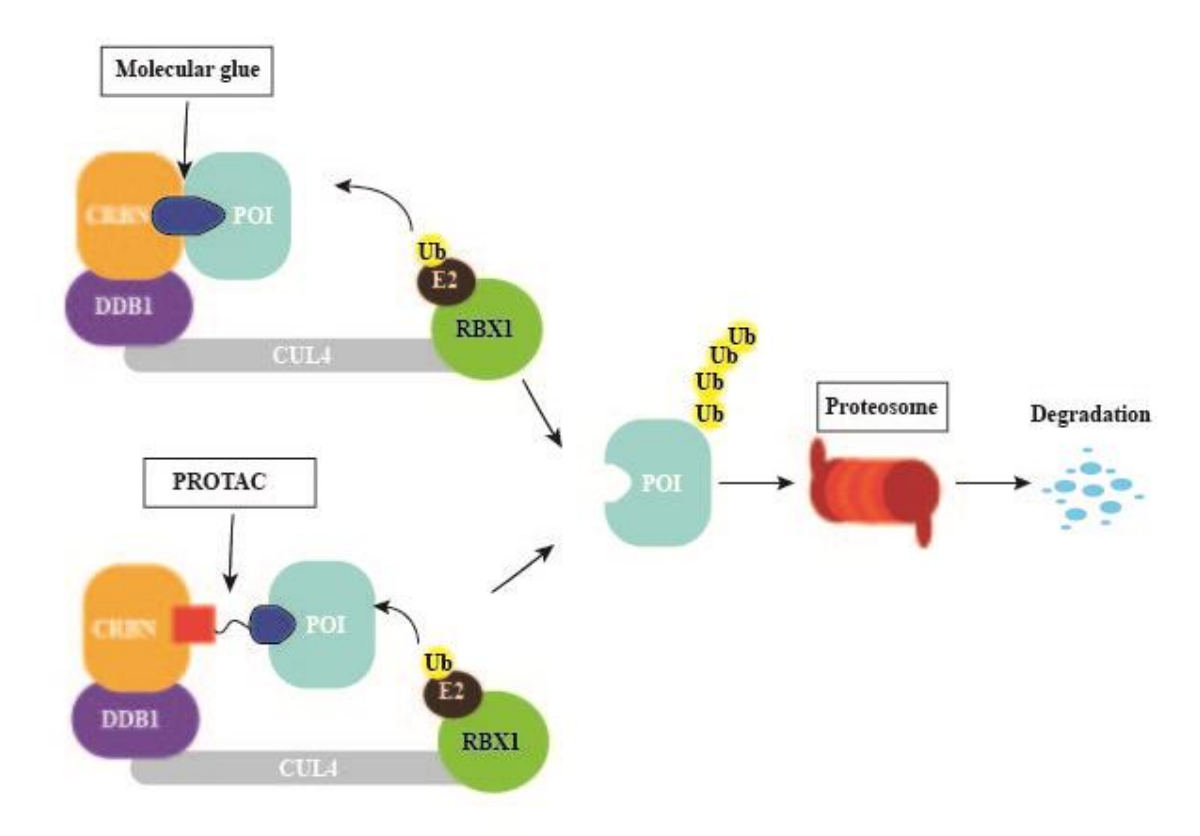


Figure 1.1.1 Scheme of PROTAC and molecular glue strategy.

PROTAC development requires structure-activity relationship (SAR) studies of target protein ligand, the linker and the E3 ligase ligand¹¹. This leads to a huge amount of synthetic work if we modify either ligand and connect them by linkers with different lengths. However, among over 600 E3 ligases in human cells, only several of them are

widely used for PROTAC¹². When the target protein binder can also be fixed, the most important factor for PROTAC development is the length of linkers.

Our lab developed a two-stage strategy to generate a potent PROTAC aiming at novel target proteins^{13,14}. This strategy provides quick access to degrader libraries with a hydrolytic labile acylhydrazone motif, which can be directly tested in biological assays. The stable versions of the hit compounds could be synthesized in the second stage. For the first generation of this strategy, it works by inciting a reaction between hydrazide A1 in the Protein of Interest (POI) ligand and aldehyde A2, which contains an E3 ligase ligand along with a variety of linkers (Figure 1.1.2). The produced PROTACs can be directly utilized in biological testing without requiring any additional purification steps. This is made possible by the high conversion rate of the reaction, generally surpassing 80%, and the fact that the only byproduct of this process is water. However, this initial approach did pose certain challenges. One of the main issues was the hydrolytic instability of the acylhydrazone motif in product A3, which could be problematic in assays requiring extended periods of treatment or storage. This was particularly the case when multiple rounds of freeze-thaw cycles were required. During the first stage of this strategy, we focused on identifying active degraders from a compound library of A3. These degraders featured an appropriate E3 ligase ligand and an optimal linker in terms of type and length. In the second stage of the strategy, we replaced the acylhydrazone motif in the linker region with a more stable isostere, such as an amide, while ensuring that the rest of the active molecule remained largely untouched.

However, it is worth noting that changing the acylhydrazone motif to its isosteres can often cause significant alterations in the activity of the degraders when the linker is relatively short and rigid. This can necessitate further optimization, which can be a time-consuming process. Additionally, the aldehyde containing partial PROTAC library A2 is not commercially available and has to be prepared through a step-by-step synthesis.

In response to these challenges, we developed a second generation Rapid-TAC platform. This platform has been meticulously designed to overcome many of the limitations in our initial strategy, while simultaneously preserving its many advantages. Central to this innovative platform is the formation of phthalimidine B3 from ortho-phthalaldehyde (OPA) **B1** and amine **B2** (**Figure 1.1.2**).

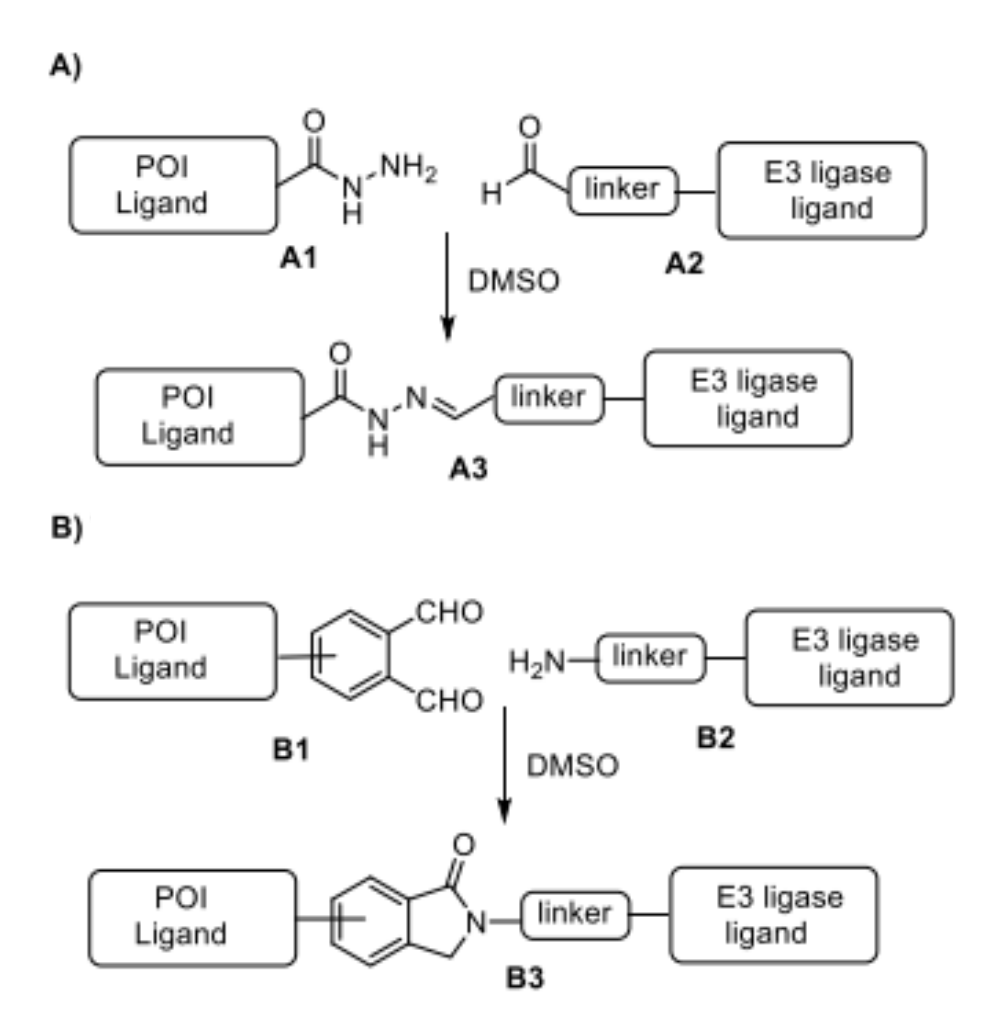


Figure 1.1.2. Platforms for the rapid synthesis of PROTACs (Rapid-TAC) under miniaturized conditions for direct screening without further manipulations. A) Our first generation RapidTAC Platform is based on hydrazide-aldehyde coupling chemistry.

B) Our second generation Rapid-TAC platform is based on OPA-amine coupling chemistry. The figure is drawn by Le Guo.

This optimized platform completes the library under miniaturized, parallel conditions in a reaction block, making it unnecessary to perform any further manipulations including purification before the cell-based screening. This is possible because the only byproduct of the reaction is water and the conversion is generally very high (over 90%). With its

streamlined process and high efficiency, we believe that our next-generation Rapid-TAC platform provides an ideal reaction environment for the development of PROTACs, propelling us further into the future of this exciting field of research.

1.2 Two-stage strategy for RIP kinase degraders development

1.2.1 Introduction

RIPK1 is a threonine/serine kinase which plays an important role in immune responses and death-inducing processes¹⁵. In most cells, necroptosis is triggered by the interaction between RIPK1 and RIPK3 ^{16,17}. RIPK1 and RIPK3 are phosphorylated and they form a complex called necrosome¹⁸. The necrosome phosphorylates MLKL and finally results in necrotic cell death¹⁹. Necroptosis is a major regulated mechanism of cellular death that is involved in inflammation^{20,21}, neuron degeneration²² and viral infection²³. Thus, targeting necroptosis has potential therapeutic applications and inhibition of RIPK1 is one of the critical steps that can block necroptosis. An increasing number of inhibitors targeting RIPK1 has already shown their effect on treatment of various diseases since Necrostatin-1 was first discovered in 2005²⁴. A novel RIPK1 inhibitor GSK2982772 has high activity in blocking necroptosis, as well as inflammation²⁵ (**Figure 1.2.1**).

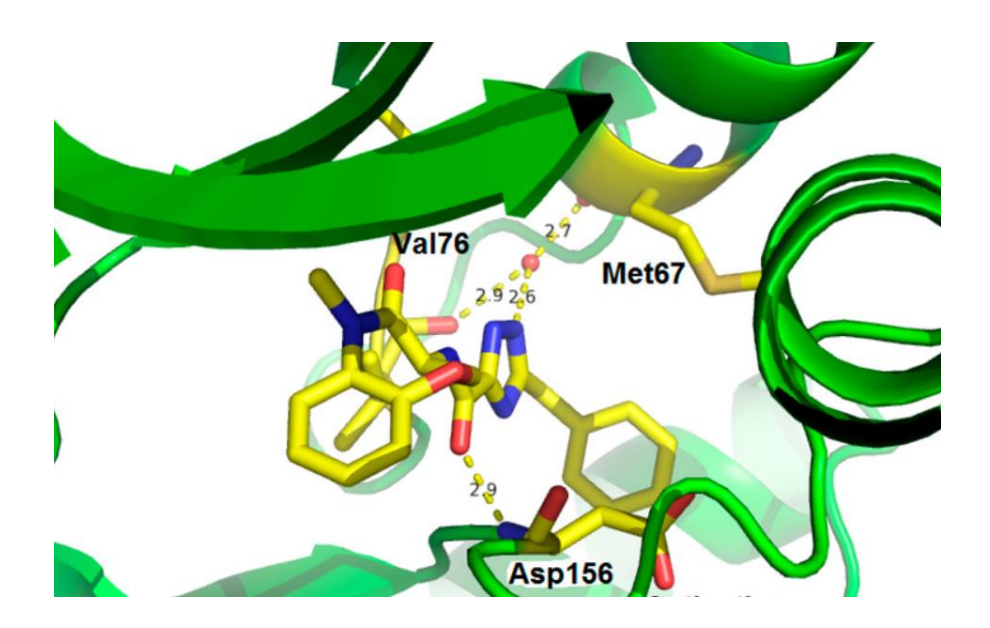


Figure 1.1.3. Co-crystallization structure of binding between RIPK1 kinase domain and GSK2982772 (PDB 5TX5)

Cancer immunotherapies have dramatically altered the landscape of cancer treatment, with immune checkpoint blockades (ICBs) making significant strides in clinical success²⁶. However, the overall response to these therapies remains notably low in several instances²⁷, emphasizing the need for understanding the defining characteristics and mechanisms of 'hot' (inflamed) and 'cold' (non-inflamed) immune tumors. This knowledge is crucial in shaping effective combination strategies to enhance antitumor immunity²⁸. Currently, various therapeutic strategies are under investigation for the transformation of 'cold' tumors into 'hot' tumors using PD1/PDL1 inhibitors²⁹. These studies, spanning both pre-clinical and clinical stages, have shown promising potential. Notably, the inflammatory responses and cell death pathways in the tumor microenvironment (TME) have emerged as critical research directions to advance cancer immunotherapies³⁰.

Receptor-interacting protein kinase 1 (RIPK1) plays a significant role in these immune responses. It regulates cell fate and proinflammatory signaling downstream of multiple innate immune pathways, including those initiated by tumor necrosis factor- α (TNF- α), toll-like receptor (TLR) ligands, and interferons (IFNs)³¹. RIPK1 exhibits dual functionality: it not only participates in apoptosis and necroptosis pathways through its kinase activity, but also operates as a kinase-independent scaffolding protein, recruiting the NF- κ B activation complex to instigate the NF- κ B pathway and promote cell survival³² (**Figure 1.2.2**). Genetic removal of RIPK1 disrupts this delicate balance between cell survival and death, triggering both RIPK3-mediated necroptosis induced by IFN γ and FADD/caspase-8–driven apoptosis incited by death receptor ligands such as TNF α ²⁸.

Recent independent studies have shed light on the function of RIPK1 in cancer immunotherapy^{28,30,32}. It has been found that the knockout of RIPK1 in cancer cells significantly sensitizes tumors to anti-PD1 therapy, leading to favorable changes in the tumor microenvironment. Interestingly, a RIPK1 kinase inhibitor developed by GSK failed to synergize with anti-PD1 therapy in a syngeneic mouse tumor model²⁸. These observations lead us to hypothesize that the development of RIPK1 degraders could mimic the genetic outcomes, potentially synergizing with ICBs to bolster antitumor immunity. This hypothesis forms the core of our research as we aim to advance the field of cancer immunotherapies.



Figure 1.2.2 Functional domains of RIPK1. Kinase domain (KD) has the function of polyubiquitination and phosphorylation. Its substrates include PELI1, TBK1, TAK1, TAB2/TAB3, etc. RHIM binds to RIPK3, TRIF and DAI. Death Domain (DD) is responsible for the RIPK1 dimerization and activation.

By using the first generation two-stage strategy, we developed active PROTACs for RIPK1. We used GSK-067, a known RIPK1 inhibitor as the ligand of target protein. For the E3 ligases, we tested both cereblon (CRBN) and Von Hippel-Lindau (VHL) because these two E3 ligases have well characterized cell permeable ligands that have been widely used in PROTAC design³³. Chemists in our lab synthesized a library containing 24 compounds with 12 for each E3 ligase ligand. My lab mate and I tested these compounds to determine the most potent degraders. I primarily focused on PROTACs that recruit VHL E3 ligase. The biological results revealed that **DY-2** was the most potent PROTAC. In stage 2, the acylhydrazone linker in **DY-2** is replaced with the amide linker to improve the stability.

Figure 1.2.3 Structures of RIPK1 degraders recruiting VHL. Synthesis was done by Dan Yin.

1.2.2 Result and discussion

The degraders were quickly screened in various cell lines (NOVAS, THP-1, HT-29 and NOMO-1) for the degradation effect of RIP kinases. Among these cells, human acute myeloid leukemia (AML) cell line NOMO-1 was the most sensitive cell line to show a down-regulated RIP expression under the treatment of our degraders. Then we performed the western blot assays on cells treated by compounds. We treated the NOMO-1 cells with 0.1 and 1 μ M of compounds DY-2 to DY-12. After 6 hours, cells were lysed for

SDS-PAGE and immunoblot. By examining the level of RIPK1 and RIPK2 protein, we observed a decrease in level of RIP1 under the treatment of several compounds (**Figure.** 1.2.4).

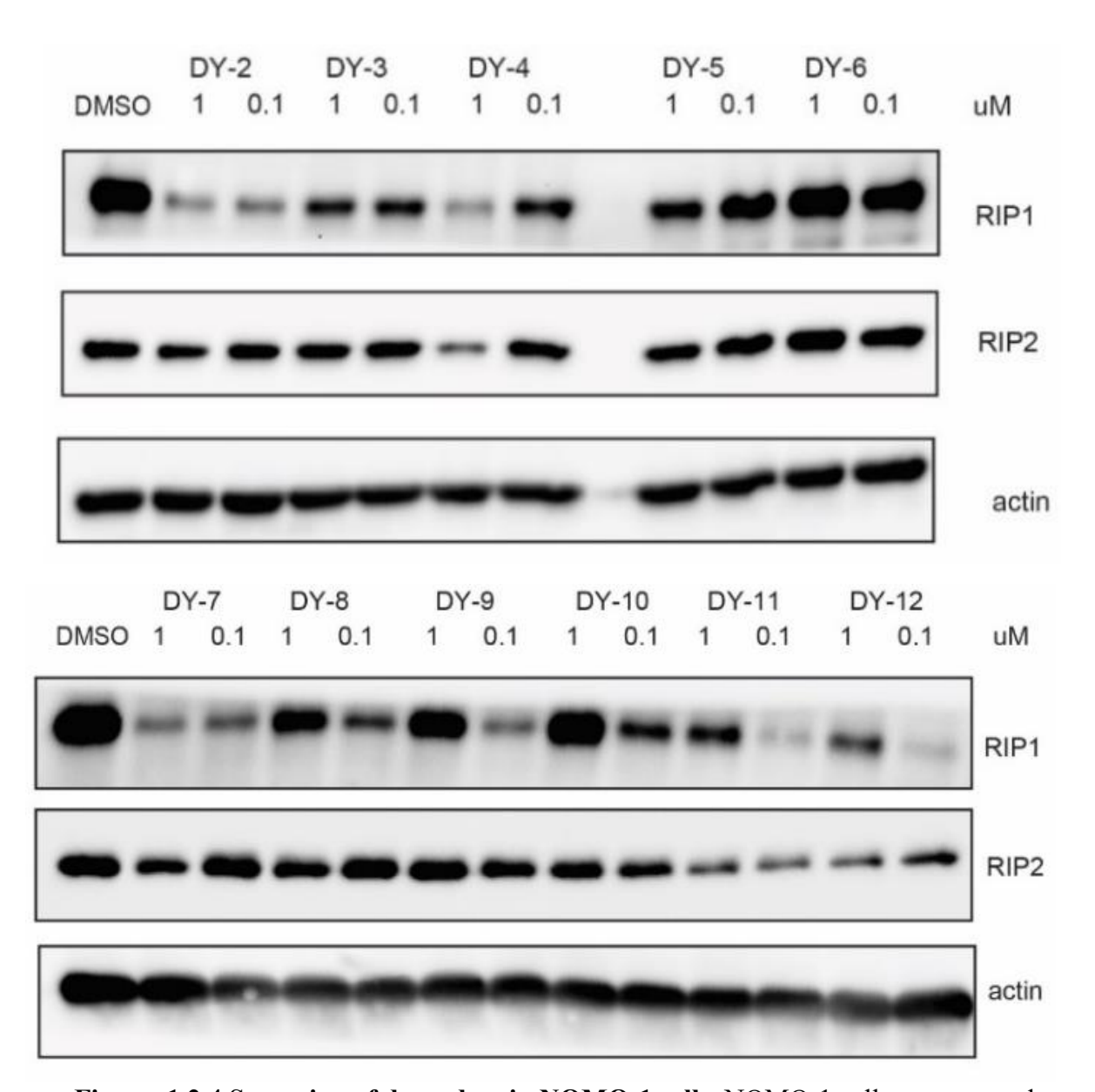


Figure. 1.2.4 Screening of degraders in NOMO-1 cells. NOMO-1 cells were treated with indicated degraders for 6 hours.

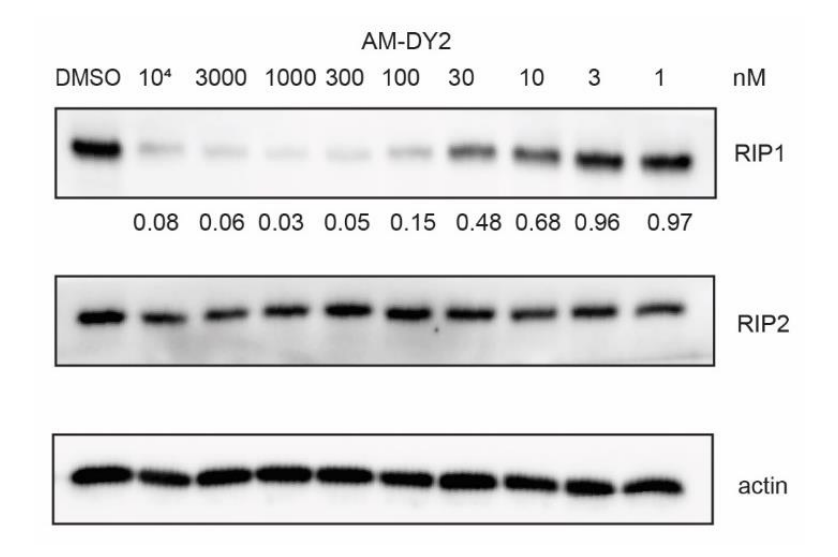
At 100 nM of dosage, RIP1 kinase can be readily degraded by most compounds tested. Although "hook effect" happened as early as 1 uM³⁴, the results showed a strong degradation effect on RIP1 at around 100 nM of the degraders. The western blot results showed that the linker length could affect the potency of the degraders. A structure-activity relationship (SAR) could be observed at 100 nM concentration. Among the alkyllinkers, degraders had higher potency as the linker length became shorter. Degrader DY-2 achieved about 60% degradation of RIP1 at 100 nM. Compared with all degraders in the PEG-linker series, DY-2 had a higher potency. This optimal linker length may be related to the distance between the E3 ligase VHL and the available ubiquitination sites of RIPK1.

Figure 1.2.5 Structure of AM-DY-2. Compound synthesized by Yunxiang Wu.

In our continued efforts to optimize the potency and stability of our PROTAC molecules, we have selected DY2 as our lead candidate, and proceeded to modify it by replacing the acylhydrazone motif with its bio isosteric amide group (**Figure 1.2.5**). This alteration was expected to enhance the compound's activity in cell-based assays by improving the stability.

To validate the activity and ascertain the effective concentration range for AM-DY2, we conducted in vitro experiments, treating cells with AM-DY2 at concentrations ranging from 1 nM to 10 µM. Immunoblotting results confirmed our hypothesis, showing that the replacement with an amide bond successfully retained the initial degradation effect of DY2, and notably, it did not show any significant hook effect even at the highest concentration (**Figure 1.2.6**.).

Our results further indicated a half-maximal degradation concentration (DC₅₀) of 14.5 nM for AM-DY2, suggesting a strong efficacy at relatively low concentrations. Importantly, AM-DY2 achieved a maximum degradation percentage (D_{max}) of 96%, thus underscoring its high effectiveness in degrading RIP1. These findings strengthen our confidence in AM-DY2's potential as a powerful tool for RIP1-related research and therapeutic applications.



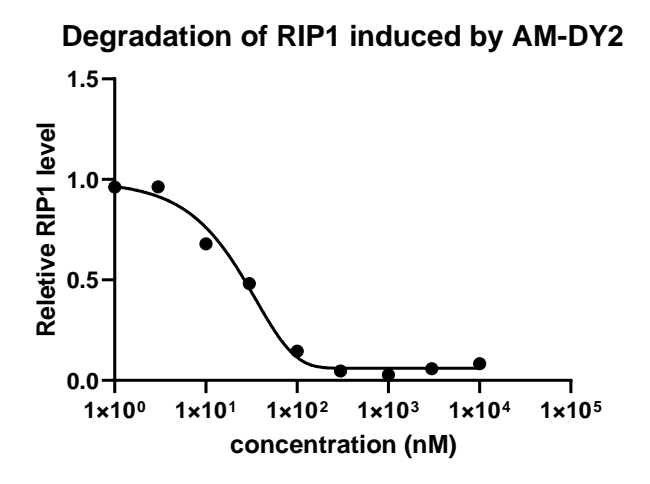


Figure 1.2.6 Western blot analysis of AM-DY2 degrading RIP1. NOMO-1 cells were treated with AM-DY2 with indicated concentration for 6 hours. The number indicates the relative signal intensity of each sample compared to the DMSO control. The RIP1 signal was normalized with the actin signal of each sample. The graph was plotted based on the relative signal intensity.

To understand the mechanism of action of our PROTAC AM-DY2, we carried out a series of experiments in NOMO-1 cells. We first treated the cells with AM-DY2 and lysed them at specific time intervals for analysis. Immunoblot results showed that at 100 nM of AM-DY2, the degradation of RIPK1 commenced after approximately 2 hours. Interestingly, a delay in degradation was observed when the AM-DY2 concentration was lowered to 10 nM, with RIPK1 degradation commencing after approximately 4 hours (**Figure 1.2.7**).

These results are critical in highlighting the efficiency and potency of AM-DY2 as a degrader of RIPK1. The rate of degradation appears to be dependent on the concentration of AM-DY2, revealing a potentially tunable mechanism for controlling the degradation process. This feature may be valuable in designing precise therapeutic applications with controlled dosages of AM-DY2 to effectively modulate RIPK1 levels in different disease contexts.

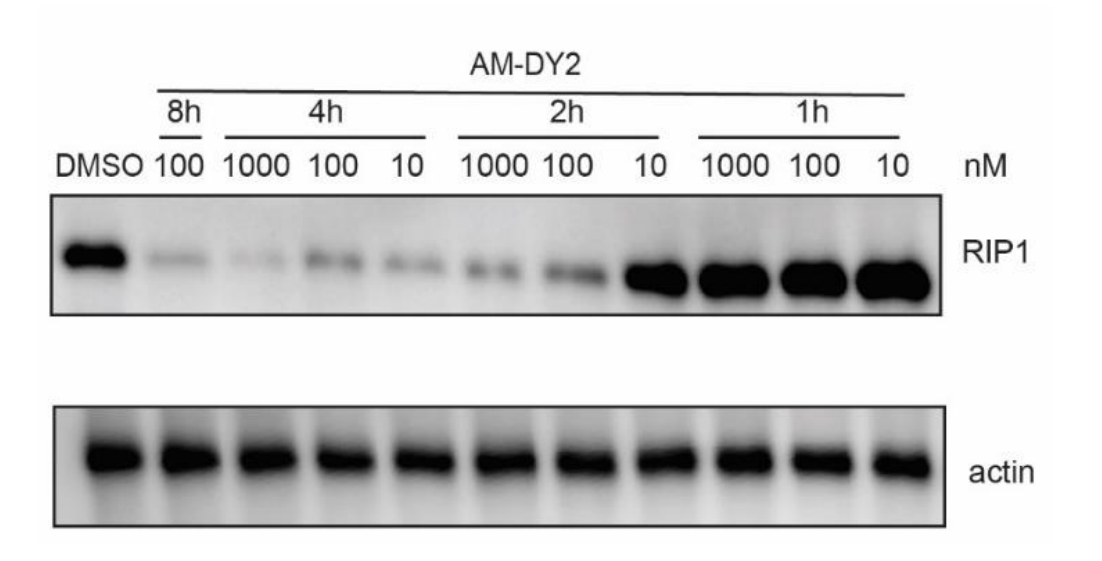


Figure 1.2.7 Time-course study of AM-DY2 in NOMO1 cells. NOMO-1 cells were treated with AM-DY2 with indicated concentration and time.

In a wash-off experiment designed to investigate the sustainability of AM-DY2's effects and the turnover rate of RIPK1, NOMO-1 cells were exposed to 100-nM AM-DY2 for a duration of 6 hours. After this incubation period, the media containing AM-DY2 was removed and replaced with normal RPMI media, thus withdrawing the AM-DY2 exposure. The cells were further incubated for up to 36 hours, after which we observed a partial recovery of RIPK1 expression levels, with a 20% recovery compared to the vehicle control (**Figure 1.2.8**).

These findings are indicative of two key insights. Firstly, even after the removal of AM-DY2, there is a lasting impact on the cellular level of RIPK1, suggesting a sustained intracellular presence of the compound or prolonged effect on RIPK1 degradation.

Secondly, the partial recovery of RIPK1 levels post wash-off implies that the turnover rate of RIPK1 is relatively slow. These observations collectively highlight the temporal dynamics of PROTAC-induced degradation and the potential of leveraging this feature for precise modulation of target protein levels in therapeutic settings.

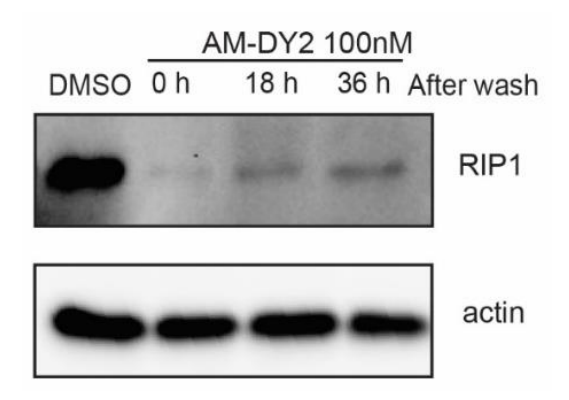


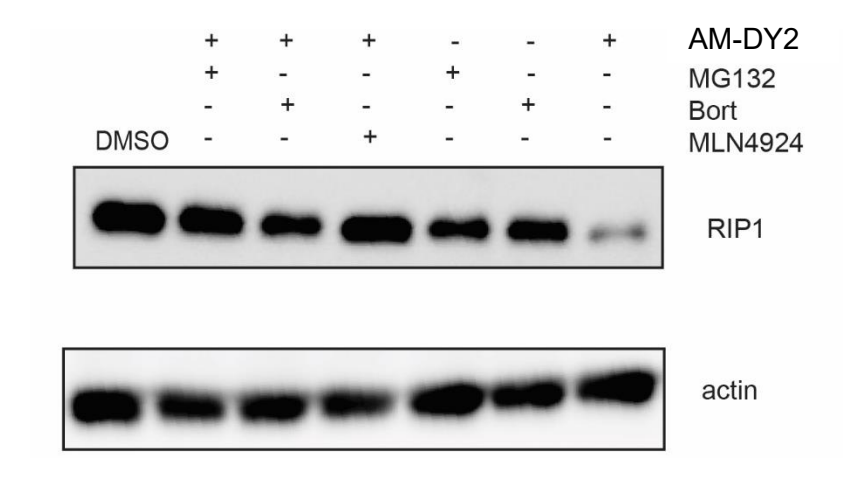
Figure 1.2.8. Wash-off study of AM-DY2. NOMO-1 cells were treated with AM-DY2 for 6 hours. Then the compound was removed and cells stayed in the fresh media for indicated hours.

PROTACs operate on a common mechanism of action that involves recruiting E3 ligase to the target protein, initiating the formation of a ternary complex, and finally, effecting proteasomal degradation of the target. To demonstrate that AM-DY2 adheres to this conventional PROTAC mechanism, we performed a series of experiments using competitive pathway inhibitors for various steps.

We observed that pre-treatment with either MG132 or Bortezomib, both of which are potent proteasome inhibitors, for one hour effectively blocked the degradation of RIPK1 induced by AM-DY2. Similarly, pre-treatment with MLN4924, an inhibitor of NEDD8-activating enzyme, which blocks the neddylation of Cullin, a crucial step in the ubiquitin-proteasome system (UPS), also nullified AM-DY2's activity. Furthermore, we found that free VHL ligand could inhibit RIPK1 degradation at relatively high concentrations (**Figure 1.2.9**).

These findings collectively substantiate that AM-DY2 operates through the typical PROTAC mechanism, facilitating the recruitment of E3 ligase and effecting proteasomal degradation to regulate the levels of RIPK1 protein.

A



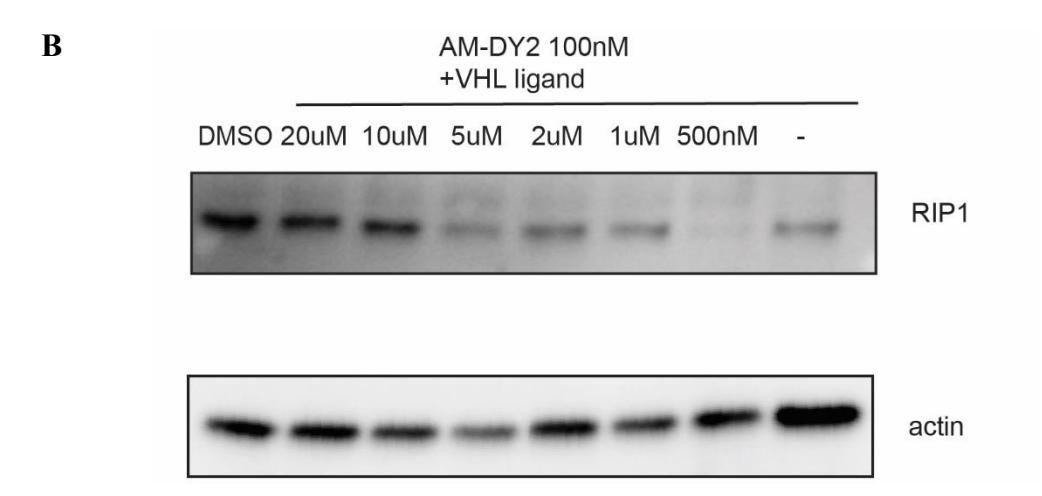


Figure 1.2.9. Mechanistic study of AM-DY2. A) One hour pretreatment of MG132, Bortizomib (Bort) or MLN4924, followed by 6-hour treatment of 100 nM AM-DY2. B) One hour pretreatment of VHL ligand, followed by 6-hour treatment of 100 nM AM-DY2.

Building upon our Rapid-TAC methodology, we have now succeeded in developing a novel PROTAC molecule that targets RIP1 kinase. This was achieved by bridging a VHL ligand to the RIP1 inhibitor GSK-067. Initial SAR explorations led to a potent degrader, DY-2, in the first stage. Subsequently, in the second stage, we synthesized one stable analogue, AM-DY2, and verified its biological activity.

Our degrader displayed the ability to selectively degrade RIP1 without affecting the levels of RIP2, indicative of its specificity. Mechanistically, AM-DY2 induced proteasomal degradation of RIP1, and the degradation effect began after only two hours of treatment with AM-DY2. This short reaction time, in comparison to that of siRNA, establishes our PROTAC as a powerful probe for studying the protein function of RIP1.

Interestingly, while catalytically inactive RIP1 inhibits necroptosis and promotes inflammation³⁵, a complete knockout of RIP1 proves lethal to mice as it renders necroptosis exclusively dependent on RIP3/MLKL, leading to systemic inflammation³⁶. In preclinical mouse models, the co-treatment of RIP1 inhibition and RIP3 gene deletion is often employed for specific diseases³⁷.

Our PROTAC molecule offers an alternative solution for temporarily knocking out RIP1, as the RIP1 level gradually recovers when the PROTAC is removed. The short onset time might not allow the cells sufficient time to compensate for the loss of function of RIP1, potentially opening new avenues for RIP1-related research and therapy.

We could also explore the application of our developed RIP1 degraders in immunotherapy. The immune modulatory effects of RIP1, particularly its role in

regulating innate immune responses, make it an attractive target for enhancing the efficiency of cancer immunotherapies. Utilizing our RIP1 degraders, we can mimic the genetic outcomes observed in RIP1 knockout models, which demonstrate significant sensitization to immunotherapies like anti-PD1 treatment. By exploring the synergies between RIP1 degradation and immune checkpoint blockade (ICB) therapies, we seek to augment the response rate of 'cold' tumors, turning them into 'hot', inflamed ones that are more susceptible to immune attack.

1.3 Second generation of Rapid-TAC platform for BRD4 degrader development

1.3.1 Introduction

Bromodomain-containing protein 4 (BRD4) has emerged as a significant target in the field of drug discovery due to its central role in various biological processes and disease pathways³⁸, particularly cancer³⁹. As a member of the BET (Bromodomain and Extra-Terminal motif) family of proteins, BRD4 acts as an epigenetic reader, binding to acetylated histones and thus regulating gene expression⁴⁰. This includes the expression of key oncogenes such as MYC, making BRD4 a crucial player in cell growth and proliferation⁴¹. The inhibition or degradation of BRD4 has been found to downregulate

these oncogenes, showing promise for potential therapeutic applications in various malignancies⁴². Consequently, the development of small molecules that can effectively degrade BRD4 is of paramount importance⁴³. Utilizing Proteolysis Targeting Chimeras (PROTACs) to achieve selective and efficient degradation of BRD4 has the potential to provide a powerful new therapeutic strategy for a range of cancer types, underscoring the relevance of our research on BRD4-targeted PROTACs.

As a means of illustrating the versatility of the ortho-phthalaldehyde (OPA) - amine coupling-based Rapid-TAC platform, we prepared a library of prospective PROTACs targeting BRD4. Our first step was to create a BRD4 ligand **6**, which contains an OPA. This was achieved through the linkage of BRD4 ligand **4**, derived from JQ1, with the bromide inclusive OPA precursor **5**, followed by a hydrolysis process.

Historically, the OPA building block included a carboxylate handle that was coupled with a ligand of the target containing an amine. In this instance, we employed an alternative strategy, utilizing a cross-coupling reaction between an aryl bromide and a ligand bearing a carboxylate derivative to prepare the vital building block 6. These OPA building blocks, 2 and 5, are well-suited for any POI ligands with an amine or carboxylate handle, respectively (Figure 1.3.1).

Figure 1.3.1 Synthesis of 21 BRD4 PROTACs using the Rapid-TAC platform.

Synthesis designed and done by Le Guo.

To validate our OPA-amine Rapid-TAC platform, we synthesized 21 potential BRD4 PROTACs (LG-BRD-1 to LG-BRD-21) swiftly in a DMSO solution under miniaturized conditions. Among these 21 products, the purity varied from 78% to 96% (**Figure 1.3.1**). The final products were then directly screened for their biological activity without any further manipulation, including purification.

1.3.2 Results and discussions

We then assessed the activity of the 21 potential BRD4 PROTACs in the MV-4-11 cell line. The results revealed no significant degradation for PROTACs LG-BRD-1 to LG-BRD-10, which were derived from pomalidomide. For PROTACs derived from VHL ligand, notably LG-BRD-12, which contains four methylene units in the linker, we observed a substantial reduction in the BRD4 protein at a concentration of 1 μ M, making it the most potent compound in this series. Interestingly, some PROTACs exhibited the classical "hook" effect at a concentration of 10 μ M (**Figure 1.3.2**).

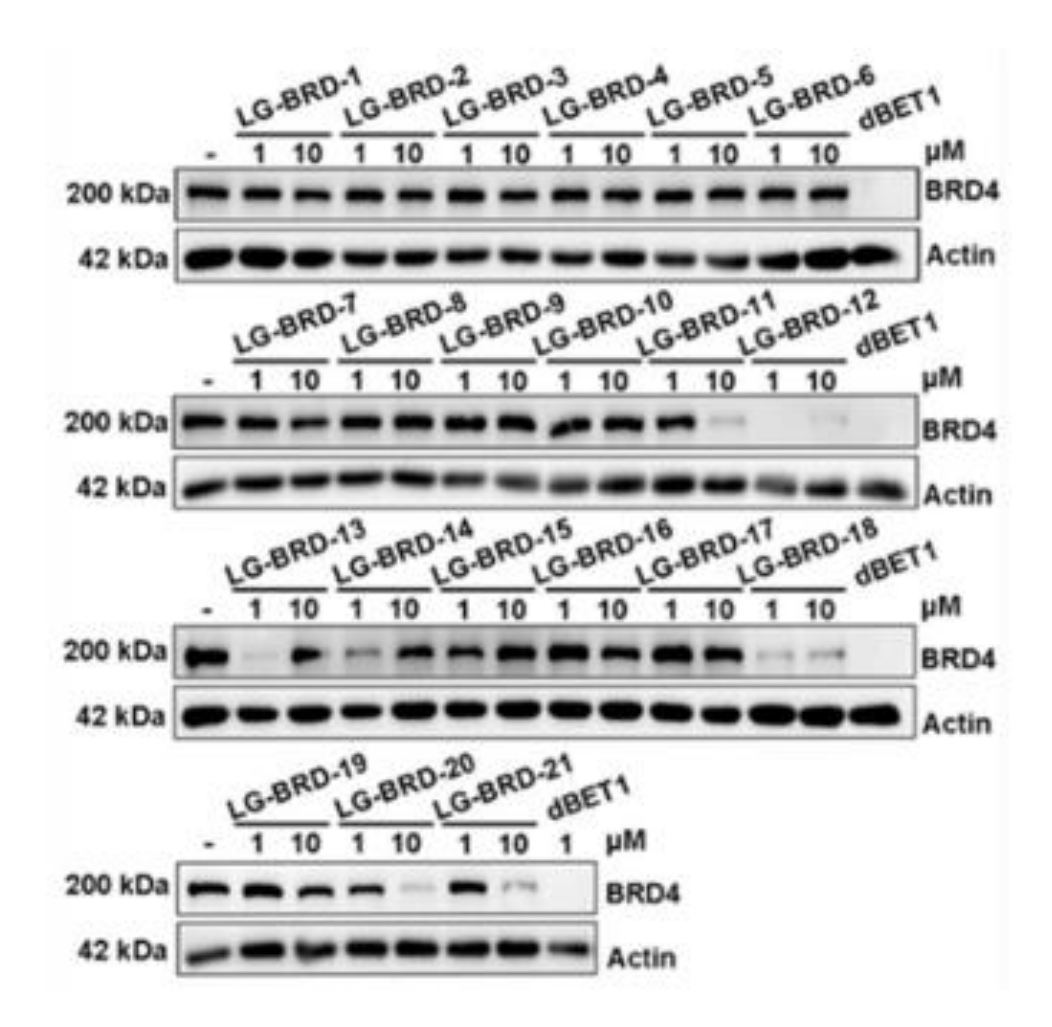
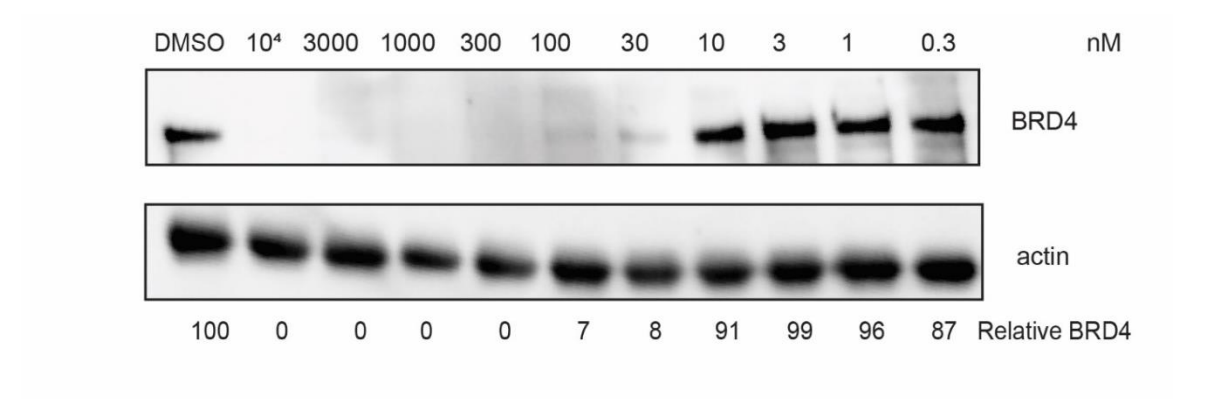


Figure 1.3.2. A library of 21 members of BRD4 PROTACs was tested by Western blot in MV-4-11 cell line for 24 h at 1 μ M and 10 μ M concentrations.

We performed a dose-response assessment of LG-BRD-12 in the MV-4-11 cell line. The results were quite promising; LG-BRD-12 achieved a DC₅₀ (the concentration at which 50% of the maximum response is observed) of just 4.9 nM (Figure 1.3.3). This demonstrates the high efficiency of our ortho-phthalaldehyde (OPA) based Rapid-TAC platform in generating potent BRD4 degraders, underscoring its potential for rapid PROTAC development and optimization.



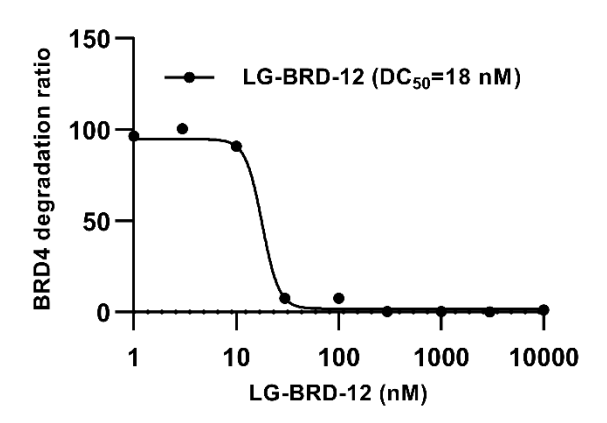


Figure 1.3.3 Dose response test for LG-BRD-12. MV-4-11 cells were treated with LG-BRD-12 for 12 hours under indicated concentrations. The numeric value of relative BRD4 levels were based on DMSO/vehicle. The dose response curve was generated from band intensity in western blot result.

The OPA-amine coupling chemistry provides a mixture of two isomers. Building upon the initial success with LG-BRD-12, we proceeded to synthesize two isomers of the BRD4 degrader, designated as LG-BRD-12A and LG-BRD-12B, where the carbonyl group is meta or para to the R2 substituent. Utilizing established chemistry and purification procedures, we compared their activities directly (**Figure 1.3.4**). We subjected cells treated with these BRD4 PROTACs for Western blot assays to evaluate

their degradation efficiency on BRD4. The findings revealed that LG-BRD-12B possessed superior degradation activity compared to LG-BRD-12A (**Figure 1.3.4**). A subsequent dose-response study conducted on LG-BRD-12B in the MV-4-11 cell line revealed a DC₅₀ of 8.9 nM (**Figure 1.3.4**). This body of evidence clearly illustrates the efficacy of our OPA-amine coupling reaction-driven Rapid-TAC platform in rapidly identifying potent BRD4 degraders.

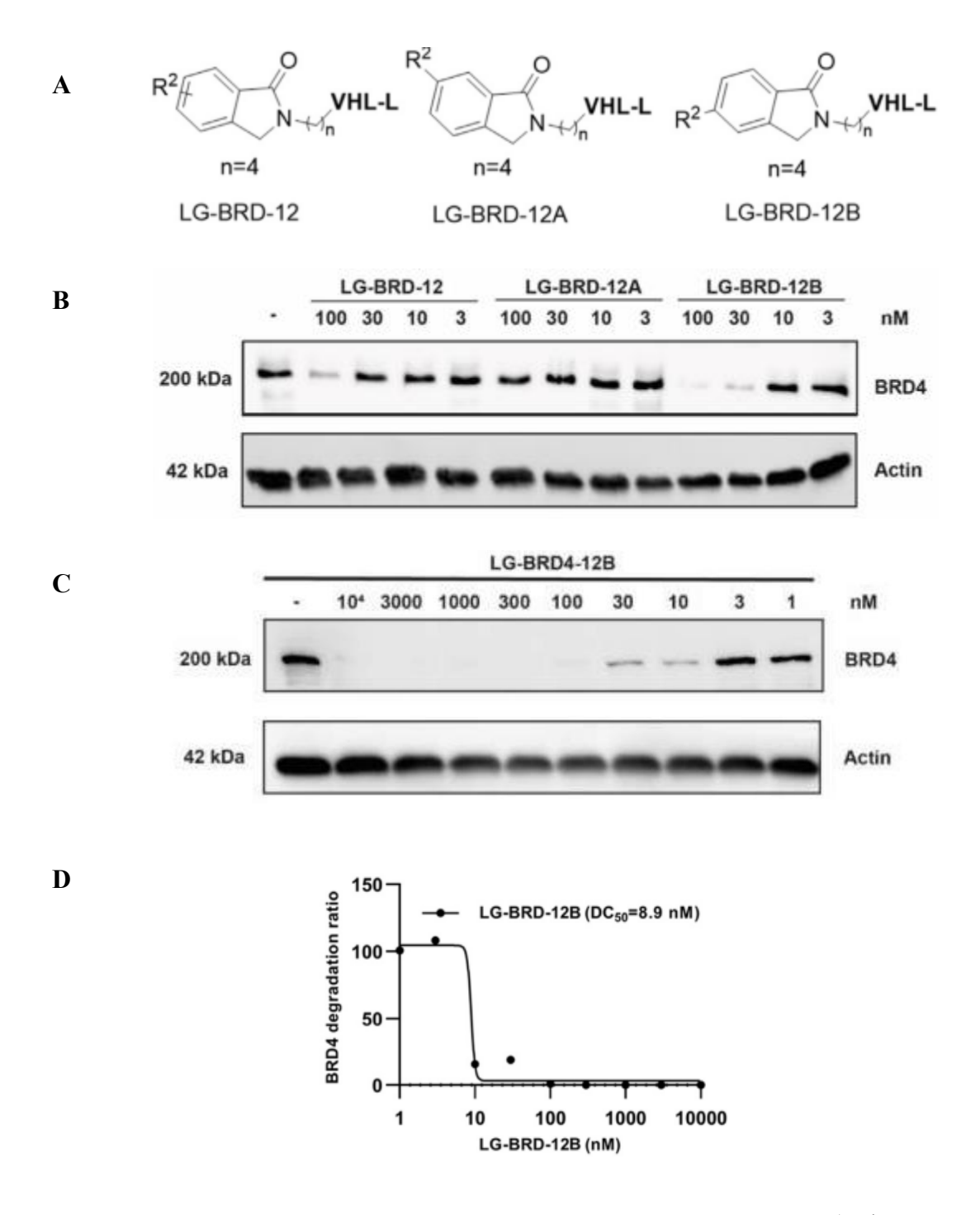


Figure 1.3.4 The western blot analysis of LG-BRD-12 enantiomers. A) The structures of two BRD4 PROTACs based on LG-BRD-12. B) BRD4 PROTACs were tested by Western blot in MV-4-11 cell line for 12 h at 100 nM, 30 nM, 10 nM and 3 nM concentrations. C) Dose response of LG-BRD-12B. MV-4-11 cells were treated with LG-

BRD-12B for 12 h at different concentrations and the results were analyzed by Western blot. D) Dose response curve of LG-BRD-12B generated from band intensity analysis in Western blot result.

In conclusion, we have successfully established a novel platform for the expedient synthesis of Proteolysis-Targeting Chimeras (PROTACs) under miniaturized conditions. This platform leverages the high efficiency of the ortho-phthalaldehyde (OPA)-amine coupling reaction, which exclusively yields water as the byproduct. Utilizing readily accessible E3 ligase ligand-linker-NH₂ building blocks, this new generation Rapid-TAC platform is capable of swiftly generating a library of stable PROTACs, featuring a range of linker lengths/types and E3 ligase ligands.

The resulting products possess adequate purity for direct utilization in cell-based screenings without any further adjustments. The OPA-amine coupling chemistry of the platform is compatible with most common functional groups, further boosting its versatility. This platform's efficiency and efficacy have been successfully validated by the swift development of active PROTACs for the Bromodomain-containing protein 4 (BRD4). In another study, its utility for the development of androgen receptor (AR) PROTACs was demonstrated by other group members. Interestingly, the two isomeric AR PROTACs derived from the active hit (e.g. the newly formed carbonyl group is meta- or para to the linker) behaved very similarly in degrading AR.

We anticipate that this innovative Rapid-TAC platform can serve as a versatile tool for the development of PROTACs against a wide range of other targets. This platform has the potential to significantly reduce the barriers to accessing PROTAC technology, a transformative methodology in the field of small molecule drug discovery. Furthermore, it can facilitate structure-activity relationship studies of PROTACs against various targets, further accelerating advancements in this exciting realm of research.

1.4. A Platform for the Rapid Synthesis of Molecular Glues(Rapid-Glue) under Miniaturized Conditions for Direct BiologicalScreening.

1.4.1 Introduction

Immunomodulatory drugs (IMiDs) as represented by thalidomide are among the earliest examples of serendipitously discovered molecular glues^{44,45}. They operate as ligands for cereblon (CRBN), the substrate receptor of the E3 ubiquitin ligase complex CUL4 (cullin 4)-RBX1-DDB1-CRBN (CRL4^{CRBN}) and instigate binding to neo-substrate proteins^{46–49}. Up to this point, a range of neo-substrates has been identified that can be targeted for degradation by the IMiDs-CRBN complex, including IKZF1^{50–52}, IKZF3^{50–52}, CK1α⁵³, GSPT1^{54–56}, ZFP91^{57,58}, ZNF98²², and more. Recent work has yielded several crystal structures^{51,54} of the ternary complex formed by thalidomide-like molecular glues, CRBN, and target proteins, revealing intriguing protein-protein interactions. Despite these advances, the rational design of molecular glues for a specific protein of interest (POI) remains challenging⁵⁹.

High-throughput screening (HTS) of compound libraries in phenotypic assays is one of the most viable and effective approaches for discovering molecular glues and their neosubstrates^{47,60,61}. Yet, traditional methods for generating molecular glue compound

libraries can be time-consuming and resource intensive. In light of this, several Rapid-TAC (rapid syntheses of PROTACs) platforms have recently been reported ^{14,62,63}. These platforms utilize efficient chemical coupling methods under miniaturized conditions and bypass the need for any chromatography purification. Our group has previously developed two such Rapid-TAC platforms. The first platform involves the coupling of a hydrazide-containing POI ligand with an aldehyde-containing E3 ligase ligand ¹⁴ and the second platform exploits the reaction between an ortho-phthalaldehyde (OPA)-containing POI ligand and an E3 ligase ligand containing a primary amine ⁶⁴. Both platforms can be conducted under miniaturized conditions and generate libraries directly usable for screening in biological assays. In 2022, Wolkenberg and coworkers reported a three-step approach using diamine building blocks to generate PROTAC libraries, which requires the use of solid phase reagents in each step for purification ⁶³.

Building on our previous Rapid-TAC platforms, we now report a new platform for the rapid synthesis of molecular glues (Rapid-Glue) (Figure 1.4.1). Unlike our previous platform, which attaches the hydrazide to the POI ligand, Rapid-Glue attaches the hydrazide motif to different positions of the E3 ligase ligand. These functionalized E3 ligase ligands then react with several hundred diverse commercially available aldehydes to form potential molecular glue products. These reactions are conducted in 96-well plates under miniaturized conditions in DMSO and can be used directly for cell-based screening due to the high-yield nature of the coupling reaction and the compatibility of the two reacting partners with diverse functional groups. Using this platform, we quickly prepared a pilot library of 1,520 compounds, including molecular glues and their corresponding negative controls, spread over sixteen 96-well plates, starting from two

CRBN ligands, two negative controls, and four 96-well plates of commercially available aryl aldehydes with diverse structures.



Figure 1.4.1 The strategy for Rapid-Glue platform. We used hydrazide-aldehyde coupling chemistry for the development of molecular glues. Synthesis was designed and done by Jingyao Li

The Rapid-Glue platform was designed based on the CRBN-recruiting molecular glues. Two hydrazide building blocks with a phenyl group attached to either the 4- or 5-position of the isoindolin-1-one were designed to create two libraries (Lib-A and Lib-B). The hydrazide was placed in different positions in each library to create compounds with distinct chemical spaces. Negative control libraries (Lib-C and Lib-D) were also generated to validate the phenotypic screening results (**Figure 1.4.2**). The addition of a small methyl substituent to the imide NH group can completely block its interaction with CRBN.⁶⁵ These four building blocks were reacted with 380 commercially available aromatic aldehydes under miniaturized conditions, generating 1,520 compounds ready for screening.

Figure 1.4.2 Design of Rapid-Glue libraries. Designed by Jingyao Li

1.4.2 Results and discussions

Our team initiated a comprehensive screening process to test the anti-proliferative effects of the compounds libraries on two cancer cell lines, RS4;11 (a leukemia cell line) and Molt4 (a lymphoma cell line). This screen was performed at a standard concentration of 1 µM. Initial screenings at a 1 µM concentration revealed that most of the compounds in Library A (Lib-A) exhibited negligible anti-proliferative activity. Nonetheless, two compounds, Lib-A-6J and Lib-A-18B, stood out with moderate anti-proliferative activity in both cell lines, as indicated by less than 80% cell viability. Notably, both compounds had a similar hydrophobic moiety, a trifluoro- and dichloro- substituted phenyl ring (Table 1.4.1).

In contrast, Library B (Lib-B) yielded more promising results, with 12 compounds demonstrating notable anti-proliferative activity in both cell lines. Further screenings of these hits from Lib-B at lower concentrations (0.5 μ M and 0.1 μ M) identified four compounds that retained anti-proliferative properties even at the lowest concentration. Interestingly, all four active compounds from Lib-B were derived from aldehyde building

blocks with heterocyclic motifs, including imidazopyridine, indole, indazole, and a thiazole ring with a piperazine substituent. This difference in results between the two libraries offers valuable insights for the future design and synthesis of molecular glues with potent anti-proliferative activities.

Table 1.4.1 Structures of compounds hit with anti-proliferation screening in Lib-A and Lib-B. Screening and analysis were done by Dr. Chunrong Li.

R ₂ N N Lib-A, R ₁ = Lib-C, R ₁ =	O N-N-O N-R ₁		Lib-C-6J	F CI Lib-A-18B Lib-C-18B
$\begin{array}{c} & & & & \\ & & & \\ & & & \\ & & & \\ & & & \\ & & & \\ & &$		R ₂ = SNNNNNNNNNNNNNNNNNNNNNNNNNNNNNNNNNNNN		Lib-B-12L Lib-D-12L
		C	N = 0	N N N N N N N N N N N N N N N N N N N
			3-15O (15O) 15O (15O-Me)	Lib-B-18J (18J) Lib-D-18J (18J-Me)
C1-		RS4;11		MOLT4
Compounds	1μM	0.5μΜ	0.1μΜ	1μΜ
Lib-A-6J	54ª	-	-	67
Lib-A-18B	47	-	-	74
Lib-C-6J	>100	-	-	>100
Lib-C-18B	>100	-	-	>100
Lib-B-5D	24	23	56	66
Lib-B-12L	25	15	46	52
Lib-B-150	15	5	52	43
				7
Lib-B-18J	11	6	86	7
Lib-B-18J Lib-D-5D	11 96	6 -	86 -	>100
		6 - -	86 - -	
Lib-D-5D	96	6 - -	86 - -	>100

^a cell viability(%) treated with RS4;11 or MOLT4 cells for 72h

To confirm that the anti-proliferative activities of the identified hit compounds were associated with cereblon (CRBN), we subjected the four hit compounds from Library B (Lib-B) and their corresponding negative controls from Library D (Lib-D) to anti-proliferative assays in three different cell lines. It was found that the compounds from Lib-B had significantly better inhibitory effects compared to their corresponding Lib-D compounds, suggesting that the anti-proliferative activity of these lenalidomide analogs is likely tied to their interaction with CRBN.

Furthermore, a comparison of the inhibitory effects showed that compounds **15O** and **18J**, both of which possess aromatic substitutions on the nitrogen of the indole or indazole rings, were more potent than Lib-B-5D and Lib-B-12L in all tested cell lines. This observation implies that the phenyl ring, which may facilitate hydrophobic interactions with pockets on the protein surface, contributed to their increased activity (**Table 1.4.2**). This data provides valuable insights that can guide the future design of more effective molecular glues that recruit CRBN.

Compounds	IC ₅₀ (μM) in RS4;11	IC ₅₀ (μM) in MOLT4	IC_{50} (μM) in MM1S
Lib-B-5D	0.071	>1	>10
Lib-B-12L	0.007	>10	>10
Lib-B-150	0.008	0.175	0.131
Lib-B-18J	0.002	0.26	0.37
Lib-D-5D	>1	>10	>10
Lib-D-12L	>10	>10	>10
Lib-D-150	>1	>1	>10
Lib-D-18J	>1	>1	>1

Table 1.4.2 Anti-proliferation results of hit compounds in 3 different cell lines.

Screening and analysis were done by Dr. Chunrong Li.

After observing significant anti-proliferation activity in three distinct cancer cell lines, including leukemia (RS4;11), multiple myeloma (MM.1S), and lymphoma (Molt4), we suspected that G1 to S phase transition 1 (GSPT1) could be a potential target. This hypothesis was based on published literature^{54,66} and our previous research experience.⁶⁷ To investigate this hypothesis, we used the two most potent compounds, 15O and 18J, and analyzed their impact on GSPT1 levels using Western blotting.

Both **15O** and **18J** induced nearly complete degradation of GSPT1 in RS4;11 cells at 1 μM after 4 hours of treatment, and at 0.1 μM after 24 hours. As anticipated, the corresponding methylated compounds, **15O-Me** and **18J-Me**, which lack CRBN binding affinity, showed no obvious GSPT1 degradation, suggesting that interaction with CRBN is crucial for GSPT1 degradation triggered by these molecular glues (**Figure 1.4.3**).

Further analysis was conducted with dose response at 12 hours treatment, and time course with 1 μ M of **15O** and **18J** in RS4;11 cells. This showed that both compounds reduced GSPT1 protein levels effectively in both dose- and time-dependent manners. Interestingly, compound **18J** showed superior degradation efficiency compared to **15O**, both in terms of potency and degradation kinetics (**Figure 1.4.3**). These results provide

robust evidence that these molecular glues can be targeted towards the degradation of GSPT1 through interaction with CRBN.

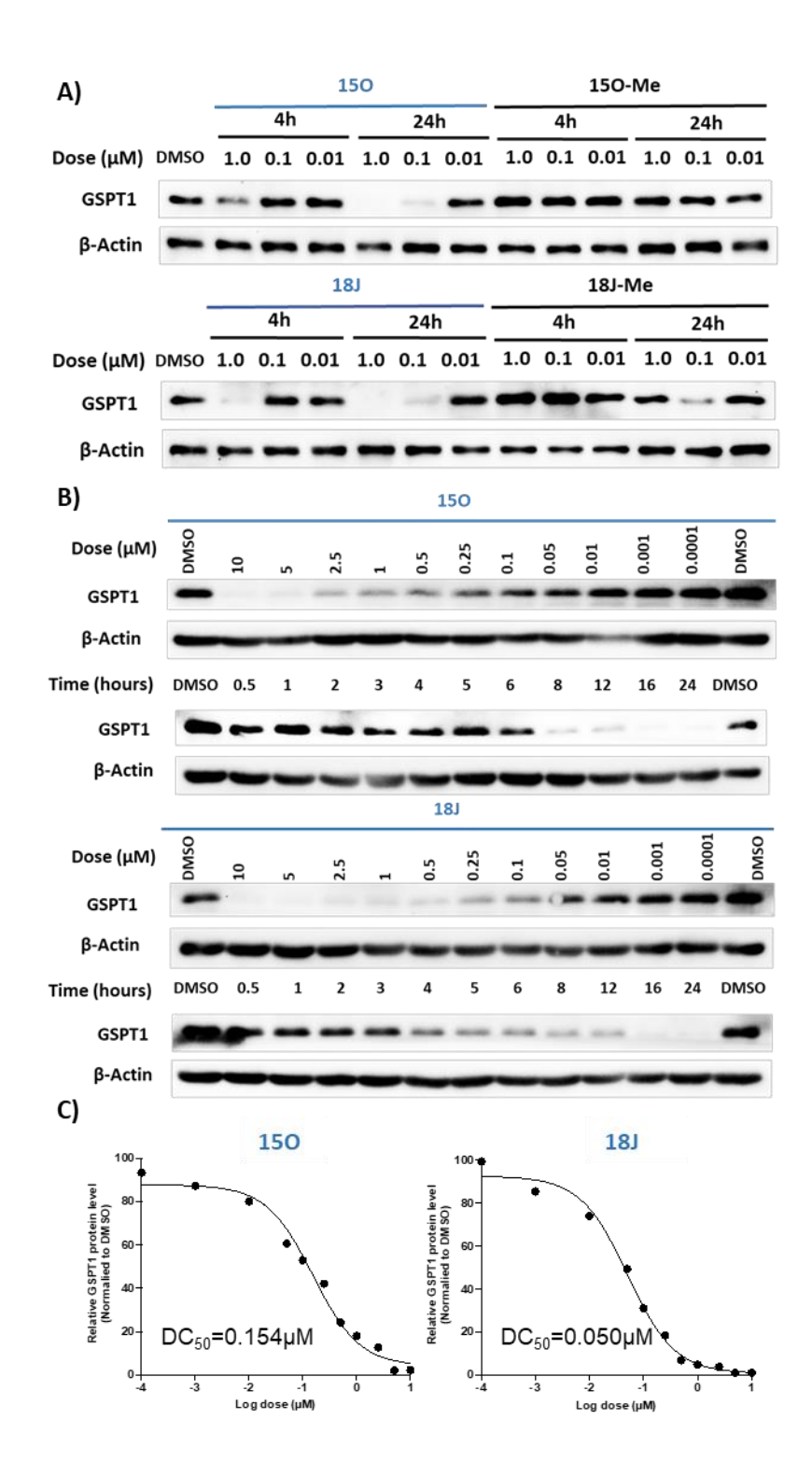


Figure 1.4.3 Potent GSPT1 degraders and their corresponding negative-control were tested by Western blot in RS4;11 cells. A) Western blot analysis of 15O, 18J, 15O-Me, 18J-Me at 1.0 μM, 0.1 μM, 0.01 μM for 4 h and 24 h in RS4;11 cells. B) Dose

response (for 12 h) and time course (at 1 μM) of GSPT1 degraders 15O and 18J. C)
Relative GSPT1 protein level at different concentrations of 15O and 18J in RS4;11 cells.
Screening and analysis were done by Dr. Chunrong Li.

To assess the selectivity of our hit compounds, **15O** and **18J**, we conducted an in-depth, quantitative proteomic analysis using tandem mass tag mass spectrometry (TMT-MS). The instruments were run by Dr. Zhiping Wu in Dr. Junming Peng's Lab of St Jude Children's Hospital. We identified and analyzed 9,520 unique proteins, corresponding to 8,126 genes, thus covering a substantial portion of proteome in a given cell line. Western blot analysis confirmed that both **15O** and **18J** significantly reduced GSPT1 levels in RS4;11 cells within a 6-hour treatment window.

Our proteomic analysis identified 5 differentially expressed (DE) proteins and 2 upregulated proteins with **15O** treatment, as well as 5 DE proteins with **18J** treatment in RS4;11 cells (p <0.05, Log2>1) (**Figure 1.4.4**). Importantly, we observed significant GSPT1 downregulation in RS4;11 cells treated with both compounds, **15O** and **18J**. Given these findings, we can categorize **15O** and **18J** as highly selective GSPT1 degraders, providing a strong basis for further investigation into their potential as targeted anti-cancer therapies.

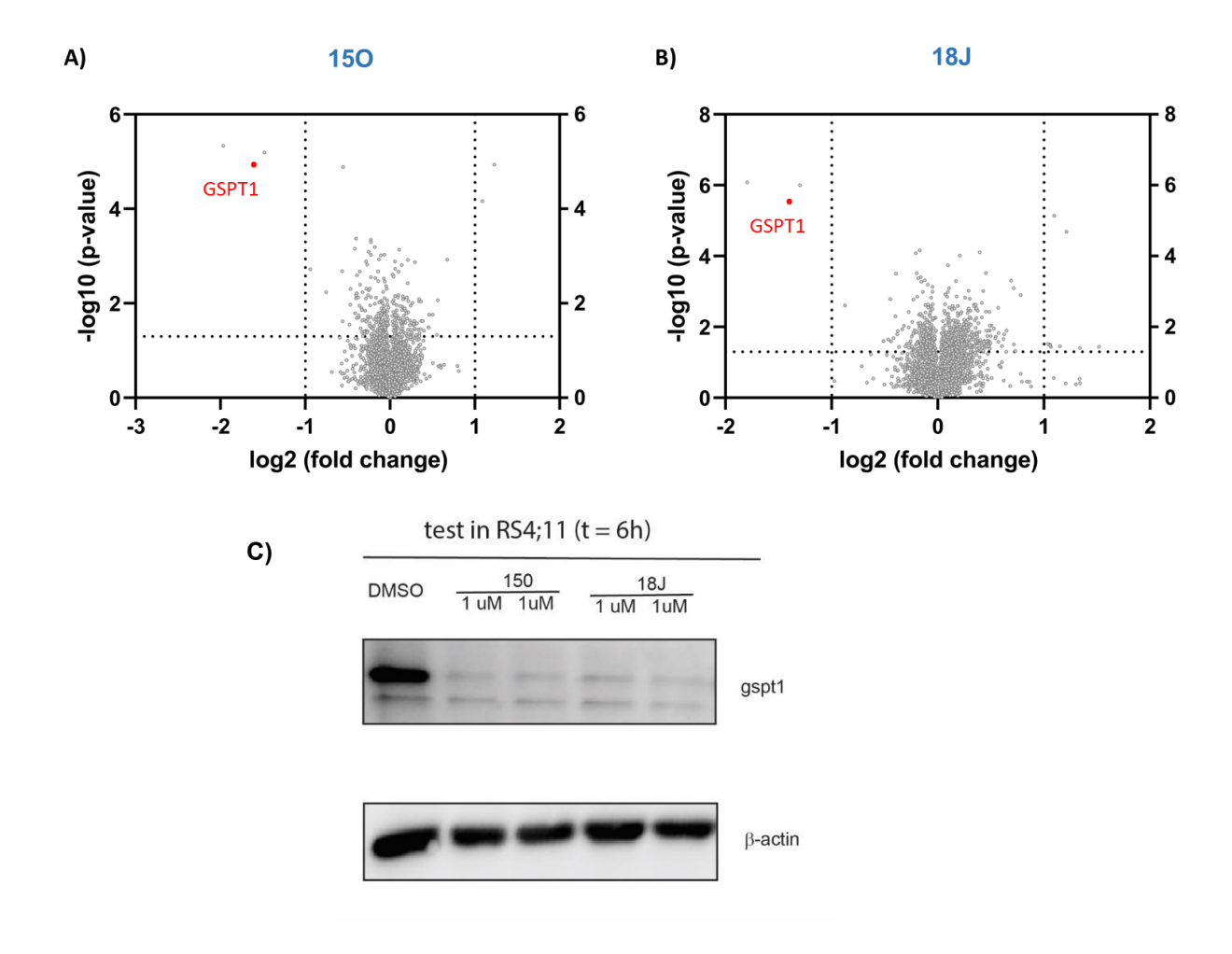


Figure 1.4.4 Proteomics analysis of 15O and 18J. A) and B). Profiling proteomic changes in RS4;11 cells after treatment with 15O and 18J at 1μM for 6h using mass spectrometry. C) Western blot analysis for confirmation of GSPT1 degradation effect induced by 15O and 18J.

The acylhydrazone linker in our lead compounds, **15O** and **18J**, was recognized as a potential point of instability due to its susceptibility to hydrolysis under acidic conditions, forming the corresponding hydrazide and aldehyde. While we initially chose aryl aldehydes to mitigate this concern due to the higher stability of the resulting

acylhydrazone, we acknowledged that the acylhydrazone motif would not be appropriate for further therapeutic development.

To address this concern, we designed three more drug-like analogues (S1-S3), where we replaced the acylhydrazone motif with a bioisosteric amide group (Figure 1.4.5). This change is aimed to maintain the overall length of the linker and property of the original molecular glues 15O and 18J. Western blot analysis revealed that all three compounds were capable of degrading GSPT1.

The potency of S1 and S2 were found to be comparable to the original hit 15O in RS4;11 cells (Figure 1.4.5). Although the potency of compound S3 was less than the original hit 18J, it still holds promise as a viable starting point for further optimization. The fact that the biological activity of all three compounds was retained indicates that the change of the linker from acylhydrazone to stable amide is viable, despite the observed decrease in activity in one case.

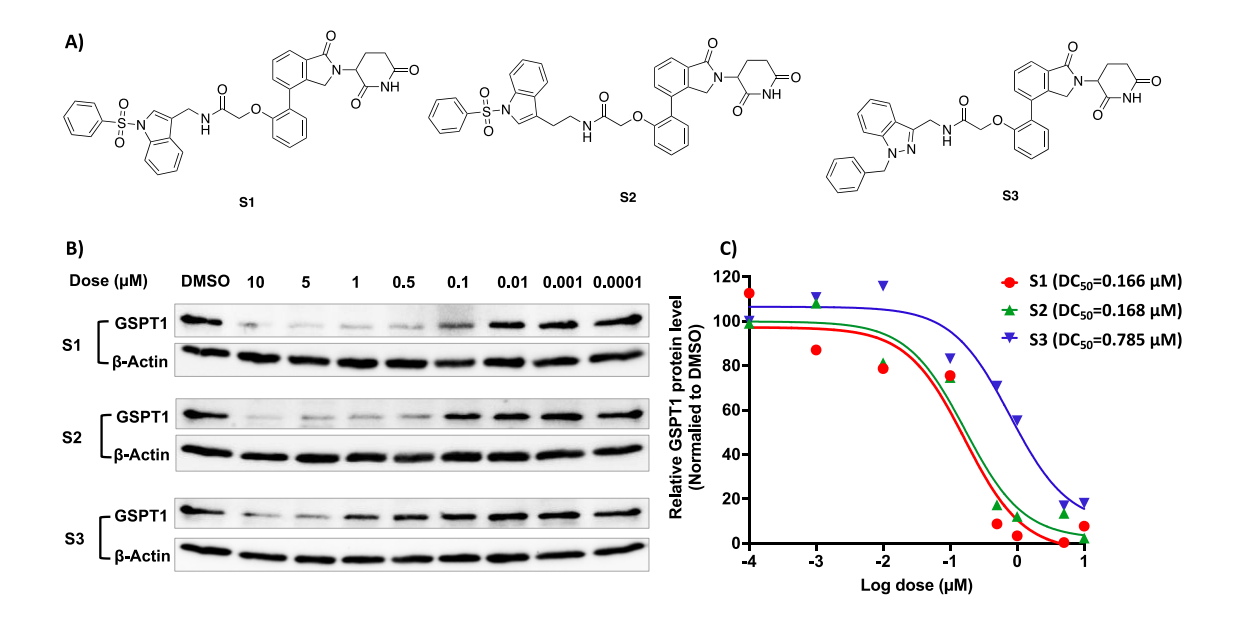


Figure 1.4.5 GSPT1 degraders with stable amide linkers were tested in RS4;11 cells. A) Structures of GSPT1 degraders. **B)** RS4;11 cells were treated with S1, S2 or S3 for 12 hours and GSPT1 level was assessed by western blots. **C)** Dose response curve generated from Western blot result **B).** Screening and analysis were done by Dr. Chunrong Li.

The Rapid-Glue platform involves rapid synthesis of acylhydrazone-containing products from hydrazides and aldehydes, high throughput phenotypic screening, proteomic profiling of the resulting hits, and replacement of the acylhydrazone motif by its bio isostere. It represents a powerful methodology for the development of molecular glues. The platform's unique ability to quickly generate a sizable library of compounds through acylhydrazone formation chemistry facilitates a broad exploration of CRBN modulators. It is important to note the negative controls included in the screening process, enabling swift identification of CRBN modulators linked to desired phenotypes.

This platform proved successful, with two potent CRBN modulators identified via antiproliferative screening and confirmed as GSPT1 degraders through immunoblotting
assays. Proteomic studies further verified the high selectivity of these GSPT1 degraders,
and molecular modeling offered insights into potential binding poses. To address the
potential instability issue, more drug-like analogues were prepared by replacing the
acylhydrazone motif with a stable amide, all of which maintained GSPT1 degradation
activity. This success underscores the platform's effectiveness and feasibility for drug
discovery.

1.5 Conclusions and future perspectives.

In conclusion, the RAPID-TAC and RAPID-GLUE platforms represent innovative approaches to drug discovery. They demonstrate the potential to revolutionize the process of developing targeted therapeutics, particularly in the realm of proteolysis targeting chimera (PROTAC) and molecular glue-based drugs. By employing robust chemistry, these platforms accelerate the synthesis of diverse libraries of potential therapeutics, aiding in the identification of novel, potent, and selective binders and degraders of disease-related proteins, such as RIPK1, BRD4 and GSPT1.

The RAPID-TAC platform facilitates the exploration of different E3 ligases, binding sites, linkers, and ligands, leading to the generation of unique PROTACs. In contrast, the RAPID-GLUE platform enables the development of molecular glues that can modulate protein-protein interactions. This platform has already shown promise, with the identification of potent CRBN modulators and the confirmation of their high selectivity for GSPT1.

Looking ahead, the potential of both platforms to drive drug discovery is vast. The future of RAPID-TAC and RAPID-GLUE platforms will likely see expansion and refinement. For RAPID-TAC, a broader range of E3 ligase ligands could be explored, allowing the investigation of a wider variety of potential therapeutic targets.

Similarly, for the RAPID-GLUE platform, extending the size of the pilot library and diversifying the types of assays for CRBN could lead to the discovery of novel neosubstrates. Moreover, the platform could be adapted for other E3 ligases with the inclusion of appropriately functionalized ligands.

Moreover, the RAPID-GLUE platform's potential to adapt acylhydrazone to stable amides will play a crucial role in enhancing the platform's future development. This adaptation maintains the degradation activity for GSPT1, offering the potential for hit optimization and drug development.

Overall, both the RAPID-TAC and RAPID-GLUE platforms promise to greatly advance the field of drug discovery and development, providing targeted, efficient, and potentially game-changing therapeutic options for various diseases.

1.6 Experimental Procedures.

1.6.1 Procedures for RIPK1 degrader development

Chemical Reagents for Biological Experiments and Antibodies

MG132 (S2619) was purchased from Selleckchem. Antibodies against RIP1, RIP2 and anti-mouse and antirabbit horseradish peroxidase (HRP)-linked antibodies were purchased from Cell Signaling Technology (CST). Antibody against α -tubulin was purchased from R&D system. HRP-linked β -Actin antibody was purchased from Santa Cruz Biotechnology.

Cell Culture.

Cell lines were obtained from American Type Culture Collection. Nomo-1 and cells were cultured in RPMI1640 media (Corning) supplemented with 10% FBS, 1% PS, 1% sodium pyruvate, and 1% N-(2-hydroxyethyl) piperazine-N'-ethanesulfonic acid (HEPES) buffer. Cell lines were grown at 37 °C in a humidified 5% CO₂ atmosphere. THP-1 cells were cultured in RPMI 1640 media supplemented with 10% FBS, 1% PS, 1% sodium pyruvate, 1% N-(2-hydroxyethyl) piperazine-N'-ethanesulfonic acid (HEPES) buffer and 0.1% 2-Mercaptoethanol (BME). MOVAS cells were cultured in Dulbecco's modified Eagle's (DMEM) medium (Corning, 4.5 g/L glucose) supplemented with 10% fetal bovine serum (FBS) and 1% penicillin–streptomycin (PS).

Western blotting.

Cells were plated at 5x10⁵ cells/well into 12-well plates using indicated media. After overnight seeding, cells were treated with indicated compounds or vehicle. After the treatment, cells were collected into 1.5 mL pipet and washed with PBS twice. Cells were

lysed with 1X RIPA lysis buffer [25 mM Tris, pH 7–8, 150 mM NaCl, 0.1% (w/v) sodium dodecyl sulfate (SDS), 0.5% sodium deoxycholate, 1% (v/v) Triton X-100, protease inhibitor cocktail (Roche, one tablet per 10 mL) and 1 mM phenylmethylsulfonyl fluoride] on ice for 10 min. Supernatant was collected after spinning down at 16 000g at 4 °C for 15 min. About 50 µg of the total protein was mixed with the 4X Laemmli Loading Dye and heated at 95–100 °C for 5 min. The heated sample was then subjected to 7.5% SDS-polyacrylamide gel electrophoresis and transferred to PVDF membrane (Bio-Rad). The membrane was blocked in 5% (w/v) nonfat milk (Bio-Rad) in the TBS-T washing buffer (137 mM NaCl, 20 mM Tris, 0.1% (v/v) Tween) and then incubated with primary antibodies at 4 °C overnight. The membrane was washed with TBS-T, incubated with secondary HRP-linked antibodies for 1 h, then washed with TBS. The Clarity ECL substrate (Bio-Rad) was incubated with the membrane for 5 min. The immunoblot was generated by ChemiDoc MP Imaging Systems (Bio-Rad) and analyzed by the Image Lab 6.0.1 software (Bio-Rad). All curves were generated with Graphpad Prisim 7.0 using a 4-parameter non-linear fit.

Mechanistic Studies

Cells were seeded 5×10^5 cells/well into a 12-well plate using RPMI 1640 supplemented with 1% stripped-FBS. After overnight seeding, the cells were pretreated with the indicated amounts of pathway blockers for 1 h. After 1 h, the indicated amount of AM-DY2 was added for 6 h and then analyzed by Western blotting.

1.6.2 Procedures for BRD4 degraders development

Cell lines and materials MV-4-11 cells were cultured in Iscove's Modified Dulbecco's Media (IMDM) supplemented with 10% FBS and 1% penicillin/streptomycin under 5% CO2 at 37 °C. b-Actin (C4) HRP (sc-47778) antibody was obtained from Santa Cruz Biotechnologies. Anti-Brd4 antibody (ab128874) was obtained from Abcam.

Western Blotting Cells were lysed in 1X RIPA lysis buffer containing 25 mM Tris, pH 7e8, 150 mM NaCl, 0.1% (w/v) sodium dodecyl sulfate (SDS), 0.5% sodium deoxycholate, 1% (v/v) Triton X-100, Roche protease inhibitor cocktail and 1 mM phenylmethylsulfonyl fluoride. Protein samples were adjusted to the equal amount after determining the concentrations by BCA assay and then loaded onto 7.5% SDS polyacrylamide gel electrophoresis. After transferring, the membrane was first blocked in 5% (w/v) nonfat milk in the TBS-T washing buffer (137 mM NaCl, 20 mM Tris, 0.1% (v/v) Tween) and then incubated with primary antibodies at 4 C overnight. Next day, the membrane was incubated with secondary HRP-linked antibodies for 1 h followed by acquisition of the immunoblot using ChemiDoc MP Imaging Systems.

1.6.3 Procedures for GSPT1 degraders development

Cell Culture

Cells (RS4;11, Molt4 and MMS1) were cultured in RPMI1640 medium supplemented with 10% FBS and 1% Penicillin/Streptomycin at 37°C in a humidified 5% CO₂ atmosphere.

Cell viability Assay (Alamar Blue)

Alamar Blue stock reagent (10X) was prepared by dissolving high purity resazurin in DPBS (pH 7.4) to 0.3 mg/mL. For the high-throughput screening, the tested compounds were loaded to a 384-well compound plate (10mM in DMSO, 30μL/well), and transferred 5nl to a 384-well cell culture plate with cells (50μL/well, 5000 cells/well) using ECHO acoustic liquid handler. Then the final concentration of compounds in 50μl media was 1μM. For the cell viability test using a 96-well plate, cells in 100μL medium were seeded in each well with serial diluted dosed of compounds. After incubating in the CO₂ incubator for 3 days. 5-10μL alamar blue was added to each well of the cell culture plates using the MicroFlo reagent dispense. The plates were incubated at 37°C for an additional 1-4 hours. The fluorescence was measured using a 560 nm excitation / 590 nm emission filter set in a plate reader. Relative cell viabilities in each well were calculated by normalizing the read value to the value of DMSO-treated wells. Growth curves were generated by plotting relative fluorescence units vs. compound concentration and graphed using GraphPad Prism software.

Immunoblot

Cells were seeded in 12 or 24-well plates and treated with compounds or DMSO.

At the designed time points, cells were collected and lysed in RIPA lysis buffer. The protein concentration was determined by Pierce BCA protein assay. Equivalent amounts of protein were separated in SDS-PAGE gels and transferred to PVDF membranes.

Membranes were blocked in 5% BSA in TBS buffer and then incubated with the appropriate primary antibodies diluted in 5% BSA in TBS with 0.1% Tween 20 (TBS-T). After being washed, the membranes were incubated with the appropriate horseradish peroxidase-conjugated secondary antibodies (Pierce, Waltham, MA) in 2.5% BSA-TBS-

T for 1 h at room temperature and then washed again. Bound antibodies were visualized by using a chemiluminescent reagent (Pierce) according to the manufacturer's instructions and imaged using ChemiDocTMMP Imaging Systems (Bio-rad). GSPT1 primary antibody and HRP-conjugated secondary antibody were purchased from Cell Singling Technology Inc. β-Actin-HRP was purchased from Santa Cruz Biotechnology Inc.

TMT mass spectrometry

The analysis was based on our optimized protocol for large-scale proteomics^{68,69}. About 6 million RS4;11 and Molt4 cells were plated in 10 cm dishes. Cells were treated with compound **15O** or **18J** at 1 μM for 6 hours. Control groups were treated with the same amount of DMSO. Three biological replicates were performed. After the treatment, cells were collected and washed with cold PBS buffer twice. Cells were lysed in lysis buffer containing 50 mM HEPES (pH 8.5), fresh 8 M urea, 0.5% sodium deoxycholate (NaDoc), 1 mM DTT and sonicated on 20s interval for 1 min at 40°C. Protein amount in the lysate were quantified by BCA method and short gel analysis as reported. About 100 μg of proteins was proteolyzed with Lys-C (1:100 (w/w)) for 2 h in lysis buffer and then further digested with trypsin (1:50 (w/w)) overnight at room temperature after reducing urea concentration from 8M to 2M. The digested peptides were reduced and alkylated before being desalted by C18 spin columns (Harvard Apparatus, catalog no. 74-7206) according to the manufacturer's instructions.

Desalted peptides were re-suspended in 50 mM HEPES (pH 8.5) buffer and labeled with TMTpro (1:1.5 (w/w) peptide:TMT reagent) for 30 min at room temperature. The reaction was then quenched with 5% hydroxylamine for 15 min. After mixing and

adjusting each sample to equal amount, the pooled peptide mixtures were desalted and fractionated by offline basic pH reverse-phase RPLC on a Waters Acuity C18 column (1.7 μm particle size, 3.0 mm × 15 cm, buffer A: 10 mM ammonium formate pH 8.0, buffer B 90% MeCN and 10 mM ammonium formate, pH 8.0). The HPLC gradient was from 15% to 45% buffer B in 155 min at a flow rate of 150 μl/min and fractions were collected every 30 s and eventually concatenated into 40 fractions. Each fraction was loaded onto a nanoscale capillary reverse-phase C18 column (75 μm x 200 mm, C18, 1.9 μm, CoAnn Technology) and analyzed by a high-performance liquid chromatography system (ThermoFisher, ultimate 3000) coupled with a LTQ Orbitrap HF mass spectrometer (ThermoFisher Scientific). Buffer A consisted of 0.2% formic acid and 3% DMSO while buffer B is the same as buffer A with addition of 62% MeCN. The peptides were eluted in a 78 min gradient from 14% to 58% B in a total of 95 min run at a flow rate of 250 nL/min. The collect MS raw data were processed by the JUMP software suite 68,70.

2. Chapter. 2. In-cell self-assembly of Proteolysis Targeting Chimeras (PROTAC) with covalent E3 ligase ligand.

Targeted protein degradation (TPD) has revolutionized the field of drug discovery,

2.1 Introduction

introducing the ability to degrade a specific proteins instead of blocking the functional sites⁷¹. Proteolysis-targeting chimeras (PROTACs) exemplify this breakthrough, as they facilitate the degradation of proteins of interest (POI) by forming a bridge to an E3 ligase, thus marking the POI for degradation via the ubiquitin-proteasome system⁴. Despite their significant potential, traditional PROTACs face challenges including high molecular weight⁷², intricate linker optimization requirements⁷³, and limited cell permeability⁷⁴. In recent years, a novel approach, CLIPTAC (in-cell click-formed proteolysis-targeting chimeras), has emerged as a potential solution to the limitations inherent in traditional PROTACs^{75,76}. CLIPTAC is an innovative concept that combines the principles of click chemistry and targeted protein degradation. It utilizes bio-orthogonal reactions to generate PROTACs in situ, directly within the cellular environment, instead of trying to make the entire PROTAC molecule cell permeable⁷⁷.

Click chemistry, specifically the inverse-electron demand Diels–Alder (IEDDA) cycloaddition between tetrazine (Tz) and trans-cyclooctene (TCO)⁷⁸, is employed in CLIPTAC to form a covalent bond between a ligand of an E3 ubiquitin ligase and a ligand of a protein of interest (POI). The concept builds upon the advantage of bio-

orthogonal click reactions being highly specific, fast, and capable of proceeding in the presence of the vast array of functional groups found in biological systems^{79–82}, making them well-suited for in-cell applications.

In the context of CLIPTAC, two separate precursor molecules, each bearing one part of the click chemistry pair and one part of the PROTAC (either the E3 ligase ligand or the POI ligand), are introduced into the cell. Once inside the cell, these precursor molecules react with each other via the click chemistry reaction to form the complete PROTAC. This in-situ formation results in PROTACs with reduced molecular weight and polar surface area compared to their pre-assembled counterparts, thus improving cell permeability.

Our research further refines the CLIPTAC approach by utilizing covalent ligands for E3 ligases, specifically targeting RNF116 and Keap1. This novel methodology, known as covalent CLIPTAC (cCLIPTAC), presents several advantages over conventional non-covalent CLIPTAC techniques (**Figure 2.1.1**).

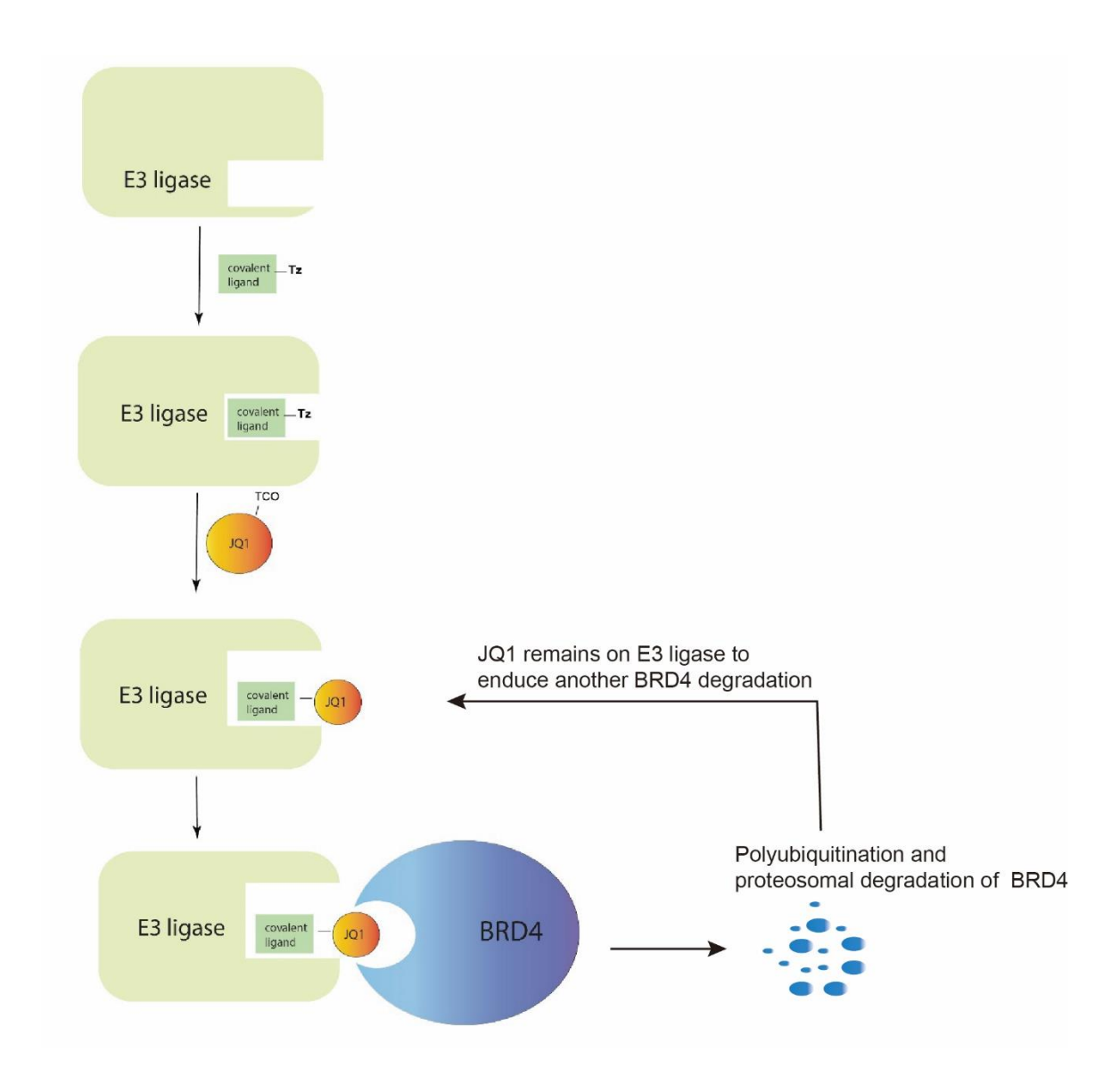


Figure 2.1.1 The scheme of cCLIPTAC. JQ1 is a known BRD4 inhibitor.

Firstly, covalent E3 ligase ligands provide the possibility of having most of the click reaction occurs intracellularly when the cells are exposed to covalent E3 ligase and the POI ligand sequentially. This may minimize the potential off-target effects resulting from forming the active PROTACs outside the cells. Additionally, covalent PROTACs would work through the formation of a binary complex between the POI and modified E3

ligase, which avoids the issue of "hook effect" for non-covalent CLIPTACs, which require the formation of a ternary complex⁸³.

Our research focused on two E3 ligases, RNF126 and Keap1, and their respective covalent ligands, JP2-196 and Piperlongumine (PL) (**Figure 2.1.1**). Ring Finger Protein 126 (RNF126) is a conserved E3 ubiquitin ligase that is critical in various cellular processes such as protein degradation, DNA damage response, and cell signaling⁸⁴⁻⁸⁶. JP2-196, a covalent ligand of RNF116, is employed in our cCLIPTAC strategy to specifically target this E3 ligase⁸⁷.

Keap1, on the other hand, serves as a substrate adaptor protein for a Cullin 3 (CUL3)-based E3 ubiquitin ligase. Keap1 is essential in managing the stability of Nrf2, playing a pivotal role in cellular defense mechanisms against oxidative stress^{88–90}. Piperlongumine (PL), a covalent ligand of Keap1, is known to bind covalently to Keap1 and is incorporated into our cCLIPTAC methodology⁹¹.

Figure 2.1.2 Structure of JP2 (left) and PL (Right).

After demonstrating the effectiveness of using covalent E3 ligase ligands for cCLIPTAC approach, we are also interested in using this platform to discover new covalent E3 ligase

ligands for the creation of novel PROTACs. With over 600 E3 ligases identified in the human proteome, only a few were currently utilized for PROTAC development^{92,93}. There are many unexplored opportunities for uncovering new E3 ligase ligands to develop effective PROTACs to target a broader spectrum of intracellular proteins.

By further understanding and exploiting the mechanism of action of cCLIPTACs, we can greatly enhance the breadth and effectiveness of targeted protein degradation. This holds substantial potential for advancing drug discovery, improving therapeutic approaches, and creating a new generation of targeted therapeutics. Through our research, we hope to contribute to these developments, driving the field of protein degradation forward and opening up new avenues for treatment.

2.2 Results and Discussions

In our proof-of-concept study, we applied the cCLIPTAC strategy to two target proteins: Bromodomain-containing protein 4 (BRD4) and Estrogen receptor α (ER α). We aimed to recruit two different E3 ligases, RNF126 and Keap1, for each of the two targets. A chemist in our lab Yunxiang Wu synthesized four molecules for this purpose: Keap1 ligand attached to tetrazine (PL-Tz), RNF126 ligand linked to tetrazine (JP2-Tz), BRD4 ligand linked to trans-cyclooctene (JQ1-TCO), and ER α ligand connected to trans-cyclooctene (ER α -TCO) (**Figure 2.2.1**). This setup allowed us to investigate four combinations of cCLIPTACs in multiple cell lines.

Figure 2.2.1 Structures of cCLIPTAC components. (Designed and prepared by Yunxiang Wu)

Our experimental testing began with BRD4 degradation in SU-DHL-4 cells, a commonly used B lymphocyte cell line for investigating the BRD protein family. Initial treatment involved PL-Tz, followed by a wash-off procedure after 2 hours to remove any remaining extracellular PL-Tz. Subsequently, we treated the cells with JQ1-TCO for a 20-hour period. The wash-off step ensured that no PL-Tz was present extracellularly, making sure

that all click reactions occurred intracellularly. The outcome showed that the sequential treatment of 1 uM PL-Tz and 1 uM JQ1-TCO effectively degraded BRD4 in SU-DHL-4 cells, whereas separate treatments with either 1 uM PL-Tz or JQ1-TCO did not influence BRD4 levels (**Figure 2.2.2**). This experiment confirmed that covalent E3 ligase ligands are effective in the cCLIPTAC strategy.

However, different results were observed with the application of the RNF126-targeted cCLIPTAC, the combination of JP2-Tz and JQ1-TCO. We found that the treatment with 1 uM JP2-Tz alone also resulted in BRD4 degradation (**Figure 2.2.2**). This unexpected outcome implies that not all E3 ligases are suitable for the cCLIPTAC strategy, underscoring the importance of the careful selection and validation of E3 ligase ligands for cCLIPTAC development.

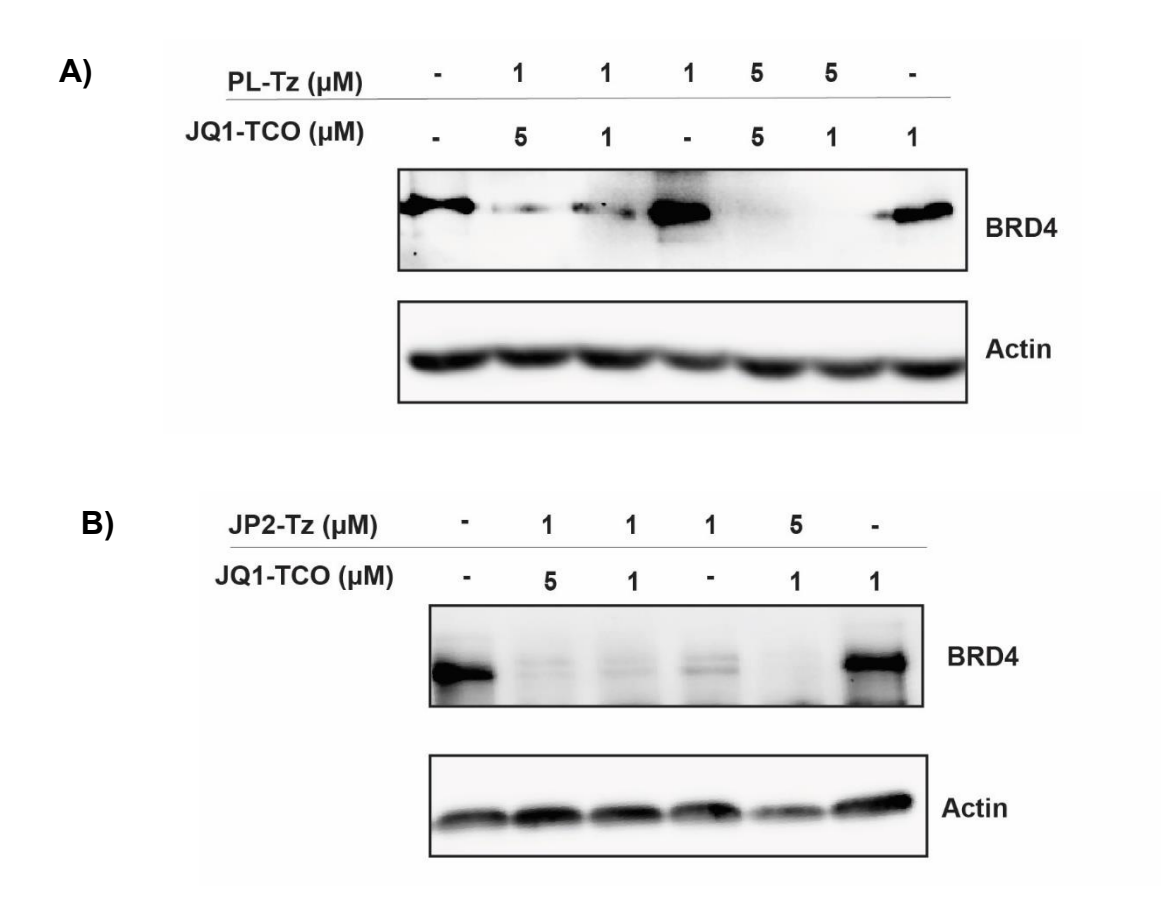


Figure 2.2.2 cCLIPTACs were tested by western blot in SU-DHL-4 cells. A) PL-Tz was first applied to the cells for 2 hours. After the wash off step, cells were treated with JQ1-TCO for 20 hours. B) The same procedure used in A) was employed for the combination of JP2-Tz and JQ1-TCO.

We sought to validate and expand the utility of our cCLIPTAC approach in other cellular contexts beyond SU-DHL-4 cells. To this end, we turned our attention to two additional cell lines - HeLa, a human cervical cancer cell line, and MCF-7, a human breast cancer cell line. These cell lines were chosen not only because of their widespread use in biological research but also for their distinctive cellular contexts which could offer

additional insights into the versatility and potential limitations of our cCLIPTAC methodology.

Similar to our earlier experimental procedure with the SU-DHL-4 cells, we began by treating HeLa and MCF-7 cells with PL-Tz. After an incubation period of 4 hours, we executed a wash-off step by replacing the medium with fresh media. After the wash-off step, we treated the cells with JQ1-TCO for a duration of 20 hours.

Our results from the HeLa cells paralleled those obtained from SU-DHL-4 cells. Western blot analyses demonstrated that the cCLIPTAC system designed to recruit Keap1 was successful in degrading BRD4. In contrast, the cCLIPTAC that recruits RNF126 was ineffective in this cell line (Figure 2.2.3). This outcome, consistent with our prior findings in SU-DHL-4 cells, affirmed the effectiveness of the cCLIPTAC strategy and its compatibility across various cell types.

The results from MCF-7 cells, however, presented an unexpected twist. Even after escalating the concentration of the PL-Tz and JQ1-TCO compounds to 10 μM, the BRD4 protein levels remained unaffected. This led us to speculate that in the context of MCF-7 cells, Keap1 may not be recruitable by our cCLIPTAC strategy. Nevertheless, when we implemented sequential treatment with 10 μM JP2-Tz and 1 μM JQ1-TCO, a detectable modest degradation of BRD4 was observed (**Figure 2.2.3**). This unanticipated finding suggested that our cCLIPTAC strategy has the potential to recruit multiple E3 ligases. However, it also underlined that the suitability of a particular E3 ligase for recruitment by cCLIPTAC might be contingent on the specific cell type under consideration.

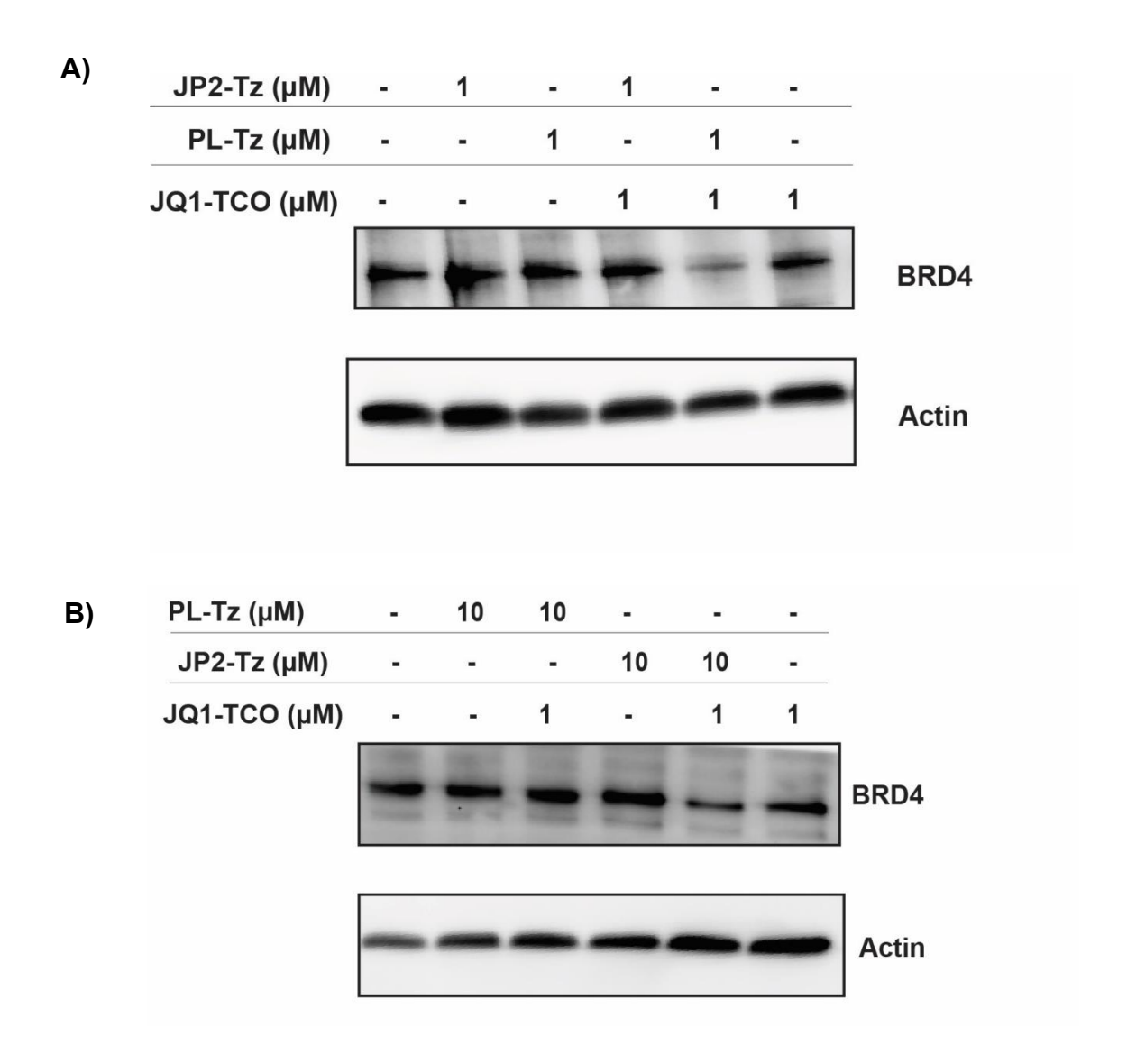


Figure 2.2.3 cCLIPTACs were tested by western blot in Hela and MCF-7 cells. A) PL-Tz or JP2-Tz was first applied to the cells for 4 hours. After the wash off step, cells were treated with JQ1-TCO for 20 hours. B) The same procedure as in A) was employed for the treatment in MCF-7 cells.

In our pursuit to confirm the functionality of RNF126 as an E3 ligase in our cCLIPTAC approach, we directed our efforts towards degrading a different target protein - Estrogen receptor α (ER α) in MCF-7 cells. The strategy remained similar to our previous experimental designs. We initially treated the MCF-7 cells with either PL-Tz or JP2-Tz for a period of two hours, followed by the wash-off step to eliminate any lingering compounds. In a change from our earlier approach, we subsequently treated the cells with ER α -TCO instead of JQ1-TCO, extending this treatment phase for a 20-hour period.

Our western blot results proved quite illuminating. It was observed that the sequential treatment of MCF-7 cells with 1 μ M JP2-Tz and ER α -TCO led to a significant reduction in the ER α protein level. On the other hand, when the cells were treated individually with either 1 μ M JP2-Tz or ER α -TCO, no such decrease in ER α protein level was noted (**Figure 2.2.4**). These findings support our hypothesis that RNF126 could function as an effective E3 ligase for the cCLIPTAC within the context of MCF-7 cells.

Intriguingly, our experiment with the Keap1 E3 ligase presented a different narrative. We found that ERα was degraded upon treatment with PL-Tz alone (**Figure 2.2.4**). This result suggested the possibility of an alternate mechanism at play within the MCF-7 cells involving Keap1 when PL-Tz was employed. This finding also reinforced our observation that the successful recruitment of specific E3 ligase for cCLIPTAC applications can be dependent on the cellular context. These results emphasize the importance of a careful and thorough evaluation of E3 ligase functionality when designing and implementing cCLIPTAC strategies.

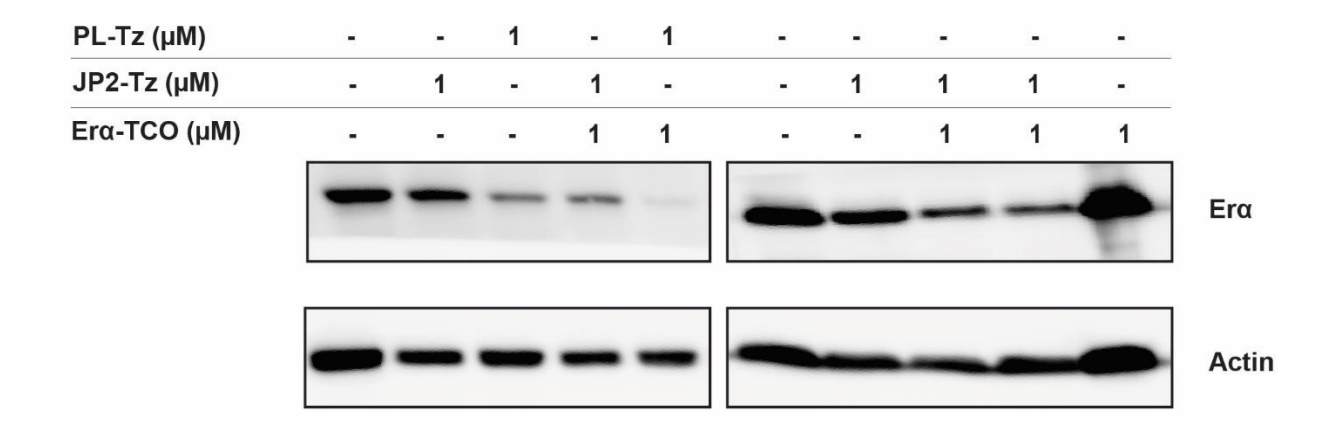


Figure 2.2.3 cCLIPTACs were tested by western blot in MCF-7 cells. PL-Tz or JP2-Tz was first applied to the cells for 4 hours. After the wash off step, cells were treated with $ER\alpha$ -TCO for 20 hours.

In a subsequent experiment, we turned our attention to the potential advantage of cCLIPTAC: improved cell permeability due to its lower molecular weight and less polar surface area compared to traditional PROTACs. Our primary objective was to compare the efficacy of a pre-assembled PROTAC mixture (PRE-MIX) to our cCLIPTAC system in the degradation of BRD4 within HeLa cells.

For the PRE-MIX condition, we prepared a 1:1 DMSO solution of PL-Tz and JQ1-TCO. The cells were treated with this solution for 4 hours, after which we performed a wash-off step to remove any remaining extracellular mixture. The cells were then incubated in fresh media for a further 20 hours.

For the cCLIPTAC condition, we utilized a double wash-off method to fairly compare with the PRE-MIX treatment. Initially, cells were treated with PL-Tz for 2 hours, followed by a wash-off step to remove the extracellular ligand. Subsequently, the cells

were treated with JQ1-TCO for another 2 hours. After a second wash-off step, the cells were also incubated in fresh media for an additional 20 hours.

The western blot analysis revealed a stark contrast between the two conditions. Most BRD4 proteins were degraded under the cCLIPTAC treatment with 5 μ M PL-Tz plus 1 μ M JQ1-TCO. Conversely, the PRE-MIX treatment, despite the concentration of 5 μ M, exhibited less degradation of BRD4 (**Figure 2.2.5**).

This outcome suggests that within the 4-hour treatment window, the cCLIPTAC components, when added sequentially, were able to permeate the cells more effectively than the pre-assembled PROTAC mixture. These results serve as evidence for our hypothesis that our cCLIPTAC strategy possesses better cell permeability when compared to traditional PROTAC molecules.

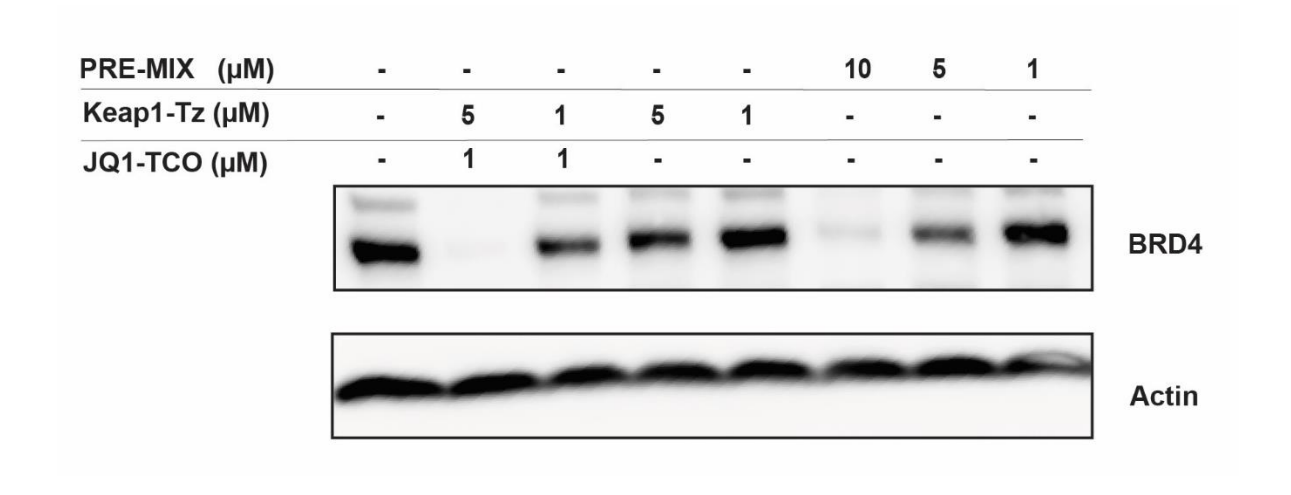


Figure 2.2.5 Comparative Analysis of Sequential cCLIPTAC and Pre-Assembled PROTAC (PRE-MIX) Treatments.

To confirm the underlying mechanism of the cCLIPTAC strategy, we turned our attention to the ubiquitin-proteasome pathway, a central process in PROTAC-mediated protein degradation. This led us to design a series of experiments employing competitive inhibitors that target various stages of the pathway promoted by PROTACs.

We noted a high level of toxicity in HeLa cells when some of the competitive inhibitors were administered for a duration of 24 hours. To circumvent this, we adopted a post-treatment approach. In the adjusted protocol, we initially introduced PL-Tz into the cell media and proceeded with a wash-off after a 2-hour incubation. We then supplemented the media with JQ1-TCO, and a post-treatment with the competitive inhibitors was conducted 6 hours later.

Our observations revealed that the degradation of BRD4 instigated by the sequential application of PL-Tz and JQ1-TCO was effectively halted upon post-treatment with either MG132 or Bortezomib (Bort), both of which are potent proteasome inhibitors. In a similar vein, the introduction of MLN4924, an inhibitor that targets the NEDD8-activating enzyme thereby inhibiting the neddylation of Cullin—a critical process in the ubiquitin-proteasome system (UPS)—also resulted in the inhibition of cCLIPTAC's effect on BRD4 degradation (Figure 2.2.6).

These collective findings reinforce the idea that cCLIPTAC operates in congruence with the conventional PROTAC mechanism. The strategy relies on facilitating the recruitment of E3 ligase and triggering proteasomal degradation, effectively regulating protein levels—in this case, the BRD4 protein. This underscores the mechanistic continuity between cCLIPTAC and the traditional ubiquitin-proteasome pathway leveraged by PROTACs.

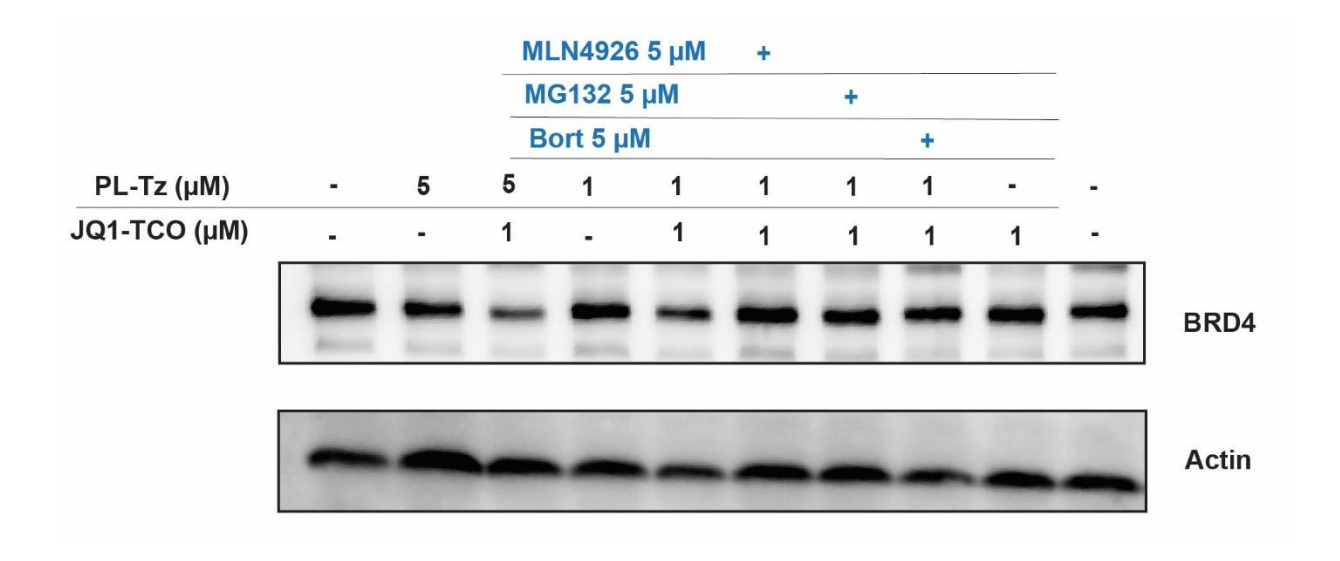


Figure 2.2.6 Validation of the Ubiquitin-Proteasome Pathway Mechanism in cCLIPTAC. PL-Tz was added first followed by a wash-off step 2 hours afterwards. Then cells were treated with JQ1-TCO. Inhibitors were applied 6 hours after JQ1-TCO was added.

2.3 Conclusions and Future perspectives.

Our work has demonstrated the potential and feasibility of applying the cCLIPTAC strategy for targeted protein degradation. We have shown that this approach can be used to recruit distinct E3 ligases such as Keap1 and RNF126 for the targeted degradation of proteins like BRD4 and ERα in different cell lines. Importantly, our results suggest that the choice of E3 ligase and target protein may be cell line-dependent, underscoring the need for careful selection and validation in future studies.

We have also demonstrated that cCLIPTAC exhibits higher activity, which are likely due to better cell permeability, than the whole PROTAC molecules, which is expected due to the lower molecular weight and less polar surface area of each of the two cCLIPTAC components. The advantage of improved cell permeability is further underscored when cCLIPTAC components are administered sequentially as compared to being pre-mixed.

Moreover, our study confirmed that cCLIPTAC operates via the ubiquitin-proteasome pathway, as does the traditional PROTAC mechanism, further cementing the notion that cCLIPTAC is a viable alternative strategy for targeted protein degradation. This was substantiated by the fact that blocking steps in the ubiquitin-proteasome pathway impeded the protein degradation caused by cCLIPTAC.

The therapeutic potential of cCLIPTAC is noteworthy. The covalent linkage to E3 ligases ensures not only a persistent interaction, improving the effectiveness of the degradation process, but also a longer retention time in the system, increasing the durability of protein degradation and possibly allowing for lower dosing frequencies. The better cell

permeability, as compared to traditional PROTACs, could potentially enhance their therapeutic effect and enabling the targeting of difficult-to-reach cell types or tissues.

Moving forward, we envision a multitude of future research directions. The ability of cCLIPTACs to recruit different E3 ligases and degrade diverse protein targets opens the possibility for broader applications in various therapeutic contexts. Comprehensive studies are needed to better understand the mechanistic underpinnings of cCLIPTAC function, including the kinetics of ligand and target protein interactions.

A deeper understanding of the mechanistic differences that contribute to the differential effectiveness of cCLIPTACs in diverse cell lines could pave the way for the design of more potent and selective CLIPTACs. Further investigation could also delve into the identification of novel covalent ligands for E3 ligases, thus expanding the repertoire of tools available for PROTAC development.

More recently, click chemistry has found novel applications in the realm of drug activation and release. For instance, 'click-to-release' strategies have been utilized to control the spatial and temporal release of caged therapeutics, offering a new level of precision in drug delivery⁵². Biorthogonal click reactions, particularly the copper-free azide-alkyne cycloaddition, have been exploited to assemble drugs in-situ, such as antibody-drug conjugates, enhancing their selectivity and reducing off-target effects^{94,95}.

In the clinical setting, click chemistry has paved the way for patient-tailored therapies. A prime example is the assembly of 3D printed personalized dosage forms using click reactions⁹⁶. Such applications of click chemistry in preclinical and clinical contexts

underscore its potential to revolutionize therapeutic design and delivery, expanding the possibilities for personalized medicine.

In summary, while much work lies ahead, our initial findings suggest that the cCLIPTAC strategy holds considerable promise as a versatile and effective tool for targeted protein degradation. It is our hope that future studies will continue to explore and refine this strategy, with the goal of developing novel, effective therapeutic interventions for diseases driven by protein dysregulation.

2.4 Experimental Procedures.

Cell Culture

Cell lines were obtained from American Type Culture Collection. SU-DHL-4 cells were cultured in RPMI1640 media (Corning) supplemented with 10% FBS, 1% PS, 1% sodium pyruvate, and 1% N-(2-hydroxyethyl) piperazine-N'-ethanesulfonic acid (HEPES) buffer. MOVAS cells were cultured in Dulbecco's modified Eagle's (DMEM) medium (Corning, 4.5 g/L glucose) supplemented with 10% fetal bovine serum (FBS) and 1% penicillin–streptomycin (PS). Cell lines were grown at 37 °C in a humidified 5% CO2 atmosphere.

For other detailed procedures, Refer to Chapter 1 section 1.6.

3. Chapter. 3. Exploring the Utility of Novel E3 Ligase Substrate Receptors DCAF1 and DCAF15 in PROTACs for Targeted Protein Degradation

3.1 Introduction

Proteolysis-targeting chimeras (PROTACs) have revolutionized therapeutic intervention, offering a unique method of degrading specific proteins in cells and reshaping the landscape of drug development⁹⁷. Central to the mechanism of PROTACs are E3 ubiquitin ligases, which mark target proteins for degradation by the proteasome through ubiquitination⁹⁸. This crucial role of E3 ligases in the functioning of PROTACs brings them to the forefront of targeted protein degradation research⁹⁹.

To date, only a small fraction of the approximately 600 E3 ligases encoded in the human genome have been successfully engaged by PROTACs. The von Hippel-Lindau protein (VHL) and cereblon (CRBN) have dominated this field 100,101. The prominence of these E3 ligases can be attributed to the availability of effective high-affinity binders and their successful engagement at low and sub-nanomolar potencies. VHL, a component of the VHL E3 ubiquitin protein ligase complex, has spearheaded PROTAC development due to its well-characterized binding interface and robust in vitro and in vivo activity 102,103.

CRBN has gained attention through its roles in thalidomide teratogenicity and the activity of immunomodulatory drugs (IMiDs)¹⁰⁴. CRBN ligand is more frequently used for PROTACs than VHL ligand due to the drug-like property of CRBN ligands compared to the peptidomimetic VHL ligands. PROTACs that recruit CRBN have been used to

degrade a range of proteins, demonstrating the expansive potential of the PROTAC approach^{65,101}. However, despite its wide usage, relying on CRBN poses certain challenges. CRBN downregulation has been observed in instances of resistance, especially in IMiD-treated multiple myeloma patients. As CRBN is a non-essential gene, loss or mutations in CRBN may present a significant liability for CRBN-targeting PROTACs¹⁰⁵. Furthermore, in about 30% of IMiD-refractory patients, alterations in CRBN levels result in reduced IMiD-mediated protein degradation^{106,107}. Thus, the reliance on CRBN alone could limit the broader utility of the PROTAC approach.

These limitations led us to explore the potential of other E3 ligases, notably the DDB1-and CUL4-associated factors (DCAFs), a family of proteins known for their diverse biological roles and involvement in various disease states¹⁰⁸. Functioning as substrate receptors in Cullin RING E3 Ligase 4 (CRL4) ubiquitin ligase complexes, DCAFs have numerous biological roles and are implicated in various disease states¹⁰⁹ (**Figure 3.1.1**).

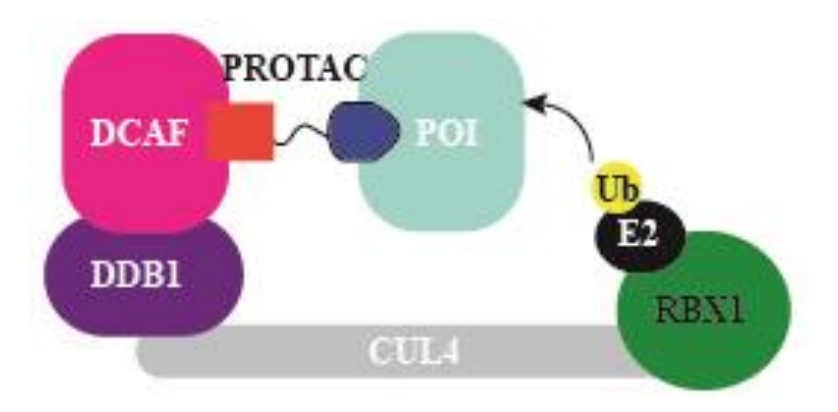


Figure 3.1.1 Scheme of PROTAC pathway recruiting DCAF1.

A key member of the DCAF family, DCAF1, also known as VprBP, functions as a multidomain substrate receptor for CRL4 ligases. Its varied physiological and disease-related roles include being hijacked by the HIV-2 virus to promote the degradation of the antiviral host protein SAMHD1^{110,111}. This interaction between DCAF1 and the viral protein Vpx occurs near the WD40 domain of DCAF1, specifically in the vicinity of C1113, which emphasizes the intricate structure-function relationships within DCAF1¹¹². Moreover, DCAF1 is an essential E3 ligase involved in several cellular processes, including cell cycle regulation and DNA repair, making it less likely to foster resistance compared to CRBN¹¹³ (**Figure 3.1.2**).

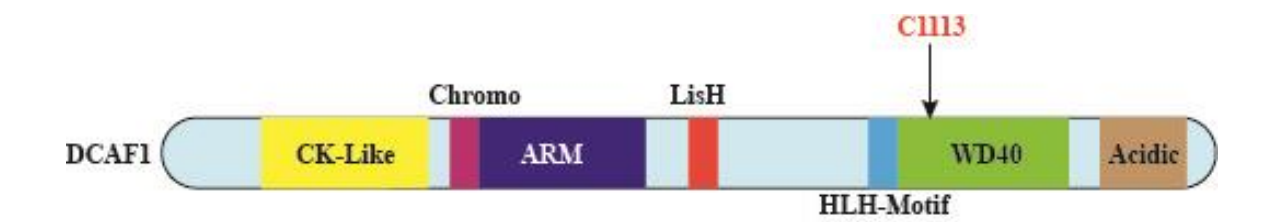


Figure 3.1.2 Domain map of DCAF1.

The recent discovery of potent DCAF1 binders suitable for PROTACs further underscores the potential of DCAF1 as an E3 ligase for targeted protein degradation¹¹⁴. On the other hand, DCAF15, albeit less characterized, has been associated with RNA splicing, and its exploration may reveal novel strategies for PROTAC development¹¹⁵. Motivated by these insights, we embarked on the development of novel PROTACs, harnessing the potential of DCAF proteins. We successfully developed PROTACs that recruit DCAF1 for the degradation of bromodomain-containing protein 4 (BRD4) and DCAF15 for the degradation of the androgen receptor (AR). This significant expansion of the E3 ligase toolkit for PROTACs open new avenues for addressing resistance in targeted protein degradation and further underscores the potential of these novel E3 ligases in therapeutic applications.

3.2 BRD4 degraders recruiting DCAF1.

To extend the E3 ligase toolkit for PROTACs, we sought to utilize DCAF1, a promising E3 ligase with the potential to bypass the limitations associated with CRBN. We first utilized a weak ligand of DCAF1, CYCA-117-70, which binds to the WD-domain of DCAF1 with a dissociation constant (K_d) of 70 μM based on literature ^{116,117}. The binding site of this ligand is adjacent to C1113, a site located in close proximity to the interaction domain between DCAF1 and the HIV-2 virus protein Vpx (**Figure 3.2.1**). This interaction is notable as the HIV-2 virus uses this site to co-opt DCAF1 and instigate the degradation of the antiviral host protein SAMHD1. As such, we hypothesized that the CYCA-117-70 ligand could be an ideal candidate for our PROTAC strategy due to its similarity in binding location to this naturally occurring degradation process.

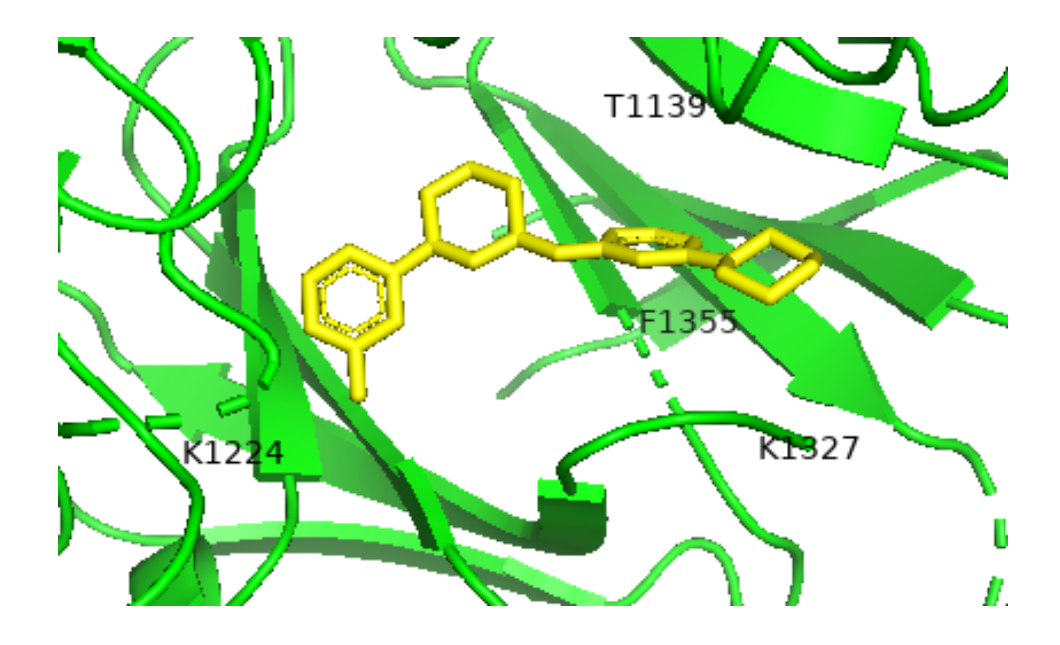


Figure 3.2.1 The binding between DCAF1 and CYCA-117-70 (PDB 7SSE).

To test this hypothesis, our chemist, Hua Tang synthesized a small library of potential PROTACs. These novel compounds were assembled by connecting CYCA-117-70 and JQ1, a potent inhibitor of bromodomain-containing protein 4 (BRD4), with various linkers (**Figure 3.2.2**). These linkers were chosen with the aim of optimizing the ternary complex formation between the target protein, E3 ligase, and the PROTAC.

Figure 3.2.2 Structures of BRD4 degrader library recruiting DCAF1. (Designed and prepared by Dr. Hua Tang.)

To further evaluate the effectiveness of our newly synthesized PROTACs, we conducted a screening of their biological functions in SU-DHL-4 and MV-4-11 cell lines. SU-DHL-4 is a B lymphocyte cell line, and MV-4-11 is a B-myelomonocytic leukemia cell line, allowing us to assess the utility of these PROTACs in different hematological malignancies.

Among all the compounds tested, HTDC1 demonstrated the most potent degradation of BRD4 in both cell lines when administered at a concentration of 5 µM for 24 hours (**Figure 3.2.3**). Notably, HTDC1 possesses the shortest linker length among all compounds in the library. This finding indicated a potential correlation between linker length and degradation efficiency of our PROTACs - as the linker length increased, the observed BRD4 degradation effect appeared to decrease.

These results not only validated our approach of using DCAF1-recruiting PROTACs for BRD4 degradation but also hinted at the pivotal role that structural optimization, specifically the linker length, plays in influencing the effectiveness of PROTACs.

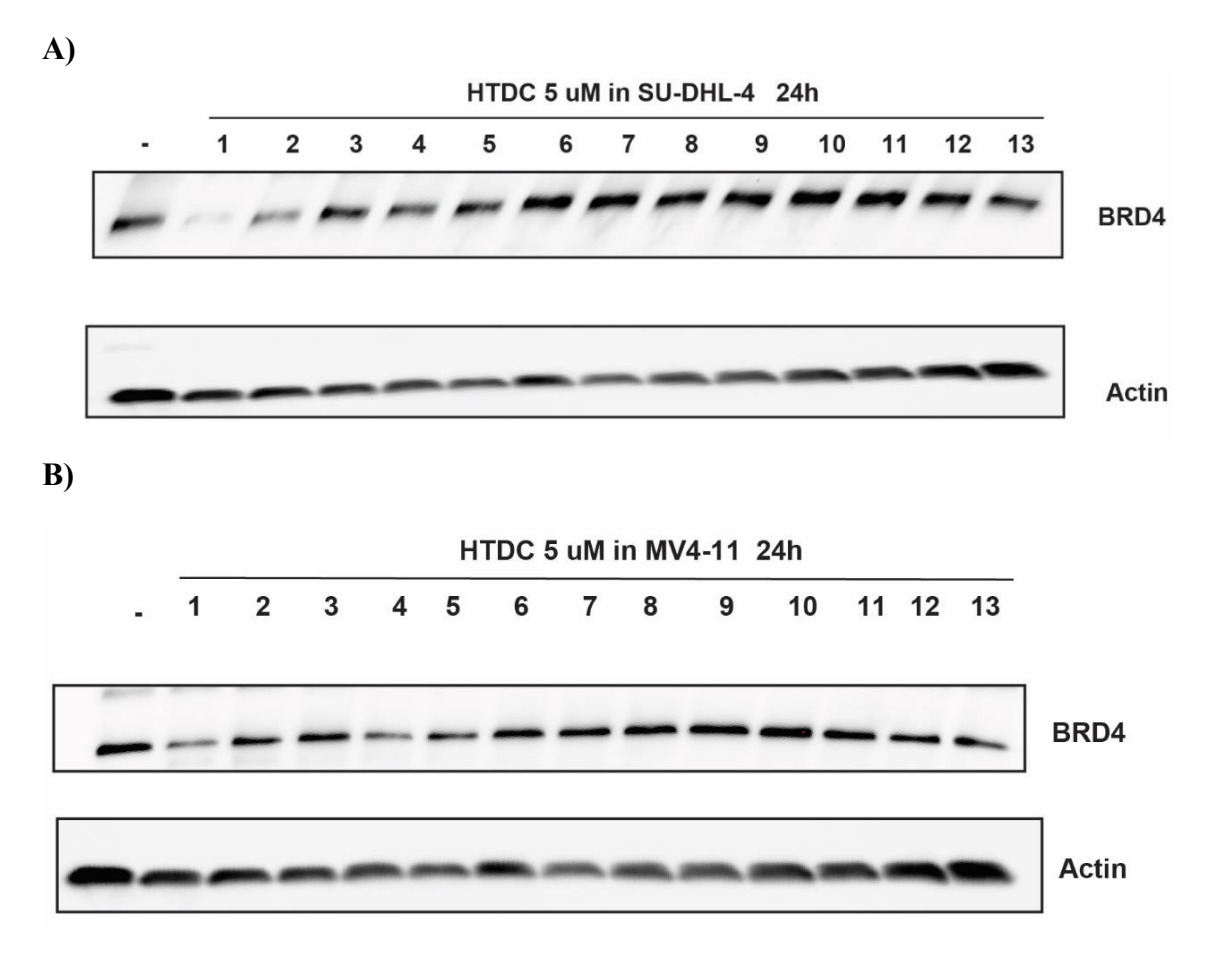


Figure 3.2.3 Screening of BRD4 degraders recruiting DCAF1. A) SU-DHL-4 cells were treated with 5 μ M of indicated compound for 24 hours. B) MV4-11 cells were treated with 5 μ M of indicated compound for 24 hours.

Several weeks after the initial screening, a more potent DCAF1 ligand, CYCA-117-70, was reported ¹¹⁶. This new compound boasted a considerably improved binding affinity to DCAF1, with a dissociation constant (Kd) of only 3 µM. With this new ligand, we sought to optimize our previous best-performing compound, HTDC1, by replacing its DCAF1 binder with CYCA-117-70, while keeping the BRD4 binder (JQ1) and the linker unchanged.

Our chemist synthesized a pair of diastereomers, designated as **2025** and **2036**, both comprised of CYCA-117-70 at one end, JQ1 at the other, and the same linker as in HTDC1 (**Figure 3.2.4**). These enantiomers presented an exciting opportunity to assess not only the influence of a more potent E3 ligase ligand but also the potential effect of stereochemistry on PROTAC performance.

Figure 3.2.4 Structure of degraders with CYCA-117-70 as DCAF1 ligand.

(Designed and prepared by Dr. Hua Tang.)

When tested in SU-DHL-4 cells, all three compounds – HTDC1, 2025, and 2036 – demonstrated impressive BRD4 degradation at a 5 µM concentration. Interestingly, at a lower concentration of 1 µM, none of the compounds were effective in degrading BRD4 (**Figure 3.2.5**). This could indicate a certain threshold concentration needed for these PROTACs to function effectively. However, the results at a 3 µM concentration proved to be pivotal. In this setting, compound 2036 outperformed the other two, showcasing superior BRD4 degradation.

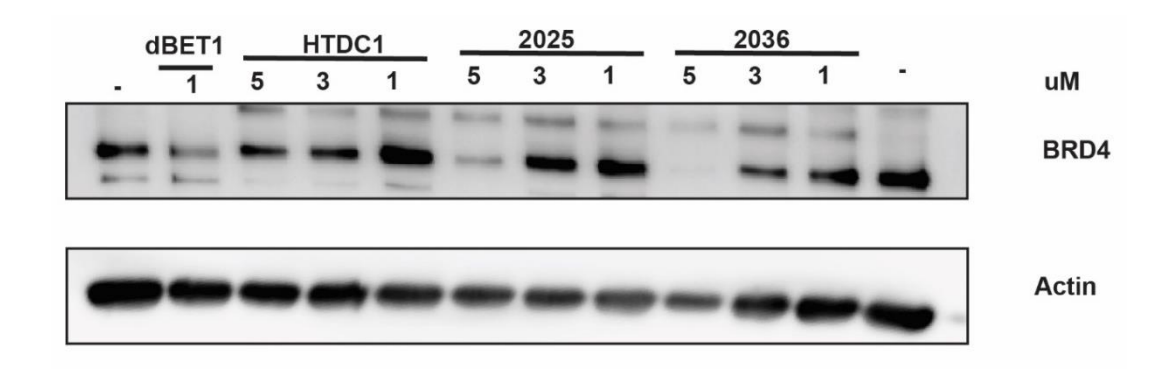


Figure 3.2.5 Western blot results of degraders tested in SU-DHL-4 cells.

Compounds were treated with 24 hours at indicated concentration. dBET1 is a well-known BRD4 degrader which was used as a positive control.

These findings confirmed our hypothesis that a stronger E3 ligase ligand could indeed enhance the degradation performance of PROTACs. Moreover, they also suggested a potential stereochemical preference in PROTAC design, as the two enantiomers demonstrated different levels of degradation efficiency.

To corroborate the mechanism of BRD4 degradation via the ubiquitin-proteasome pathway, we implemented a series of experiments using competitive inhibitors of various stages in the proteasomal pathway. Initially, the direct pre-treatment of these inhibitors resulted in high toxicity when applied for 24 hours in SU-DHL-4 cells, which led us to reconsider our experimental approach.

Instead of a pre-treatment setup, we decided to post-treat cells with the competitive inhibitors. To do so, cells were initially treated with a 3 µM dose of compound 2036. Then, the post-treatment of competitive inhibitors was performed. As expected, the BRD4 degradation induced by 2036 was effectively obstructed following post-treatment with MG132, a well-known proteasome inhibitor. Similarly, post-treatment with

MLN4924, an inhibitor of the NEDD8-activating enzyme that blocks cullin neddylation—a crucial step in the ubiquitin-proteasome system (UPS)—also abrogated the BRD4 degradation effect of 2036 (**Figure 3.2.6**).

In addition to investigating the involvement of the proteasome pathway, we aimed to confirm the role of DCAF1 in this degradation process. To this end, we conducted a competitive assay, pre-treating cells with a 10 µM dose of CYCA-117-70—the original DCAF1 ligand—before introducing 2036. As expected, the pretreatment with the DCAF1 ligand effectively inhibited the degradation effect of 2036, thus confirming DCAF1's critical role in this degradation pathway (**Figure 3.2.6**).

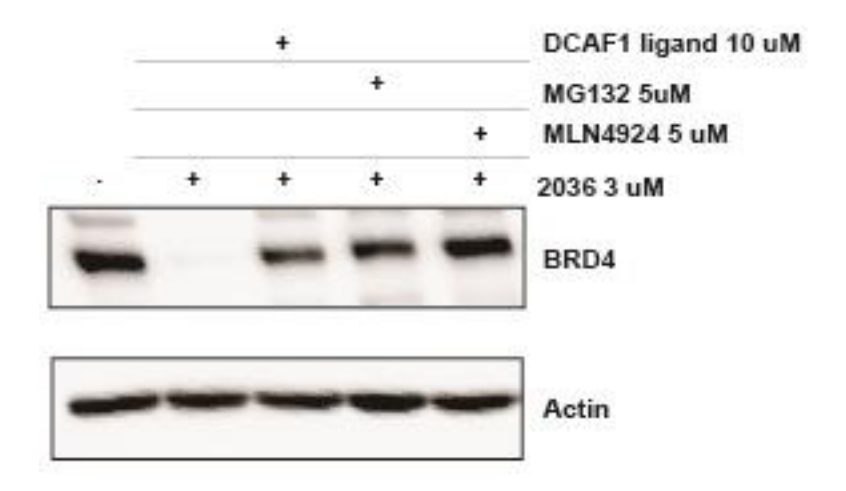


Figure 3.2.6 Mechanistic study of 2036. DCAF1 ligand was pre-treated for 1 hour. 2036 was treated for 24 hours. MG132 and MLN4924 was treated 12 hours after 2036 was applied to SU-DHL-4 cells.

Altogether, these findings corroborate that compound 2036 functions via the prototypical PROTAC mechanism: it recruits DCAF1, thereby instigating proteasomal degradation to effectively regulate the levels of the BRD4 protein.

3.3 AR degraders recruiting DCAF15.

In addition to DCAF1, another pivotal player in the realm of substrate receptors is DCAF15, an intricate protein made up of two primary domains rich in β -sheets. These are the N-terminal domain (NTD, encompassing residues 30-264) and the C-terminal domain (CTD, housing residues 383-600)¹¹⁸. The DCAF15 protein attaches to DDB1 via a helix-loop-helix motif, thereby creating contacts with the two β -propeller domains of DDB1, BPA and BPC. Interestingly, this interaction mirrors the helix-loop-helix motif found in CSA and DDB2 proteins¹¹⁹.

Interestingly, DCAF15 does not conform to the common structural characteristics observed in most DDB1 and CUL4-associated factors (DCAFs). It lacks a canonical WD40 β -propeller fold, setting it apart from other CRL substrate receptors in terms of structural homology.

E7820, a ligand of DCAF15, associates within a superficial pocket formed at the interface between the NTD and CTD of DCAF15. This binding pocket resides in a minimally conserved surface groove located in close proximity to DDB1 (**Figure 3.3.1**). This unique binding interaction offers a promising potential avenue for therapeutic exploitation, further broadening the realm of possible targets for the PROTAC approach.

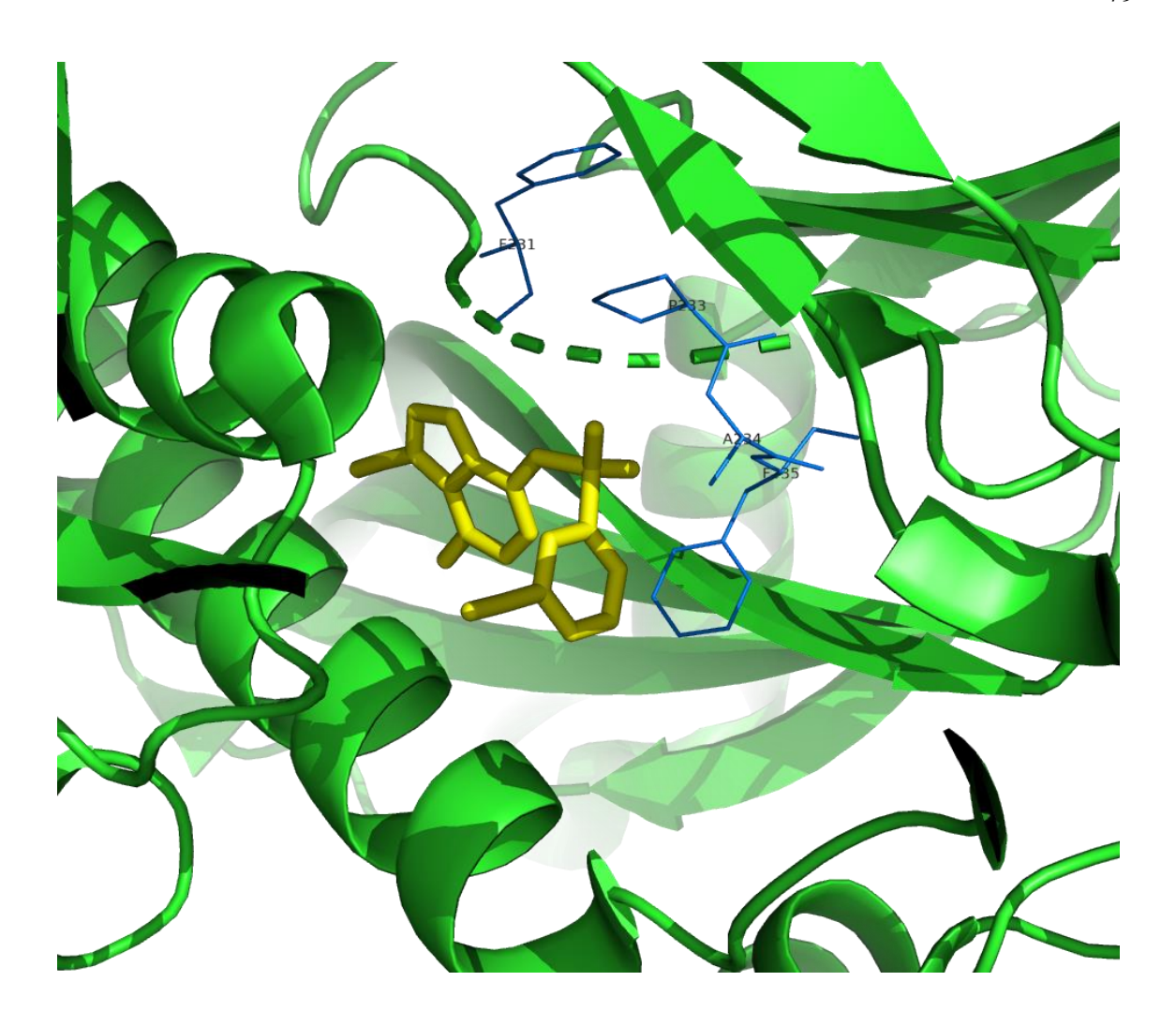


Figure 3.3.1 Binding between E7820 and DCAF15. E7820 was labeled as yellow and the amino acids interacting with E7820 was labeled as blue. (PDB 6Q0R)

In the pursuit of an effective PROTAC strategy for androgen receptor (AR) degradation, our chemist Zhen Zhang, synthesized a diverse array of AR degraders (**Figure 3.3.2**). These degraders featured E7820 at one end, a compound designed to recruit the E3 ligase DCAF15, and an AR ligand at the other end. Bridging these two moieties was a variety of different linkers, each potentially influencing the overall activity and effectiveness of the degraders.

z0z-1-103 z0z-1-104

z0z-1-105

Figure 3.3.2 Structure of the AR degraders recruiting DCAF15. (Designed and prepared by Dr. Zhen Zhang.)

The library of these bespoke degraders was then tested in LN-CAP cells, a prostate cancer cell line known for its dependence on AR signaling. Among the first three compounds synthesized, only one exhibited noticeable degradation effects on AR. This degradation, however, was not particularly potent, as it necessitated a high concentration ($10 \mu M$) and extended exposure time (24 hours) to elicit noticeable AR degradation (**Figure 3.3.3**).

Although these initial results could be deemed unsatisfactory in terms of potency, they nonetheless signify a crucial first step in the iterative process of PROTAC development.

The understanding gained from these preliminary findings will inform the design of subsequent iterations, guiding modifications to enhance the activity of our AR degraders.

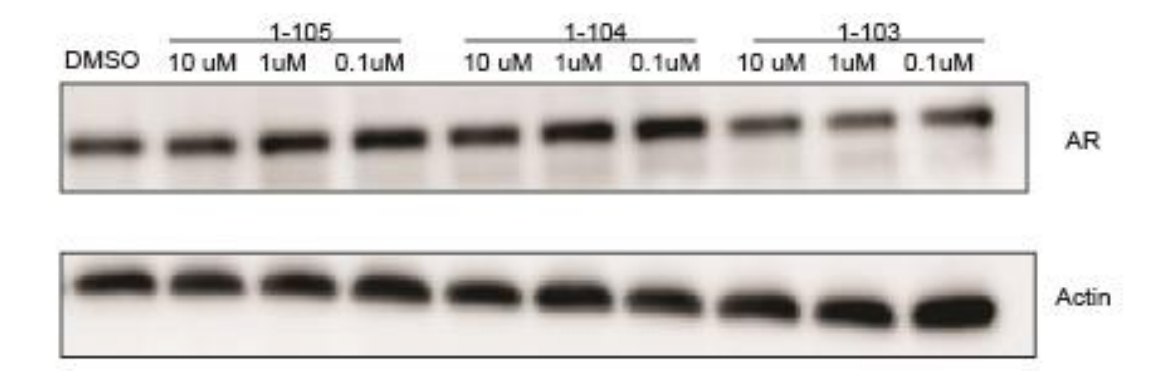


Figure 3.3.4 Western blot results for AR degraders. LN-CAP cells were treated with compounds of indicated concentration for 24 hours.

Further efforts to optimize the AR degraders were made by implementing a series of Structure-Activity Relationship (SAR) studies based on the structure of compound 103. Our chemist, Zhen Zhang, synthesized an additional set of six compounds, aiming to investigate the impact of subtle structural modifications on the degradation activity (**Figure 3.3.5**).

0 1 111	CN
z0z-1-111	O ZH
	CI———NH
z0z-1-095-9	CI NC
z0z-1-095-10	CI NC
z0z-1-095-13	CI C
z0z-1-095-16	CI O NH
z0z-1-135-2	CI NC NH HZ CN

Figure 3.3.5 Structure of second AR degraders library. (Designed and prepared by Dr. Zhen Zhang.)

After rigorous biological testing, only one compound, labeled as 135-2, demonstrated a similar weak degradation effect to 103, needing a concentration of 10 μ M to trigger discernible AR degradation. Importantly, the initial compound, 103, maintained its weak degradation effect under these test conditions, demonstrating consistency in its performance (**Figure 3.3.6**).

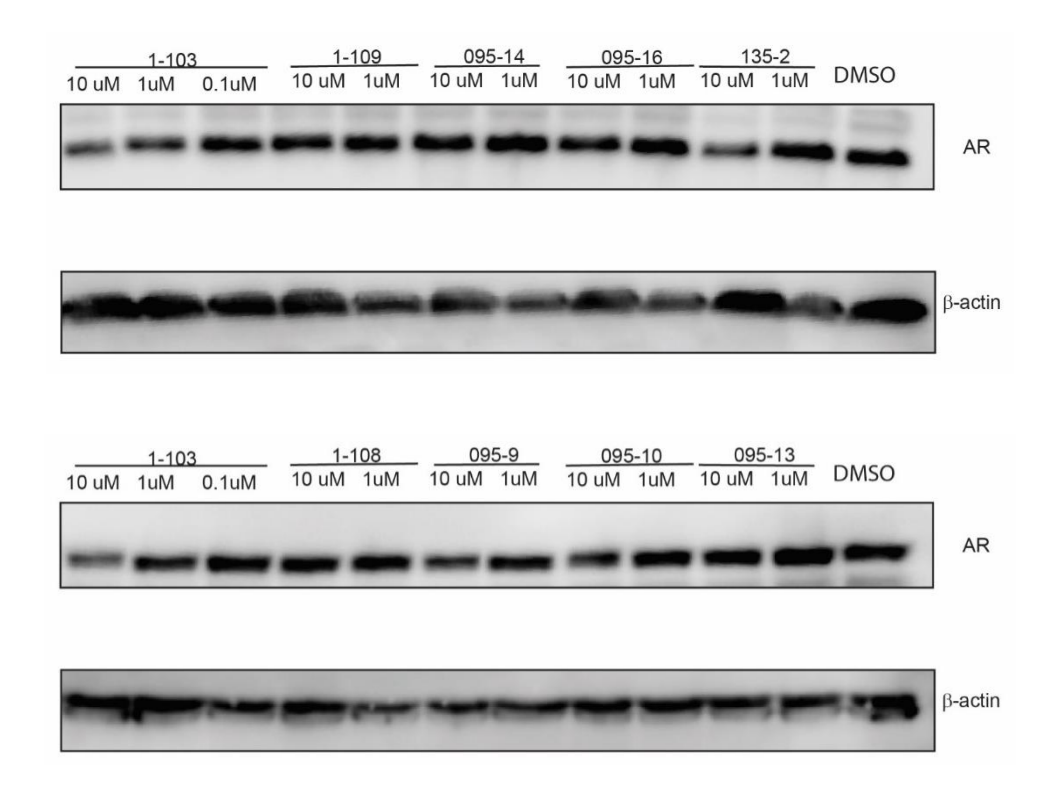


Figure 3.3.7 Western blot results for second AR degraders library. LN-CAP cells were treated with compounds of indicated concentration for 24 hours.

Our commitment to uncover a potent AR degrader continued with the expansion of our SAR studies. Our chemist, Zhen Zhang, synthesized an additional 14 AR degraders, each reflecting the structural characteristics of the initial compound 103 (**Figure 3.3.8**). Our goal was to explore a wider chemical space while maintaining the key features of the prototype molecule.

z0z-1-095-15	CI NC
z0z-1-095-11	CI NC
z0z-1-095-12	CI ON HIN CN
z0z-1-136	
z0z-1-137-2	CI NC N N N N N N N N N N N N N N N N N
z0z-1-137-3	CI NC
z0z-1-137-5	CI TO NO
z0z-1-137-6	CI NC

Figure 3.3.8 Structure of the third AR degraders library. (Designed and prepared by Dr. Zhen Zhang.)

The new compounds were subjected to extensive biological testing, using western blot screening as the principal assay. Unfortunately, none of the new candidates showed a detectable degradation effect on AR, suggesting that the structural modifications implemented did not improve the degrader's efficacy (**Figure 3.3.9**).

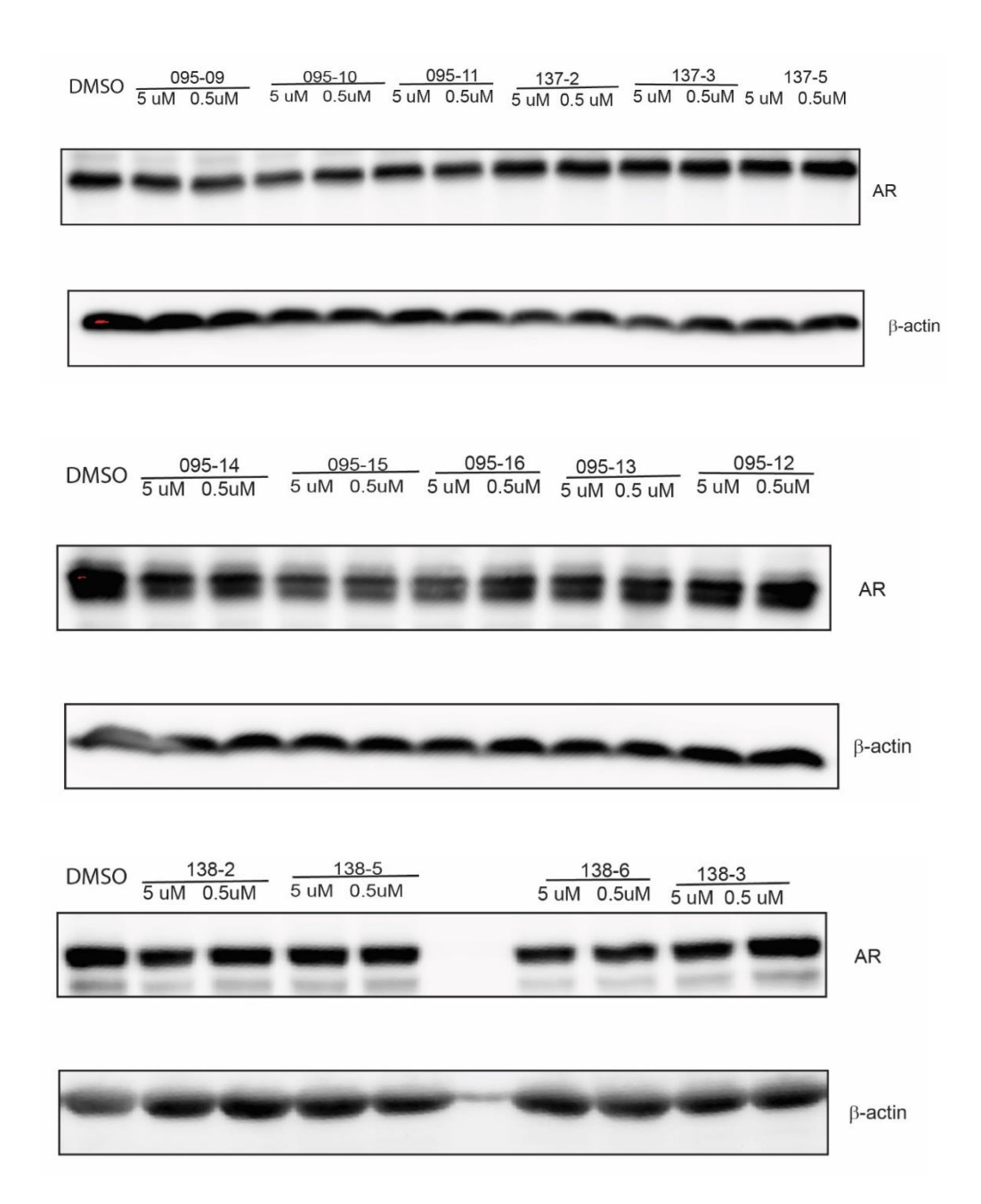


Figure 3.3.9 Western blot results for third AR degraders library. LN-CAP cells were treated with compounds of indicated concentration for 24 hours.

While these results might seem discouraging, they add valuable information to our understanding of the SAR of AR degraders. Each non-reactive compound serves to delineate the bounds of effectiveness, enabling us to fine-tune our chemical strategies. We

remain hopeful that our continued investigation will eventually lead to the discovery of an effective and potent AR degrader, built on the foundation of knowledge that these studies provide.

Before devoting more efforts to the synthesis, we decided to confirm the functional outcome and mechanism of action of the two weak AR degraders, 1-103 and 135-2. The next step in our investigation entailed evaluating the antiproliferative effects of these two compounds in the LN-CAP prostate cancer cell line.

For this, we treated LN-CAP cells with 10 µM of either 1-103 or 135-2 for a span of 72 hours and assessed the impact on cell proliferation. The data unveiled that both degraders could reduce the viability of LN-CAP cells by 30-40 percent following the 72-hour treatment period. This suggested a moderate cytotoxic impact and hinted at the potential utility of these compounds in limiting the growth of prostate cancer cells (**Figure 3.3.10**). In contrast, it was noteworthy that treatment with either E7820 or AR ligand alone, the two components of our degraders, had a negligible effect on cell proliferation under the same conditions. This observation underscored the value of the PROTAC strategy, as the combinatory action of the ligand and the E3 ligase recruiter, linked via a judiciously selected spacer, offered superior anticancer effects. It also served to emphasize the possibility that the cytotoxic effects we observed might be due, at least in part, to the specific degradation of AR rather than to other off-target effects.

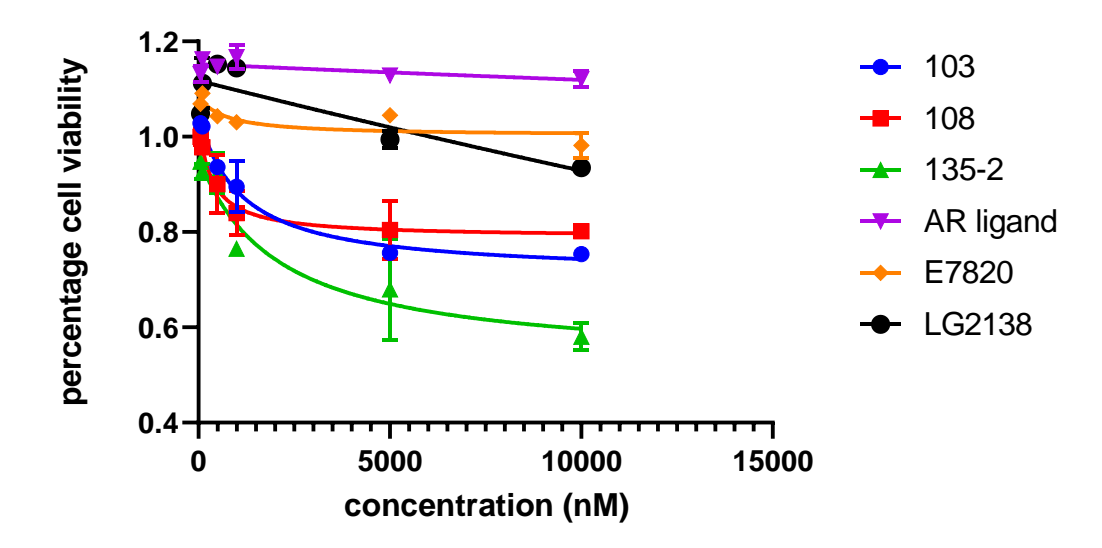


Figure 3.3.10 Antiproliferation effect for 72-hour treatment in LN-CAP cells.

Percentage cell viability was normalized with vehicle treatment of DMSO.

To gain further insight into the activity of our AR degraders, we turned to the NanoBRET assay to verify the formation of a ternary complex among DCAF15, AR, and our PROTAC molecule. This highly sensitive technique allows the examination of protein-protein interactions within the cellular context. The approach is based on the principle that when two proteins tagged with NanoLuc and HaloTag ligands are brought into close proximity, luminescence is emitted, indicative of an interaction.

We transfected HEK293 cells with AR-NanoLuc and DCAF15-HaloTag plasmids, followed by a pre-treatment with a proteasome inhibitor to prevent any degradation of AR that might occur. Next, we treated the cells with our degraders for 6 hours and then quantified the luminescent signal. This step was essential in providing data on the spatial proximity of DCAF15 and AR in the presence of our PROTACs (**Figure 3.3.11**).

The results were promising, with treatment using 103 revealing a significantly higher signal ratio compared to the vehicle control. Importantly, this elevation in signal was not

observed when cells were treated with E7820, AR ligand, or MG132 alone. This outcome suggested that these individual components were not capable of mediating the interaction between DCAF15 and AR.

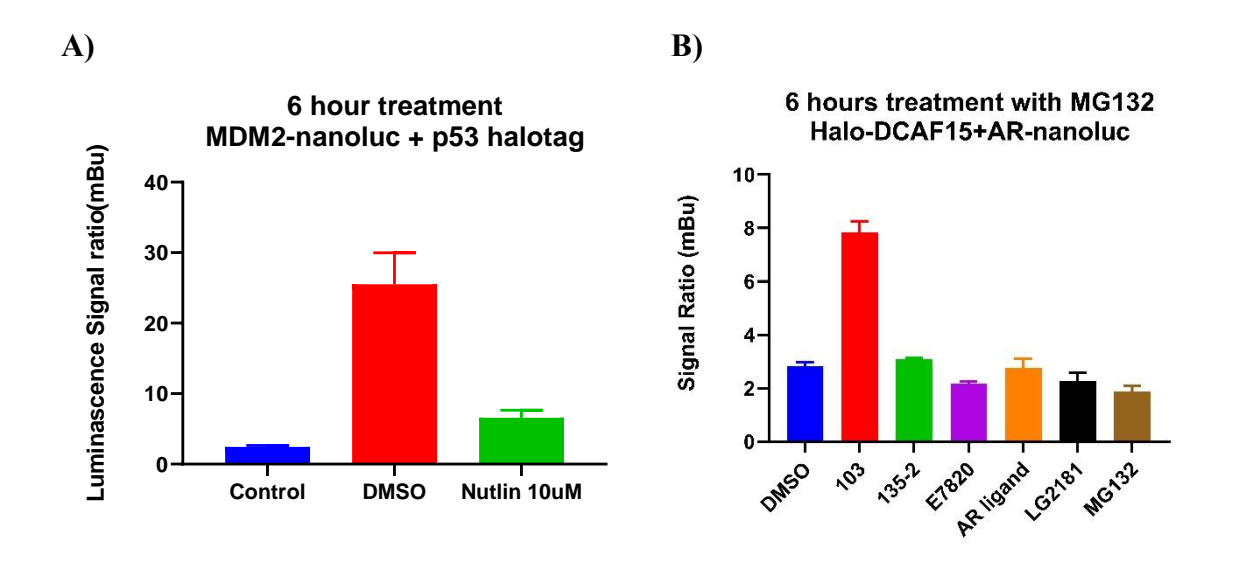


Figure 3.3.11 nanoBRET assay for confirming ternary complex formation. A)

Validation of nanoBRET assay. 10 uM nutlin treatment inhibited the interaction between MDM2 and p53. The cells treated with nutlin had 5 times lower luminescence signal ratio than the Vehicle. **B)** The nanoBRET results of ternary complex formation among DCAF15, AR and 103. Cells treated with 103 had 5 times higher signal ratio than that of vehicle control.

Taken together, our findings provided compelling evidence that **treatment** with 103 indeed facilitated the formation of a ternary complex between DCAF15, AR, and the PROTAC molecule. This complex formation is critical in the PROTAC mechanism, as it enables the recruitment of the substrate protein to the E3 ligase for subsequent ubiquitination and degradation. As such, these findings further support the viability of our

approach in targeting AR for degradation as a potential therapeutic strategy for prostate cancer.

In this study, we have systematically explored and demonstrated the potential of two

3.4 Discussion and Future perspectives

novel E3 ligases, DCAF1 and DCAF15, as effectors for PROTAC-based therapeutic interventions. We have developed effective and selective degraders for the proteins BRD4 and AR, harnessing the potential of the DCAF1 and DCAF15 E3 ligases, respectively.

Our findings on DCAF1 recruitment through the ligand CYCA-117-70 have extended our understanding of PROTAC design and opened up new possibilities in the domain of targeted protein degradation. DCAF1, previously overlooked due to its multi-domain nature and extensive physiological roles, has been shown to play a pivotal role in targeted protein degradation. The discovery of a weak ligand for DCAF1, followed by its subsequent enhancement through the introduction of a more potent ligand, elucidated the direct correlation between the potency of an E3 ligase ligand and the efficiency of degradation.

Furthermore, we validated the PROTAC mechanism of action by confirming that our designed molecules operated through the ubiquitin-proteasome pathway. The success of our DCAF1-recruiting BRD4 degrader underpins the potential of this E3 ligase in TPD, offering an alternative to the widely used CRBN and VHL E3 ligases, thus providing a promising strategy to circumvent resistance induced by PROTACs that recruit CRBN or VHL.

Our exploration of DCAF15 in this study further diversified the E3 ligase toolbox. This E3 ligase, which binds in a unique manner to its ligand E7820, was shown to successfully mediate AR degradation in the LN-CAP prostate cancer cell line. While our initial degraders were weak, the anti-proliferative effects and the confirmation of ternary complex formation by the NanoBRET assay indicated the potential for future optimization.

The application of PROTACs for targeted protein degradation is still rapidly evolving. Future perspectives include further optimization of our existing DCAF1 and DCAF15 recruiters, as well as the exploration of additional under-utilized E3 ligases. Further, expanding the range of targeted proteins could bring novel therapeutic opportunities. Our studies have also highlighted the importance of comprehensive SAR studies and biological testing, which will continue to be a cornerstone of PROTAC development.

In addition, as resistance is an issue in cancer therapeutics, understanding the mechanisms of resistance to PROTAC therapy will be of paramount importance.

Studying how cancer cells may adapt to PROTACs and how this resistance can be circumvented will be a significant focus going forward. Further studies on the physiological and disease functions of different E3 ligases will also be essential in developing a more nuanced understanding of PROTAC biology.

In conclusion, our study has broadened the scope of E3 ligases for PROTAC development and provided new directions in the quest for effective and selective protein degradation. This work has the potential to reshape our understanding of disease mechanisms and open new avenues for the development of innovative therapeutics.

3.5 Experimental Procedures

Plasmids Preparation.

The NanoLuc-MDM2 and p53-Halotag plasmids were generously provided by Deininger Lab Versiti / Blood Research Institute.

Digestion of the Parent Plasmids: The human AR plasmids purchased from Addgene were digested with appropriate restriction enzymes. The enzymes chosen would have been determined by the sequences of the plasmids, targeting specific recognition sites that flank the desired fragment. The digestion reaction was carried out following the manufacturer's instructions.

Purification of DNA fragments: The digested plasmids were subjected to agarose gel electrophoresis to separate the DNA fragments. The band corresponding to the AR fragment from the human AR plasmid and the NanoLuc fragment from the NanoLuc-MDM2 plasmid were excised from the gel. DNA was extracted from the gel slices using a Gel Extraction Kit according to the manufacturer's instructions.

Ligation of AR onto NanoLuc Plasmid: The purified AR and NanoLuc fragments were ligated together using T4 DNA Ligase. The reaction was set up according to the manufacturer's instructions and incubated at 16°C overnight.

Transformation of Recombinant Plasmids into Competent Cells: The ligated plasmid was then transformed into competent E. coli cells using heat shock at 42°C for 90

seconds followed by ice cooling. Transformed cells were then plated onto agar plates containing the appropriate antibiotic for selection and incubated overnight at 37°C.

Verification of the Recombinant Plasmid: Colonies were picked and plasmid DNA was isolated using a Plasmid Miniprep Kit. The presence of the AR fragment in the NanoLuc plasmid was confirmed by sequencing.

Bioluminescence Resonance Energy Transfer (BRET) Assay

reaction following the manufacturer's instructions.

HEK293 cells were cultured in DMEM supplemented with 10% FBS and maintained at 37°C in a humidified atmosphere of 5% CO2. When the cells reached approximately 70% confluence, they were transiently co-transfected with AR-NanoLuc and DCAF15-HaloTag plasmids using Lipofectamine 3000 according to the manufacturer's instructions. Following 48 hours post-transfection to allow for the expression of the fusion proteins, cells were optionally pre-treated with MG132 (10 μM) for 2 hours to prevent protein degradation during the BRET assay. After pre-treatment, cells were treated with either degraders or control compounds at indicated concentrations and incubated for 6 hours.

Upon completion of treatment, cells were incubated with HaloTag® NanoBRET™ 618

Ligand (Promega) at a final concentration of 100 nM for 10 minutes at 37°C.

Subsequently, NanoLuc substrate (Promega) was added to the cells to initiate the BRET

Finally, the BRET signal was measured using a dual-filter luminometer with readings taken at the donor emission wavelength of 460 nm and the acceptor emission wavelength

of 618 nm. The BRET ratio was then calculated as the ratio of the acceptor emission to the donor emission. Data are presented as the mean \pm standard deviation of three independent experiments.

For other information, please refer to section 1.6.

Abbreviations

AML acute myeloid leukemia

AR androgen receptor

BET Bromodomain and Extra-Terminal motif

Bort bortezomib

BRD4 bromodomain-containing protein 4

CLIPTAC click-formed proteolysis targeting chimeras

CRBN cereblon

CRL4^{CRBN} CUL4 (cullin 4)-RBX1-DDB1-CRBN

DCAF DDB1- and CUL4-associated factors

DC₅₀ half-maximal degradation concentration

D_{max} maximum degradation percentage

DMSO Dimethylsulfoxide

GSPT1 G1 To S Phase Transition 1

HTS High-throughput screening

OPA ortho-phthalaldehyde

ICB immune checkpoint blockades

IEDDA inverse-electron demand Diels-Alder

IFNs interferons

IKZF Ikaros zinc finger

IMiDs Immunomodulatory drugs

PD1 Programmed cell death protein 1

PEG polyethylene glycol

PL piperlongumine

POI protein of interest

PROTAC Proteolysis-targeting chimeric

Rapid-TAC rapid synthesis of PROTACs

RIPK Receptor-interacting serine/threonine-protein kinase

SAR structure-activity relationship

TCO trans-cyclooctene

TME tumor microenvironment

TMT-MS tandem mass tag mass spectrometry

TNF-α tumor necrosis factor-α

TLR toll-like receptor

Tz tetrazine

UPS ubiquitin-proteasome system

VHL Von Hippel-Lindau

References

- Yang K, Wu H, Zhang Z, et al. Development of Selective Histone Deacetylase 6
 (HDAC6) Degraders Recruiting von Hippel-Lindau (VHL) E3 Ubiquitin Ligase.
 ACS Med Chem Lett. Published online 2020.
 doi:10.1021/acsmedchemlett.0c00046
- Sakamoto KM, Kim KB, Kumagai A, Mercurio F, Crews CM, Deshaies RJ.
 Protacs: Chimeric molecules that target proteins to the Skp1-Cullin-F box complex for ubiquitination and degradation. *Proc Natl Acad Sci U S A*. 2001;98(15):8554-8559. doi:10.1073/PNAS.141230798/ASSET/96E10B62-DC16-4F76-94AF-64F8B7059B8E/ASSETS/GRAPHIC/PQ1412307006.JPEG
- Luh LM, Scheib U, Juenemann K, Wortmann L, Brands M, Cromm PM. Prey for the Proteasome: Targeted Protein Degradation—A Medicinal Chemist's Perspective. *Angew Chemie - Int Ed.* 2020;59(36):15448-15466. doi:10.1002/ANIE.202004310
- 4. Lai AC, Crews CM. Induced protein degradation: an emerging drug discovery paradigm. *Nat Rev Drug Discov 2016 162*. 2016;16(2):101-114. doi:10.1038/nrd.2016.211
- Mullard A. Targeted protein degraders crowd into the clinic. Nat Rev Drug Discov.
 2021;20(4):247-250. doi:10.1038/D41573-021-00052-4
- 6. Gao H, Sun X, Rao Y. PROTAC Technology: Opportunities and Challenges. *Cite This ACS Med Chem Lett.* 2020;11:240. doi:10.1021/acsmedchemlett.9b00597
- 7. Nowak RP, Deangelo SL, Buckley D, et al. Plasticity in binding confers selectivity in ligand-induced protein degradation article. *Nat Chem Biol*. 2018;14(7):706-714.

- doi:10.1038/s41589-018-0055-y
- 8. Lai AC, Crews CM. Induced protein degradation: An emerging drug discovery paradigm. *Nat Rev Drug Discov*. 2017;16(2):101-114. doi:10.1038/NRD.2016.211
- Bondeson DP, Smith BE, Burslem GM, et al. Lessons in PROTAC Design from Selective Degradation with a Promiscuous Warhead. *Cell Chem Biol*.
 2018;25(1):78-87.e5. doi:10.1016/J.CHEMBIOL.2017.09.010
- Belcher BP, Ward CC, Nomura DK. Ligandability of E3 Ligases for Targeted Protein Degradation Applications. *Biochemistry*. 2023;62(3):588-600. doi:10.1021/ACS.BIOCHEM.1C00464
- 11. Wang Y, Jiang X, Feng F, Liu W, Sun H. Degradation of proteins by PROTACs and other strategies. *Acta Pharm Sin B*. 2020;10(2):207-238.
 doi:10.1016/j.apsb.2019.08.001
- 12. Ottis P, Toure M, Cromm PM, Ko E, Gustafson JL, Crews CM. Assessing Different E3 Ligases for Small Molecule Induced Protein Ubiquitination and Degradation. ACS Chem Biol. 2017;12(10):2570-2578. doi:10.1021/acschembio.7b00485
- Li J, Li C, Zhang Z, et al. A platform for the rapid synthesis of molecular glues (Rapid-Glue) under miniaturized conditions for direct biological screening. Eur J Med Chem. 2023;258. doi:10.1016/j.ejmech.2023.115567
- 14. Roberts BL, Ma ZX, Gao A, et al. Two-Stage Strategy for Development of Proteolysis Targeting Chimeras and its Application for Estrogen Receptor Degraders. ACS Chem Biol. 2020;15(6):1487-1496. doi:10.1021/ACSCHEMBIO.0C00140

- 15. Zhang D, Lin J, Han J. Receptor-interacting protein (RIP) kinase family. *Cell Mol Immunol*. 2010;7(4):243-249. doi:10.1038/cmi.2010.10
- 16. Upton JW, Kaiser WJ, Mocarski ES. DAI/ZBP1/DLM-1 complexes with RIP3 to mediate virus-induced programmed necrosis that is targeted by murine cytomegalovirus vIRA. *Cell Host Microbe*. 2012;11(3):290-297. doi:10.1016/j.chom.2012.01.016
- 17. Berghe T Vanden, Linkermann A, Jouan-Lanhouet S, Walczak H, Vandenabeele P. Regulated necrosis: The expanding network of non-apoptotic cell death pathways. *Nat Rev Mol Cell Biol*. 2014;15(2):135-147. doi:10.1038/nrm3737
- 18. Sun L, Wang H, Wang Z, et al. Mixed lineage kinase domain-like protein mediates necrosis signaling downstream of RIP3 kinase. *Cell*. 2012;148(1-2):213-227. doi:10.1016/j.cell.2011.11.031
- Petrie EJ, Czabotar PE, Murphy JM. The Structural Basis of Necroptotic Cell
 Death Signaling. *Trends Biochem Sci.* 2019;44(1):53-63.
 doi:10.1016/j.tibs.2018.11.002
- Meng L, Jin W, Wang X. RIP3-mediated necrotic cell death accelerates systematic inflammation and mortality. *Proc Natl Acad Sci U S A*. 2015;112(35):11007-11012. doi:10.1073/pnas.1514730112
- 21. Harris PA, Berger SB, Jeong JU, et al. Discovery of a First-in-Class Receptor Interacting Protein 1 (RIP1) Kinase Specific Clinical Candidate (GSK2982772) for the Treatment of Inflammatory Diseases. *J Med Chem*. 2017;60(4):1247-1261. doi:10.1021/acs.jmedchem.6b01751
- 22. Vandenabeele P, Galluzzi L, Vanden Berghe T, Kroemer G. Molecular

- mechanisms of necroptosis: An ordered cellular explosion. *Nat Rev Mol Cell Biol*. 2010;11(10):700-714. doi:10.1038/nrm2970
- Cho YS, Challa S, Moquin D, et al. Phosphorylation-Driven Assembly of the RIP1-RIP3 Complex Regulates Programmed Necrosis and Virus-Induced Inflammation. *Cell.* 2009;137(6):1112-1123. doi:10.1016/j.cell.2009.05.037
- 24. Degterev A, Huang Z, Boyce M, et al. Chemical inhibitor of nonapoptotic cell death with therapeutic potential for ischemic brain injury. *Nat Chem Biol*. 2005;1(2):112-119. doi:10.1038/nchembio711
- Liu Y, Liu T, Lei T, et al. RIP1/RIP3-regulated necroptosis as a target for multifaceted disease therapy (Review). *Int J Mol Med*. 2019;44(3):771-786. doi:10.3892/ijmm.2019.4244
- 26. Sharma P, Allison JP. Immune checkpoint targeting in cancer therapy: toward combination strategies with curative potential. *Cell*. 2015;161(2):205-214. doi:10.1016/J.CELL.2015.03.030
- 27. Ju E, Park KA, Shen HM, Hur GM. The resurrection of RIP kinase 1 as an early cell death checkpoint regulator—a potential target for therapy in the necroptosis era. *Exp Mol Med 2022 549*. 2022;54(9):1401-1411. doi:10.1038/s12276-022-00847-4
- 28. Cucolo L, Chen Q, Qiu J, et al. The interferon-stimulated gene RIPK1 regulates cancer cell intrinsic and extrinsic resistance to immune checkpoint blockade. *Immunity*. 2022;55(4):671-685.e10. doi:10.1016/j.immuni.2022.03.007
- 29. Powles T, Eder JP, Fine GD, et al. MPDL3280A (anti-PD-L1) treatment leads to clinical activity in metastatic bladder cancer. *Nature*. 2014;515(7528):558-562.

- doi:10.1038/NATURE13904
- 30. Manguso RT, Pope HW, Zimmer MD, et al. In vivo CRISPR screening identifies Ptpn2 as a cancer immunotherapy target. *Nature*. 2017;547(7664):413-418. doi:10.1038/nature23270
- 31. Cabal-Hierro L, O'Dwyer PJ. TNF signaling through RIP1 kinase enhances SN38-induced death in colon adenocarcinoma. *Mol Cancer Res.* 2017;15(4):395-404. doi:10.1158/1541-7786.MCR-16-0329
- 32. Hou J, Wang Y, Shi L, et al. Integrating genome-wide CRISPR immune screen with multi-omic clinical data reveals distinct classes of tumor intrinsic immune regulators. *J Immunother Cancer*. 2021;9(2):1-14. doi:10.1136/jitc-2020-001819
- Pettersson M, Crews CM. PROteolysis TArgeting Chimeras (PROTACs) Past, present and future. *Drug Discov Today Technol*. 2019;31:15-27.
 doi:10.1016/j.ddtec.2019.01.002
- 34. Moreau K, Coen M, Zhang AX, et al. Proteolysis-targeting chimeras in drug development: A safety perspective. *Br J Pharmacol*. 2020;177(8):1709-1718. doi:10.1111/BPH.15014
- 35. Newton K, Dugger DL, Maltzman A, et al. RIPK3 deficiency or catalytically inactive RIPK1 provides greater benefit than MLKL deficiency in mouse models of inflammation and tissue injury. *Cell Death Differ*. 2016;23(9):1565-1576. doi:10.1038/cdd.2016.46
- Rickard JA, O'Donnell JA, Evans JM, et al. RIPK1 regulates RIPK3-MLKL-driven systemic inflammation and emergency hematopoiesis. *Cell*.
 2014;157(5):1175-1188. doi:10.1016/j.cell.2014.04.019

- 37. Zhou T, Wang Q, Phan N, et al. Identification of a novel class of RIP1/RIP3 dual inhibitors that impede cell death and inflammation in mouse abdominal aortic aneurysm models. *Cell Death Dis.* 2019;10(3). doi:10.1038/s41419-019-1468-6
- 38. Raina K, Lu J, Qian Y, et al. PROTAC-induced BET protein degradation as a therapy for castration-resistant prostate cancer. *Proc Natl Acad Sci U S A*. 2016;113(26):7124-7129. doi:10.1073/PNAS.1521738113
- 39. Lu J, Qian Y, Altieri M, et al. Hijacking the E3 Ubiquitin Ligase Cereblon to Efficiently Target BRD4. *Chem Biol.* 2015;22(6):755-763. doi:10.1016/J.CHEMBIOL.2015.05.009
- 40. Filippakopoulos P, Qi J, Picaud S, et al. Selective inhibition of BET bromodomains. *Nature*. 2010;468(7327):1067. doi:10.1038/NATURE09504
- 41. BRD4 Bromodomain Gene Rearrangement in Aggressive Carcinoma with

 Translocation t(15;19) ScienceDirect. Accessed July 12, 2023.

 https://www.sciencedirect.com/science/article/pii/S0002944010630490?casa_toke
 n=0mAPzH2Q4HMAAAAA:ZXOFuRUiMu6Yu0Qa65q_6ozeOuAu_4XllwUkzGhpAMeMm3GqtOFoaEnTgMIwoc5t6MFcYRbl
 Q
- 42. Belkina AC, Denis G V. BET domain co-regulators in obesity, inflammation and cancer. *Nat Rev Cancer*. 2012;12(7):465-477. doi:10.1038/NRC3256
- 43. Carmony KC, Kim K-B. PROTAC-induced proteolytic targeting. *Methods Mol Biol.* 2012;832:627-638. doi:10.1007/978-1-61779-474-2 44
- 44. Lopez-Girona A, Mendy D, Ito T, et al. Cereblon is a direct protein target for immunomodulatory and antiproliferative activities of lenalidomide and

- pomalidomide. Leukemia. 2012;26(11):2326-2335. doi:10.1038/LEU.2012.119
- 45. Chamberlain PP, Cathers BE. Cereblon modulators: Low molecular weight inducers of protein degradation. *Drug Discov Today Technol*. 2019;31:29-34. doi:10.1016/j.ddtec.2019.02.004
- Dong G, Ding Y, He S, Sheng C. Molecular Glues for Targeted Protein
 Degradation: From Serendipity to Rational Discovery. *J Med Chem*.
 2021;64(15):10606-10620. doi:10.1021/ACS.JMEDCHEM.1C00895
- Domostegui A, Nieto-Barrado L, Perez-Lopez C, Mayor-Ruiz C. Chasing molecular glue degraders: screening approaches. *Chem Soc Rev*.
 2022;51(13):5498-5517. doi:10.1039/D2CS00197G
- 48. Geiger TM, Schäfer SC, Dreizler JK, Walz M, Hausch F. Clues to molecular glues. *Curr Res Chem Biol.* 2022;2:100018. doi:10.1016/j.crchbi.2021.100018
- 49. Kozicka Z, Thomä NH. Haven't got a glue: Protein surface variation for the design of molecular glue degraders. *Cell Chem Biol*. 2021;28(7):1032-1047. doi:10.1016/j.chembiol.2021.04.009
- Fischer ES, Böhm K, Lydeard JR, et al. Structure of the DDB1–CRBN E3 ubiquitin ligase in complex with thalidomide. *Nat 2014 5127512*.
 2014;512(7512):49-53. doi:10.1038/nature13527
- 51. Sievers QL, Petzold G, Bunker RD, et al. Defining the human C2H2 zinc finger degrome targeted by thalidomide analogs through CRBN. *Science* (80-). 2018;362(6414). doi:10.1126/SCIENCE.AAT0572
- 52. Hansen JD, Correa M, Nagy MA, et al. Discovery of CRBN E3 Ligase Modulator CC-92480 for the Treatment of Relapsed and Refractory Multiple Myeloma. *J*

- Med Chem. 2020;63(13):6648-6676. doi:10.1021/ACS.JMEDCHEM.9B01928
- 53. Petzold G, Fischer ES, Thomä NH. Structural basis of lenalidomide-induced CK1α degradation by the CRL4 CRBN ubiquitin ligase. *Nature*. 2016;532(7597):127-130. doi:10.1038/NATURE16979
- 54. Matyskiela ME, Lu G, Ito T, et al. A novel cereblon modulator recruits GSPT1 to the CRL4 CRBN ubiquitin ligase. *Nature*. 2016;535(7611):252-257. doi:10.1038/NATURE18611
- 55. Hao B bing, Li X jing, Jia X long, et al. The novel cereblon modulator CC-885 inhibits mitophagy via selective degradation of BNIP3L. *Acta Pharmacol Sin*. 2020;41(9):1246-1254. doi:10.1038/S41401-020-0367-9
- 56. Surka C, Jin L, Mbong N, et al. CC-90009, a novel cereblon E3 ligase modulator, targets acute myeloid leukemia blasts and leukemia stem cells. *Blood*. 2021;137(5):661-677. doi:10.1182/blood.2020008676
- 57. Matyskiela ME, Zhang W, Man HW, et al. A Cereblon Modulator (CC-220) with Improved Degradation of Ikaros and Aiolos. *J Med Chem.* 2018;61(2):535-542. doi:10.1021/ACS.JMEDCHEM.6B01921
- 58. Hagner PR, Man HW, Fontanillo C, et al. CC-122, a pleiotropic pathway modifier, mimics an interferon response and has antitumor activity in DLBCL. *Blood*. 2015;126(6):779-789. doi:10.1182/blood-2015-02-628669
- 59. Lipinski CA. Lead- and drug-like compounds: The rule-of-five revolution. *Drug Discov Today Technol*. 2004;1(4):337-341. doi:10.1016/j.ddtec.2004.11.007
- 60. Schreiber SL. The Rise of Molecular Glues. *Cell*. 2021;184(1):3-9. doi:10.1016/j.cell.2020.12.020

- Dong G, Ding Y, He S, Sheng C. Molecular Glues for Targeted Protein
 Degradation: From Serendipity to Rational Discovery. *J Med Chem*.
 2021;64(15):10606-10620.
 doi:10.1021/ACS.JMEDCHEM.1C00895/ASSET/IMAGES/LARGE/JM1C00895
 _0012.JPEG
- 62. Guo L, Zhou Y, Nie X, et al. A platform for the rapid synthesis of proteolysis targeting chimeras (Rapid-TAC) under miniaturized conditions. *Eur J Med Chem*. 2022;236:114317. doi:10.1016/J.EJMECH.2022.114317
- 63. Hendrick CE, Jorgensen JR, Chaudhry C, et al. Direct-to-Biology Accelerates PROTAC Synthesis and the Evaluation of Linker Effects on Permeability and Degradation. *ACS Med Chem Lett.* 2022;13(7):1182-1190. doi:10.1021/ACSMEDCHEMLETT.2C00124
- 64. Guo L, Zhou Y, Nie X, et al. A platform for the rapid synthesis of proteolysis targeting chimeras (Rapid-TAC) under miniaturized conditions. *Eur J Med Chem*. 2022;236. doi:10.1016/j.ejmech.2022.114317
- 65. Wu H, Yang K, Zhang Z, et al. Development of Multifunctional Histone Deacetylase 6 Degraders with Potent Antimyeloma Activity. *J Med Chem*. 2019;62(15):7042-7057. doi:10.1021/acs.jmedchem.9b00516
- 66. Powell CE, Du G, Che J, et al. Selective Degradation of GSPT1 by Cereblon Modulators Identified via a Focused Combinatorial Library. ACS Chem Biol. 2020;15(10):2722-2730. doi:10.1021/ACSCHEMBIO.0C00520
- 67. Wang B, Liu J, Tandon I, et al. Development of MDM2 degraders based on ligands derived from Ugi reactions: Lessons and discoveries. *Eur J Med Chem*.

- 2021;219. doi:10.1016/j.ejmech.2021.113425
- 68. Wang Z, Yu K, Tan H, et al. 27-Plex Tandem Mass Tag Mass Spectrometry for Profiling Brain Proteome in Alzheimer's Disease. *Anal Chem.* 2020;92(10):7162-7170. doi:10.1021/ACS.ANALCHEM.0C00655
- 69. Bai B, Vanderwall D, Li Y, et al. Proteomic landscape of Alzheimer's Disease: novel insights into pathogenesis and biomarker discovery. *Mol Neurodegener*. 2021;16(1). doi:10.1186/S13024-021-00474-Z
- 70. Wang X, Li Y, Wu Z, Wang H, Tan H, Peng J. JUMP: A tag-based database search tool for peptide identification with high sensitivity and accuracy. *Mol Cell Proteomics*. 2014;13(12):3663-3673. doi:10.1074/mcp.O114.039586
- 71. Deshaies RJ. Protein degradation: Prime time for PROTACs. *Nat Chem Biol*. 2015;11(9):634-635. doi:10.1038/NCHEMBIO.1887
- 72. Papatzimas JW, Gorobets E, Brownsey DK, Maity R, Bahlis NJ, Derksen DJ. A General Strategy for the Preparation of Thalidomide-Conjugate Linkers. *Synlett*. 2017;28(20):2881-2885. doi:10.1055/S-0036-1588539
- 73. Corson TW, Aberle N, Crews CM. Design and applications of bifunctional small molecules: Why two heads are better than one. *ACS Chem Biol*. 2008;3(11):677-692. doi:10.1021/CB8001792
- 74. Pettersson M, Crews CM. PROteolysis TArgeting Chimeras (PROTACs) Past, present and future. *Drug Discov Today Technol*. 2019;31:15-27. doi:10.1016/j.ddtec.2019.01.002
- 75. Protein Degradation by In-Cell Self-Assembly of Proteolysis Targeting Chimeras |

 ACS Central Science. Accessed July 16, 2023.

- https://pubs.acs.org/doi/10.1021/acscentsci.6b00280#
- 76. Lebraud H, Wright DJ, Johnson CN, Heightman TD. Protein degradation by incell self-assembly of proteolysis targeting chimeras. ACS Cent Sci. 2016;2(12):927-934.
 doi:10.1021/ACSCENTSCI.6B00280/ASSET/IMAGES/LARGE/OC-2016-002802_0004.JPEG
- 77. Pajouhesh H, Lenz GR. Medicinal chemical properties of successful central nervous system drugs. *NeuroRx*. 2005;2(4):541-553. doi:10.1602/NEURORX.2.4.541
- 78. Blackman ML, Royzen M, Fox JM. Tetrazine ligation: Fast bioconjugation based on inverse-electron-demand Diels-Alder reactivity. *J Am Chem Soc*. 2008;130(41):13518-13519. doi:10.1021/JA8053805
- Selvaraj R, Fox JM. Trans-Cyclooctene-a stable, voracious dienophile for bioorthogonal labeling. *Curr Opin Chem Biol*. 2013;17(5):753-760. doi:10.1016/J.CBPA.2013.07.031
- 80. Tsai YH, Essig S, James JR, Lang K, Chin JW. Selective, rapid and optically switchable regulation of protein function in live mammalian cells. *Nat Chem*. 2015;7(7):554-561. doi:10.1038/NCHEM.2253
- 81. Yang KS, Budin G, Reiner T, Vinegoni C, Weissleder R. Bioorthogonal imaging of Aurora Kinase A in live cells. *Angew Chemie Int Ed.* 2012;51(27):6598-6603. doi:10.1002/ANIE.201200994
- 82. Reiner T, Earley S, Turetsky A, Weissleder R. Bioorthogonal Small-Molecule Ligands for PARP1 Imaging in Living Cells. *ChemBioChem*. 2010;11(17):2374-

- 2377. doi:10.1002/CBIC.201000477
- 83. Chaudhry C. Mathematical Model for Covalent Proteolysis Targeting Chimeras: Thermodynamics and Kinetics Underlying Catalytic Efficiency. *J Med Chem*. 2023;66(9):6239-6250. doi:10.1021/ACS.JMEDCHEM.2C02076/ASSET/IMAGES/LARGE/JM2C02076 _0010.JPEG
- 84. Krysztofinska EM, Martínez-Lumbreras S, Thapaliya A, Evans NJ, High S, Isaacson RL. Structural and functional insights into the E3 ligase, RNF126. *Sci Rep.* 2016;6. doi:10.1038/SREP26433
- Rodrigo-Brenni MC, Gutierrez E, Hegde RS. Cytosolic Quality Control of Mislocalized Proteins Requires RNF126 Recruitment to Bag6. *Mol Cell*.
 2014;55(2):227-237. doi:10.1016/J.MOLCEL.2014.05.025
- 86. Hu X, Wang L, Wang Y, et al. RNF126-Mediated Reubiquitination Is Required for Proteasomal Degradation of p97-Extracted Membrane Proteins. *Mol Cell*. 2020;79(2):320-331.e9. doi:10.1016/J.MOLCEL.2020.06.023
- 87. Toriki ES, Papatzimas JW, Nishikawa K, et al. Rational Chemical Design of Molecular Glue Degraders. ACS Cent Sci. Published online May 24, 2022. doi:10.1021/ACSCENTSCI.2C01317/ASSET/IMAGES/LARGE/OC2C01317_00 05.JPEG
- 88. Tong B, Luo M, Xie Y, et al. Bardoxolone conjugation enables targeted protein degradation of BRD4. *Sci Rep.* 2020;10(1):15543. doi:10.1038/s41598-020-72491-9
- 89. Wei J, Meng F, Park KS, et al. Harnessing the E3 ligase KEAP1 for targeted

- protein degradation. *J Am Chem Soc.* 2021;143(37):15073-15083. doi:10.1021/jacs.1c04841
- 90. Suzuki T, Yamamoto M. Stress-sensing mechanisms and the physiological roles of the Keap1–Nrf2 system during cellular stress. *J Biol Chem*. 2017;292(41):16817-16824. doi:10.1074/jbc.r117.800169
- 91. Pei J, Xiao Y, Liu X, et al. Piperlongumine conjugates induce targeted protein degradation. *Cell Chem Biol*. 2023;30(2):203-213.e17. doi:10.1016/j.chembiol.2023.01.004
- 92. Mi D, Li Y, Gu H, Li Y, Chen Y. Current advances of small molecule E3 ligands for proteolysis-targeting chimeras design. *Eur J Med Chem*. 2023;256. doi:10.1016/j.ejmech.2023.115444
- 93. Zhong Y, Chi F, Wu H, et al. Emerging targeted protein degradation tools for innovative drug discovery: From classical PROTACs to the novel and beyond. *Eur J Med Chem.* 2022;231. doi:10.1016/J.EJMECH.2022.114142
- 94. Hartung KM, Sletten EM. Bioorthogonal chemistry: Bridging chemistry, biology, and medicine. *Chem.* Published online 2023. doi:10.1016/J.CHEMPR.2023.05.016
- 95. Sletten EM, Bertozzi CR. Bioorthogonal chemistry: fishing for selectivity in a sea of functionality. *Angew Chemie*. 2009;48(38):6974-6998. doi:10.1002/ANIE.200900942
- Goyanes A, Wang J, Buanz A, et al. 3D Printing of Medicines: Engineering Novel
 Oral Devices with Unique Design and Drug Release Characteristics. *Mol Pharm*.
 2015;12(11):4077-4084.
 - doi:10.1021/ACS.MOLPHARMACEUT.5B00510/ASSET/IMAGES/MEDIUM/

- MP-2015-005109 0009.GIF
- 97. Békés M, Langley DR, Crews CM. PROTAC targeted protein degraders: the past is prologue. *Nat Rev Drug Discov*. 2022;21(3):181-200. doi:10.1038/S41573-021-00371-6
- 98. Ciechanover A. Proteolysis: From the lysosome to ubiquitin and the proteasome.

 Nat Rev Mol Cell Biol. 2005;6(1):79-86. doi:10.1038/NRM1552
- 99. Hughes SJ, Ciulli A. Molecular recognition of ternary complexes: A new dimension in the structure-guided design of chemical degraders. *Essays Biochem*. 2017;61(5):505-516. doi:10.1042/EBC20170041
- Buckley DL, Gustafson JL, Van-Molle I, et al. Small-molecule inhibitors of the interaction between the E3 ligase VHL and HIF1α. Angew Chemie Int Ed.
 2012;51(46):11463-11467. doi:10.1002/ANIE.201206231
- 101. Jevtić P, Haakonsen DL, Rapé M. An E3 ligase guide to the galaxy of small-molecule-induced protein degradation. *Cell Chem Biol.* 2021;28(7):1000-1013. doi:10.1016/J.CHEMBIOL.2021.04.002
- Burslem GM, Smith BE, Lai AC, et al. The Advantages of Targeted Protein
 Degradation Over Inhibition: An RTK Case Study. *Cell Chem Biol*.
 2018;25(1):67-77.e3. doi:10.1016/J.CHEMBIOL.2017.09.009
- 103. Toure M, Crews CM. Small-molecule PROTACS: New approaches to protein degradation. *Angew Chemie Int Ed.* 2016;55(6):1966-1973. doi:10.1002/ANIE.201507978
- 104. Zuo X, Liu D. Mechanism of immunomodulatory drug resistance and novel therapeutic strategies in multiple myeloma. *Hematol (United Kingdom)*.

- 2022;27(1):1110-1121. doi:10.1080/16078454.2022.2124694
- 105. Wang T, Wei JJ, Sabatini DM, Lander ES. Genetic screens in human cells using the CRISPR-Cas9 system. *Science* (80-). 2014;343(6166):80-84. doi:10.1126/SCIENCE.1246981
- 106. Shalem O, Sanjana NE, Hartenian E, et al. Genome-scale CRISPR-Cas9 knockout screening in human cells. *Science* (80-). 2014;343(6166):84-87. doi:10.1126/SCIENCE.1247005
- Tsherniak A, Vazquez F, Montgomery PG, et al. Defining a Cancer Dependency
 Map. Cell. 2017;170(3):564-576.e16. doi:10.1016/J.CELL.2017.06.010
- 108. Hrecka K, Gierszewska M, Srivastava S, et al. Lentiviral Vpr usurps Cul4-DDB1[VprBP] E3 ubiquitin ligase to modulate cell cycle. *Proc Natl Acad Sci U S A*. 2007;104(28):11778-11783. doi:10.1073/PNAS.0702102104
- 109. Zhang X, Crowley VM, Wucherpfennig TG, Dix MM, Cravatt BF. Electrophilic PROTACs that degrade nuclear proteins by engaging DCAF16. *Nat Chem Biol*. 2019;15(7):737-746. doi:10.1038/S41589-019-0279-5
- 110. Schabla NM, Mondal K, Swanson PC. DCAF1 (VprBP): Emerging physiological roles for a unique dual-service E3 ubiquitin ligase substrate receptor. *J Mol Cell Biol.* 2019;11(9):725-735. doi:10.1093/JMCB/MJY085
- 111. Chen Z, Zhang L, Ying S. SAMHD1: A novel antiviral factor in intrinsic immunity. *Future Microbiol*. 2012;7(9):1117-1126. doi:10.2217/FMB.12.81
- 112. Schwefel D, Groom HCT, Boucherit VC, et al. Structural basis of lentiviral subversion of a cellular protein degradation pathway. *Nature*. 2014;505(7482):234-238. doi:10.1038/NATURE12815

- 113. Laguette N, Sobhian B, Casartelli N, et al. SAMHD1 is the dendritic- and myeloid-cell-specific HIV-1 restriction factor counteracted by Vpx. *Nature*. 2011;474(7353):654-657. doi:10.1038/NATURE10117
- 114. Schröder M, Renatus M, Liang X, et al. Reinstating targeted protein degradation with DCAF1 PROTACs in CRBN PROTAC resistant settings. *bioRxiv*. Published online April 14, 2023:2023.04.09.536153. doi:10.1101/2023.04.09.536153
- 115. Nijhuis A, Sikka A, Yogev O, et al. Indisulam targets RNA splicing and metabolism to serve as a therapeutic strategy for high-risk neuroblastoma. *Nat Commun* 2022 131. 2022;13(1):1-16. doi:10.1038/s41467-022-28907-3
- 116. Owen J, Shahani V, Kimani S, et al. Designing chemical probes for DCAF1 using match maker TM. Accessed July 24, 2023. https://www.rcsb.org/structure/7SSE
- 117. wwPDB: 7SSE. Accessed July 30, 2023.

 https://www.wwpdb.org/pdb?id=pdb_00007sse
- 118. Structural basis of indisulam-mediated RBM39 recruitment to DCAF15 E3 ligase complex | Nature Chemical Biology. Accessed July 24, 2023.
 https://www.nature.com/articles/s41589-019-0411-6
- 119. Bussiere DE, Xie L, Srinivas H, et al. Structural basis of indisulam-mediated RBM39 recruitment to DCAF15 E3 ligase complex. *Nat Chem Biol* 2019 161. 2019;16(1):15-23. doi:10.1038/s41589-019-0411-6